CELL AND DEVELOPMENTAL BIOLOGY

THE ROLE OF RAB11-FIP2 IN EPITHELIAL CELLS

NICOLE ANNETTE DUCHARME

Dissertation under the direction of Professor James R Goldenring

The small GTPase Rab11 family proteins have been implicated in the plasma membrane recycling system in such diverse model systems as H/K-ATPase trafficking in parietal cells to GLUT4 trafficking in heart and skeletal muscle. Rab11 family interacting protein 2 (Rab11-FIP2) was previously identified as binding to both Rab11a and the motor protein, myosin Vb. Therefore, we hypothesized that Rab11-FIP2 is a critical regulator of the plasma membrane recycling system. In these studies, we sought to characterize the role of Rab11-FIP2 function in polarized epithelial cells. To address the role of Rab11-FIP2, we uncovered a new role for Rab11-FIP2 in the establishment of polarity. We found that Rab11-FIP2 is phosphorylated by MARK2, and that this phosphorylation is necessary for the proper formation of the adherens junction. Next, we characterized a new dominant mutant Rab11-FIP2 mutant, which has unique effects on the recycling system than all previously characterized mutants. Analysis of the data suggests that FIP2 is involved in multiple stages in passage through the Rab11a associated recycling system. Multiple points of entry into the Rab11a/ FIP2 recycling system may be exploited depending upon the origin of the protein and possibly, its destination. This model supports a dynamic vision of the recycling system trafficking.

We also analyzed new Rab11-FIP2 interacting proteins utilizing a novel approach of immunoprecipitation from stable cell lines overexpressing either wild type Rab11-FIP2 or its mutants followed by identification of the associated proteins using mass spectrometry. This proteomics approach revealed novel interactions with proteins known to be involved in trafficking (dynein and Rab10) in early endosomal membrane regulation (Rab5b and EpsinR), and vesicle coat proteins (AP-1 and clathrin heavy chain). Validation of these interactions proves that this methodology reveals robust interactions that are readily confirmed. All together, this body of work significantly advances our understanding of the diverse roles of Rab11-FIP2 in the regulation of epithelial cell function.

Approved: Dr James R Goldenring

THE ROLE OF RAB11-FIP2 IN POLARIZED MDCK CELLS

By

Nicole Annette Ducharme

Dissertation

Submitted to the Faculty of the

Graduate School of Vanderbilt University

in partial fulfillment of the requirements

for the degree of

DOCTOR OF PHILSOPHY

in

Cell and Developmental Biology

May, 2007

Nashville, Tennessee

Approved:

Dr James R Goldenring

Dr Susan R Wente

Dr Stephen R Hann

Dr Ann Richmond

Dr Anne K Kenworthy

Dr Robert J Coffey

TABLE OF CONTENTS

LIST OF TABLES

LIST OF FIGURES

LIST OF ABBREVIATIONS

AEE	Apical Early Endosome
AKAP	A Kinase Anchoring Protein
AP-2	Adaptor-Related Protein-2
ARE	Apical Recycling Endosome
ARF	ADP-ribosylation factor
BEE	Basolateral Early Endosome
CE	Common Endosome
CFTR	Cystic Fibrosis Transmembrane Receptor
EE	Early Endosome
EEA1	Early Endosome Antigen 1
EGF	Epidermal Growth Factor
EGFP	Enhanced Green Fluorescent Protein
EGFR	Epidermal Growth Factor Receptor
EHD	Eps15 Homology Domain
EMK1	ELKL Motif Kinase 1
GAP	GTPase Activating Proteins
GEF	Guanine Nucleotide Exchange Factors
GP135	Glycoprotein
IQGAP	IQ motif containing GTPase activating protein
LC-MS/MS	Liquid Chromatography/Mass Spectrometry/Mass Spectrometry
LDL	Low Density Lipoprotein

MARK2	Microtubule Affinity-Regulating Kinase 2
MDCK	Madin-Darby Canine Kidney
mRFP	monomeric Red Fluorescent Protein
NOEL	No Eleven Binding Domain
PAR1-B	Partitioning-Defect 1
PATJ	Pals1-Associated Tight Junction Protein
pIgA	Polymeric Immunoglobulin A
pIgAR	Polymeric Immunoglobulin A Receptor
Rab	Ras genes from rat brain
Rab11-FIP	Rab11 Family Interacting Protein
Rab11-FIP(ΔC2)	Rab11-FIP2(129-512)
Rab11-FIP2(SARG)	Rab11-FIP2(S229A/Rab11-FIP2(R413G)
RCP	Rab Coupling Protein
ZO-	Zonula Occludens -1, -2, -3

CHAPTER I

INTRODUCTION

Cells have evolved complex processes to maintain a functional dynamic equilibrium. One of the fundamental tasks of a cell is to interact with its environment. In order to respond accurately to external stimuli, the cell has evolved an intricate system for the regulation of its plasma membrane proteins. Much of this pathway is facilitated by the movement of proteins to and from the cell surface via vesicular structures along the cytoskeleton. This system is ubiquitous in many aspects of cell physiology from nutrient internalization to receptor and ion channel recycling (Takei and Haucke, 2001), collectively known as trafficking.

Epithelial Cell polarization

The defining characteristic of an epithelial cell is the involvement of directionality in the cell. The cell defines its top, or apical, side as well as its bottom, or basal/basalateral, side. The existence of these different sides of the cell is fundamental to all aspects of epithelial cell-specific functions. The process of defining the apical and basolateral domains is known as polarization. A cell begins to polarize in response to signals sent from neighboring cells and the extracellular matrix, which the cells have adhered to and forms the basis of the basolateral domain (Shin *et al.*, 2005). As a cell polarizes, two distinct junctions are formed that help to define the polarized domains: the adherens junction and the tight junction.

The adherens junction forms at the site of cell-cell adhesion where calcium dependent cell-to-cell binding occurs. E-cadherins from one cell bind to those in the neighboring cell forming the adherens junction (Lock and Stow, 2005b). E-cadherin also binds a number of internal proteins that serve to stabilize the complex. As E-cadherin is synthesized, it binds to beta-catenin. Once E-cadherin is trafficked to the plasma membrane, it interacts with cytosolic p120-catenin (Lock and Stow, 2005b). However, approximately 13% of the E-cadherin is in a constantly recycling pool (Le *et al.*, 1999). If cells are incubated at 18° C, a temperature that results in accumulation of endocytosed proteins in early or sorting endosomes, recycling E-cadherin accumulates in a Rab5 positive early endosomal structure (Le *et al.*, 1999).

The tight junction forms a physical barrier between two adjacent cells that serves to regulate the flow of materials across the epithelial monolayer between cells as well as to maintain the distinction between the apical and basolateral membrane domains (Kobayashi *et al.*, 2002). This physiological significance of the tight junction is exemplified by a phenotype of severe dehydration leading to death in mice lacking the barrier function afforded by these junctions (Tunggal *et al.*, 2005). Proteins destined for the tight junction are transported in vesicles to the lateral domain (Kobayashi *et al.*, 2002). Numerous tight junction proteins have been identified and tracked through the polarization process. The first known protein to move apically is PATJ, which begins the definition and formation of the tight junction (Figure 1). Another protein, ZO-1, is brought with E-cadherin to the site of cell-cell adhesion (Stevenson and Keon, 1998; Shin *et al.*, 2005). Shortly after the movement of PATJ, ZO-1 assembles with ZO-2 and ZO-3 at the adherens junction (Stevenson and Keon, 1998) before moving to the tight junction

(Shin *et al.*, 2005). In fact, in PATJ knock-down studies, ZO-1 had a delayed progression to the tight junction (Shin *et al.*, 2005) and PATJ is required for occludin and ZO-3 localization to tight junctions (Michel *et al.*, 2005). The tight junction proteins interact with filamentous actin found at the apical membrane (Shin *et al.*, 2005) (Figure 1). If the actin is disrupted, the tight junction looses its barrier function and internalizes the junctional proteins ZO-1 and occludin (Shin *et al.*, 2005). The generation of polarity in epithelia is dependent upon microtubules. Microtubules have intrinsic directionality with their plus ends directed basally and their minus ends directed apically. The kinase MARK2 promotes microtubule assembly at the lateral membrane essentially initiating polarity (Musch, 2004). Specifically, junctional assembly requires microtubules and microtubule motors: first dynein tethers the complex and then kinesin mediates transport along microtubules (Caviston and Holzbaur, 2006).

Following the formation of junctional complexes, the cell has defined apical and basolateral domains. All subsequently synthesized proteins must be targeted to the correct domain. Some proteins have defined directionality cues. Sorting to the apical membrane is driven by N- and O-linked glycosylation or GPI anchors (Folsch, 2005). Delivery to the basolateral membrane is directed by the presence of a tyrosine or dileucine motif in the cytoplasmic tail of the newly synthesized protein (Folsch, 2005). Recent reports suggest that individualized endocytosis routes may exist for different receptors. For example, the transferrin receptor utilizes AP-2 as its clathrin adaptor protein while LDL receptor and EGFR employ Epidermal growth factor receptor pathway substrate 15 (Eps 15) as its clathrin adaptor (Perret *et al.*, 2005). The orchestration of delivery of proteins to apical and basal domains is mediated by trafficking events.

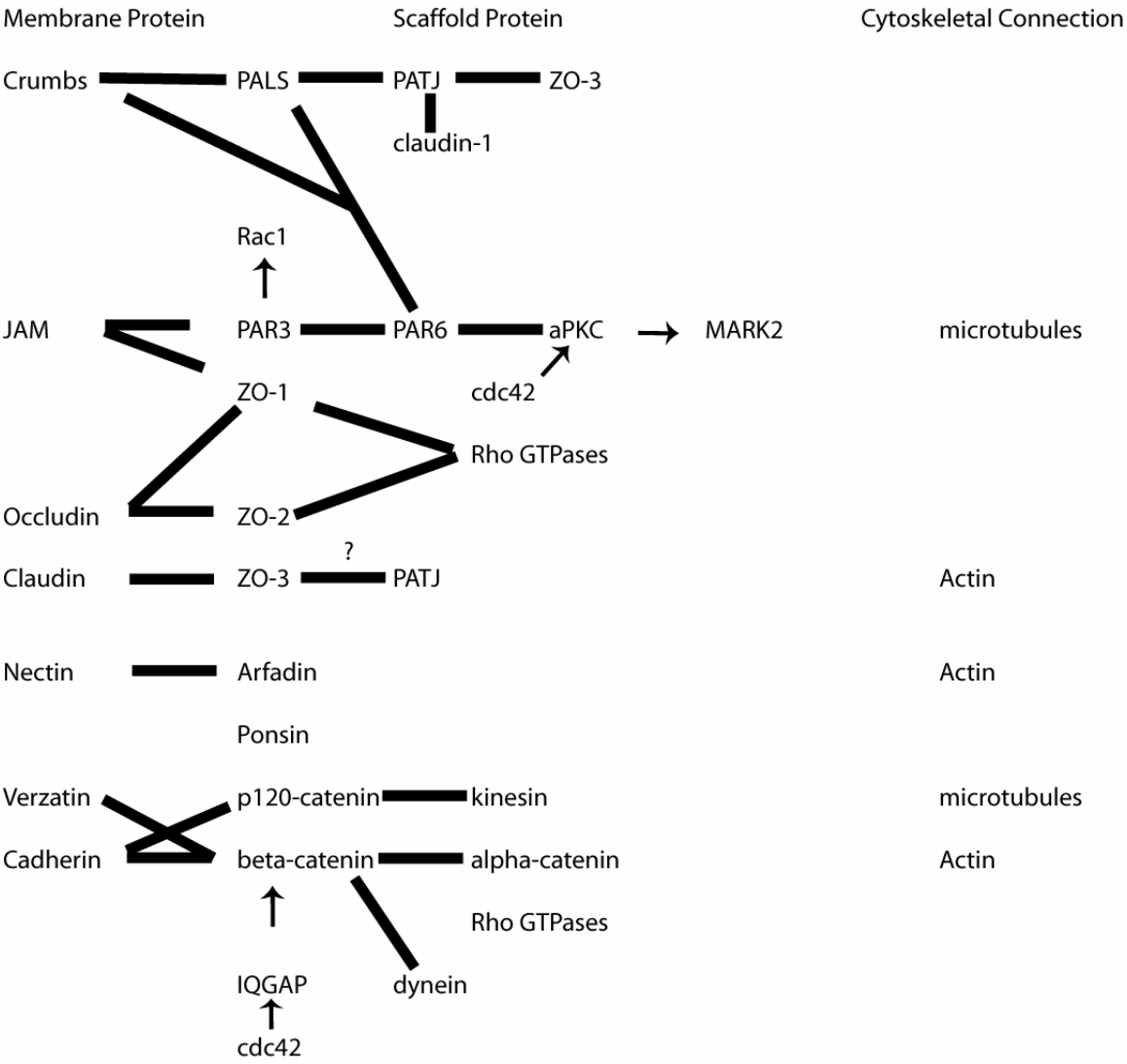

Figure 1: A Schematic Depicting a Portion of the Known Junctional Proteins

Modified from ((Bryant and Stow, 2004); (Matter et al., 2005); (Nelson, 2003); (Shin et al., 2005); (Ivanov et al., 2006); (Gumbiner, 2005)). Arrows indicate the protein at the arrow head is activated by the initial protein. Lines indicate that the proteins interact with each other.

Cells can internalize and direct vesicles in four distinct ways. A cell can internalize a vesicle from the apical side and return it back to the apical side, known as apical recycling. Alternatively, a cell can utilize basolateral recycling when it internalizes a vesicle from the basolateral side and recycles it back to that same side. The cell can also transport a vesicle from one side of the cell to the other in a process known as

transcytosis. Finally, a cell can target the contents of vesicles for degradation by the lysosome (2).

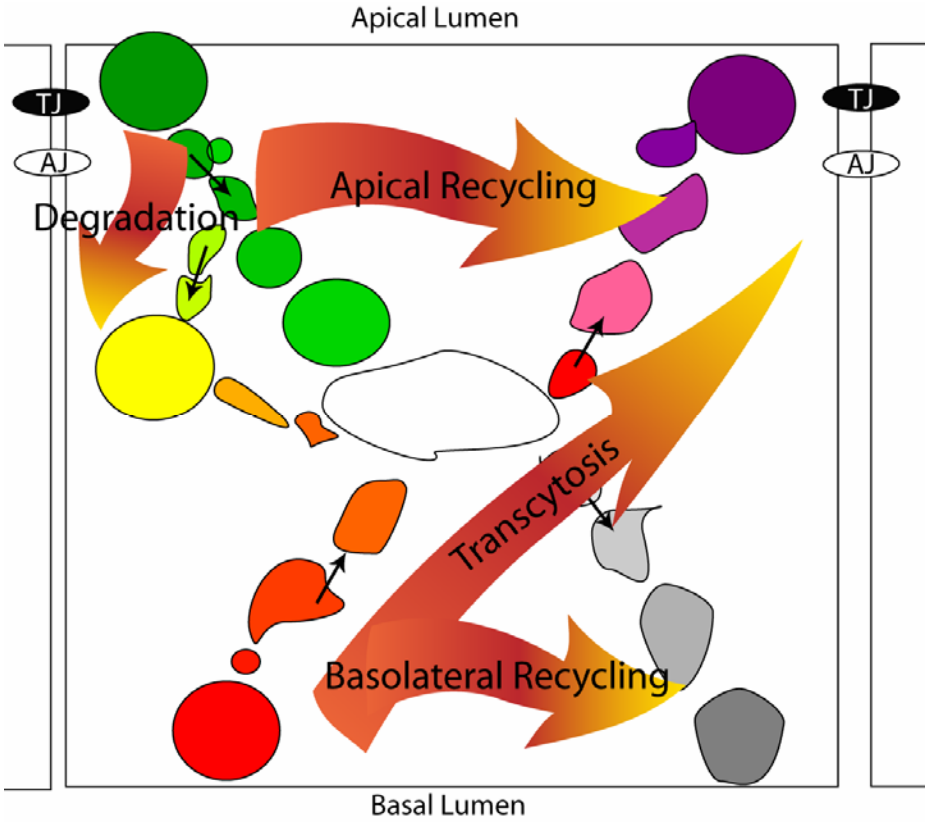

Figure 2: Schematic of the potential trafficking routes in polarized cells

A cell can internalize cargo and direct it to a variety of different places. A cell can send the cargo to the lysosome for degradation. Alternatively, cargo endocytosed, from the apical membrane can enter an apical recycling pathway that brings it back out to the apical membrane. A cell can also internalize cargo from the basolateral membrane. This cargo can either be trafficked to the apical membrane, known as transcytosis, or send it back out to the basolateral membrane, known as basolateral recycling. TJ refers to tight junction while AJ refers to adherens junction.

Small GTPases

Small GTP-binding proteins are monomeric proteins with molecular masses of 20-40 kDa (Takei and Haucke, 2001). The small GTPase superfamily currently has been subdivided into five families: Ras, Rho/Rac/cdc42, Ran, Arf/Sar, and Rab. Each of these

small GTPases share structural homology but have functional specificity. The first protein class described in the family was Ras. Ras was subsequently found to regulate cell proliferation, differentiation, morphology, and apoptosis (Takei and Haucke, 2001). Rho/Rac/Cdc42 proteins regulate cytoskeletal reorganization in response to extracellular signals in mammalian cells (Wennerberg and Der, 2004). Ran regulates nuclear import and export through the nuclear pore complex (Madrid and Weis, 2006). The Arf/Sar family of proteins regulates vesicle budding and formation (Kahn *et al.*, 2005). Finally, the Rab family regulates vesicle trafficking (Takei and Haucke, 2001). The work described herein specifically furthers our understanding of Rab proteins.

The Importance of Rab Proteins

Investigations over the past decade have demonstrated that a family of small GTPases, known as Rab ('Ras genes from rat brain') proteins, regulates many diverse aspects of vesicle trafficking within both non-polarized and polarized cells (Pfeffer, 2001). Researchers have identified over sixty mammalian Rabs to date, each with a unique role in cellular trafficking. Each Rab helps to define a subsection of vesicular membranes, which, while dynamic, is generally exclusive for each type of Rab (Sonnichsen *et al.*, 2000). In many cases, the membrane domains are continuous (Brown *et al.*, 2000) yet functionally distinct (Sonnichsen *et al.*, 2000). It has become a standard practice in the trafficking field to use Rabs to define distinct subdomains within a continuous membrane (Seabra and Coudrier, 2004) (see below for examples).

Rabs are critical for the regulation of vesicle budding and fusion during trafficking events. The Tavitian lab first identified and named mammalian Rabs 1 through 4 in 1987 (Touchot *et al.*, 1987). Subsequently, further work revealed that Rabs

can have such high conservation from yeast through mammals that they often can substitute for each other in *in vitro* situations (Stenmark and Olkkonen, 2001). Rab family members have a carboxyl-terminal CC or CXC sequence, which allows isoprenylation with a geranylgeranyl motif (Khosravi-Far *et al.*, 1991), accounting for their membrane association. Double geranylgeranylation is necessary for proper membrane targeting and activation of Rabs (Gomes *et al.*, 2003). Finally, Rabs cycle between an active (GTP-bound) and inactive (GDP bound). The transition between these states utilizes guanine-nucleotide exchange factors (GEFs) to exchange GDP for GTP and GTPase-activating proteins (GAPs) to aid in GTP hydrolysis to GDP (reviewed in (Segev, 2001)) (Figure 3).

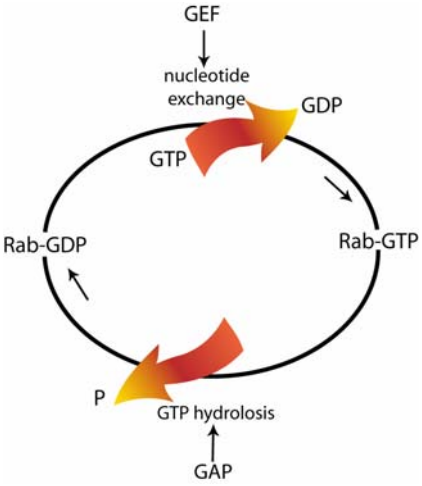

Figure 3: Common Features of Rab Proteins

Rab GTPase Cycle. Rab proteins cycle between an active GTP bound form and an inactive GDP bound form. GTPase-activating proteins (GAPs) enhance the exchange from GDP to GTP. The hydrolysis of GTP to GDP is facilitated by guanine nucleotide exchange factors (GEFs).

Rab Protein Function

In the early 1990s, two hypotheses emerged to explain the functional importance of Rab proteins: 1) Rab proteins serve as switches/timers or 2) Rab proteins coordinate

protein complex assembly. The first hypothesis was suggested in 1991 based upon a comparison with other small GTPases (Khosravi-Far *et al.*, 1991). This work suggested that because small GTPases had a common structure, they would also have a common function. By comparing EF-Tu to the other GTPase families, Bourne *et al* concluded that the hydrolysis of GTP to GDP served as a timer to turn off the core function of the GTPase. Further support of this hypothesis found that Rab5 could undergo GTP-binding and hydrolysis without causing endosome fusion (Rybin *et al.*, 1996). However, the fusion event did require hydrolysis. This work suggested that the binding of GDP or GTP regulated the recruitment of interacting proteins, which would in turn slow the hydrolysis step. This work set the stage for the second hypothesis that the primary role of Rab proteins is to recruit other effector molecules. The specificity of Rab localization facilitates the assembly of all components in a complex necessary for vesicle formation (Schimmoller *et al.*, 1998; Hammer and Wu, 2002). For example, Rab5-GTP specifically recruits Rabaptin-5 to the Rab5 positive membrane (Rybin *et al.*, 1996). Thus, these two hypotheses were unified into the postulate that the binding of GTP to Rab proteins served as a timer to recruit the appropriate proteins in order for a vesicle to correctly form (Woodman, 1998).

A seminal paper reported that the carboxy-terminal variable region of Rab proteins determines their subcellular localization (Chavrier *et al.*, 1991). This work exchanged portions of the Rab2, 5 or 7 proteins with each other creating chimeric proteins. They found that the carboxy-terminal domain conferred specificity. For example, N-terminal Rab5 fused to C-terminal Rab7 caused localization of the chimera to the late endosome (Chavrier *et al.*, 1991). These results supported a hypothesis that Rab

localization was dependent on C-terminal protein interactions (Seabra and Wasmeier, 2004).

The original work comparing the classes of small GTPases used sequence homology to determine putative functions for conserved sequences (Khosravi-Far *et al.*, 1991). They suggested the GTP binding region was divided into three regions based upon the known function in EF-Tu: region 1 bound α and β-phosphate of GDP and/or GTP; region 2 was used to bind the coordinating Mg ion; and region 3 bound the γ-phosphate of GTP (Khosravi-Far *et al.*, 1991) (Figure 4). Recent work analyzing crystal structures of Rab proteins have supported this general hypothesis (Pfeffer, 2005).

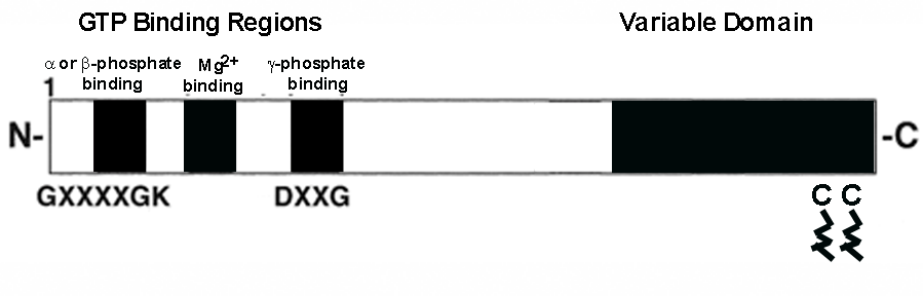

Figure 4: Small GTPase Protein Structure

Small GTPase proteins are characterized by GTP binding regions and a variable domain. Three GTP binding domains are used to bind separate components of GTP: Region 1 binds the α- or β-phosphate of GDP and GTP; Region 2 binds magnesium; and Region 3 binds the γ-phosphate of GTP. The C-terminal variable domain consists of the last 30 amino acids.

Rab11 Family

Over the past 10 years, a number of studies have led to the recognition that Rab11 family members regulate the plasma membrane recycling system. Rab11a was cloned as the Sec4 homolog in MDCK cells in 1990 (Chavrier *et al.*, 1990a; Chavrier *et al.*, 1990b). The Rab11 Family now consists of Rab11a, Rab11b, and Rab25, all of which share a

similar genomic structure (Bhartur *et al.*, 2000). To date, Rab11a is the best-characterized member of the family. Tissues with high levels of secretion such as the brain, lung, fundus, and ileum, as well as the parietal cell have enriched levels of Rab11 protein (Goldenring *et al.*, 1994). In non-polarized cells such as HeLa or CHO cells, Rab11a is associated with perinuclear recycling endosomes. Rab11a colocalizes with transferrin receptor in the recycling endosome (Ullrich *et al.*, 1996; Green *et al.*, 1997). GTP hydrolysis is required for the recycling of these vesicles, while carboxy-terminal prenylation is required for Rab11a association with recycling vesicles (Ren *et al.*, 1998).

Following the identification of the basic characteristics of Rab11a, more detailed work sought to understand more fully the role of this protein in the cell. Early work began in non-polarized cells and began to define sorting compartments. The early endosome initially was characterized as a pre-lysosomal compartment in the receptor-mediated endocytotic pathway (Helenius and Marsh, 1982). Gradually, these compartments became defined by the presence of Rab proteins. Rab5, one of the first Rabs isolated in mammalian cells was associated with the early endosome (Chavrier *et al.*, 1990a). Rab11a was associated with a perinuclear structure termed the recycling endosome that was defined as the last step before delivery to the plasma membrane (Ullrich *et al.*, 1996). The trafficking field quickly developed a canonical pathway marked by specific Rab proteins (). The first defined compartment following endocytosis is the peripheral vesicles known as early endosomes. Rab5 is associated both with the plasma membrane and these early endosomes. Rab4 parses out cargo to different destinations in a sorting endosome (Mohrmann *et al.*, 2002). Cargo destined for degradation is directed towards the Rab7 positive late endosome and subsequently to the

lysosome (Ren *et al.*, 1998). Proteins that are recycling back to the plasma membrane traverse a Rab11 positive recycling endosome (Chen *et al.*, 1998; Ren *et al.*, 1998).

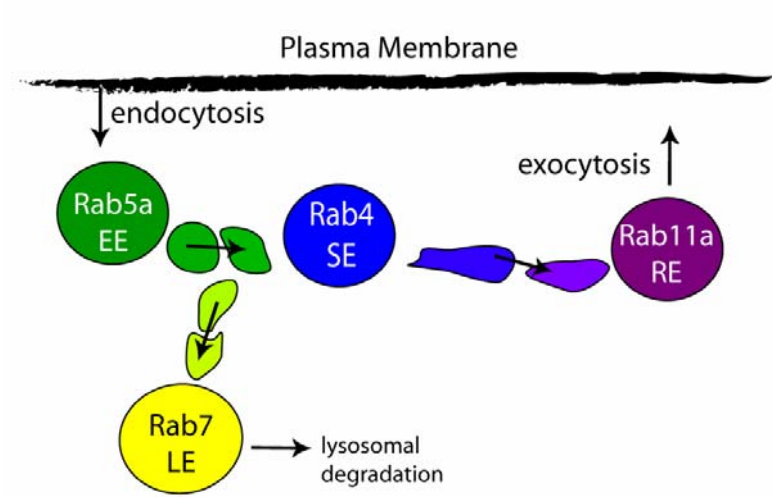

Figure 5: Vesicle Trafficking Pathway in non-polarized cells

Cargo is internalized from the plasma membrane via endocytosis into a Rab5 positive early endosome (EE). It is then either targeted for degradation by trafficking to the Rab7 positive late endosome (LE) followed by the lysosome or is sent to the Rab4 positive sorting endosome (SE). Finally, cargo traffics to the Rab11 recycling endosome (RE) before returning to the membrane and undergoing exocytosis.

Original work in the Rab field hypothesized that each Rab marked a unique membrane population. As mentioned above, a Rab5 positive structure was synonymous with the EEA1 positive early endosome. However, as additional Rab proteins were characterized, it became clear that such a rigid framework was not always accurate. For example, Rab 21 (Simpson *et al.*, 2004) and Rab22 (Magadan *et al.*, 2006) are also on EEA1 positive early endosomes. Therefore, the canonical view of one Rab per vesicle was replaced with a multiple Rabs per vesicle hypothesis. In addition, the concept that a particular lab is present only on a vesicle population is also no longer supported by recent studies. This work suggested that Rabs mark trafficking pathways rather than specific

vesicle populations. For example, a single endosome contained both Rab 5 and Rab4 or Rab4 and Rab11 when followed over time (Sonnichsen *et al.,* 2000). Further studies found that staining for Rab5 decreased as Rab7 increased during vesicle maturation (Rink *et al.,* 2005).

At the same time, numerous physiologic implications for Rab11 were emerging. For example, Rab11 interacts with Presenilin 1 and 2, important proteins in the progression of Alzheimer's disease (Dumanchin *et al.,* 1999). Estrogen signaling via the ER-alpha receptor induces Rab11, and this regulation is hypothesized to initiate a cascade of proteins to enter into the secretory pathway during implantation (Chen *et al.,* 1999). In addition, Rab11 is involved in the trafficking of the H/K ATPase in parietal cells allowing for acid secretion in the stomach (Duman *et al.,* 1999).

Rab11 was emerging as an important regulator in the membrane recycling endosomal pathway. Therefore, two labs began screening for proteins that interact with Rab11a. These labs identified the same protein, Rab11BP/Rabphillin reported in 1999, which was enriched in Rab11a positive endosomes (Mammoto *et al.,* 1999; Zeng *et al.,* 1999). The characterization of this protein determined that it was not a GAP or a GEF for Rab11 (Mammoto *et al.,* 1999) but did interact very specifically with the GTP-bound form of Rab11a. Rab11BP/Rabphillin was primarily cytosolic but required membrane binding to interact with Rab11a (Zeng *et al.,* 1999). Subsequently, Prekeris *et al* found that pp75/rip11 bound to Rab11a-GTP and was involved in the transcytotic pathway. pp75/rip11 had a cytosolic form akin to Rab11BP/Rabphillin, but cytosolic pp75/rip11 was phosphorylated. The group hypothesized that de-phosphorylation was necessary for membrane association and interaction with Rab11a (Prekeris *et al.,* 2000). Our lab

followed with the identification of a Rab11 interaction with the unconventional myosin, myosin Vb. Generally, myosins are known as actin motor proteins. We found that myosin Vb was unexpectedly associated with microtubules since taxol treatment caused mislocalization (Lapierre *et al.*, 2001).

The Cloning of Rab11a interacting proteins: FIPs

Our lab sought to identify additional proteins that interacted with Rab11a employing a yeast two-hybrid library screen. This approach resulted in the characterization of the founding member of the Rab11-Family Interacting Proteins (Rab11-FIPs), Rab11-FIP1. Rab11-FIP1 uses its carboxy-terminus to bind to Rab11a, and thus this area was called the Rab11 Binding Domain (RBD) (Figure 6). Homology searches using the sequence of the RBD identified three other proteins as family members: Rab11-FIP2, eferin (now termed Rab11-FIP3), and pp75 (now termed Rab11-FIP5). All four proteins bind to the three Rab11 Family members, Rab11a, Rab11b, and Rab25.

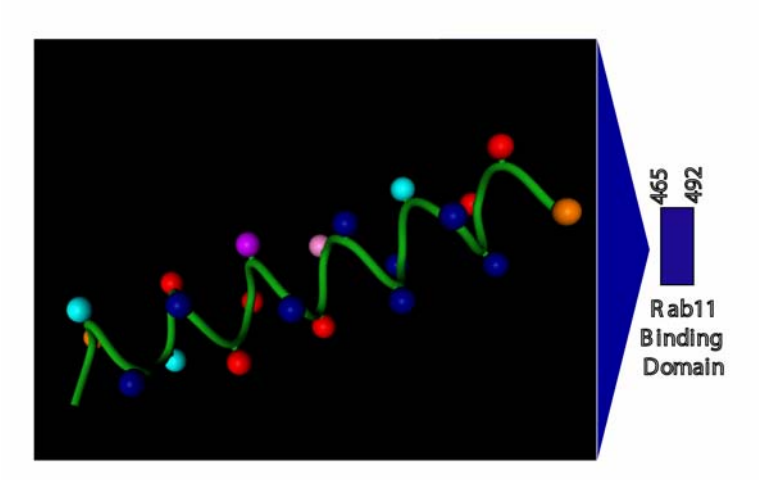

Figure 6: Rab11-FIP2 has a Rab11 binding domain comprised of an amphipathic alpha helix

Each Rab11-FIP has a Rab11 binding domain comprised of an amphipathic alpha helix. This diagram of the Rab11-FIP2 helix is representative of this domain, which occurs between amino acids 465 and 492 in Rab11-FIP2. Image courtesy of Joseph Roland, www.cytogrpahica.com.

However, Rab11-FIP2 had three distinctive characteristics that set it apart from the other family members. First, it was able to bind to both Rab11a-GDP (dominant negative) and Rab11-GTP (dominant active), while the other members only interacted with the GTP bound form. Rab11-FIP2 was also able to interact with the motor protein myosin Vb. Finally, Rab11-FIP2 only partially co-localized in MDCK cells with Rab11a, while Rab11-FIP1 and Rab11-FIP5 seem to entirely co-localize with Rab11a (Hales *et al.*, 2001).

Another lab independently confirmed the interaction of Rab11a with Rab11-FIP3 (Prekeris *et al.*, 2001) and Rab11-FIP5 (Prekeris *et al.*, 2000; Prekeris *et al.*, 2001). Shortly after the report of the cloning of the Rab11-FIPs, an additional lab cloned Rab11-FIP4 (Wallace *et al.*, 2002). Finally, Rab Coupling Protein (RCP) was cloned as a Rab4 interacting protein that colocalized with Rab11a (Lindsay *et al.*, 2002). Recent work has determined that the Rab11-FIP1 gene codes for seven splice variants, one of which is RCP. Therefore, this protein is now characterized as Rab11-FIP1C/RCP while the original FIP1 is now FIP1A (Jin and Goldenring, 2006). Thus, the family now contains six family members in mammalian cells (Figure 7).

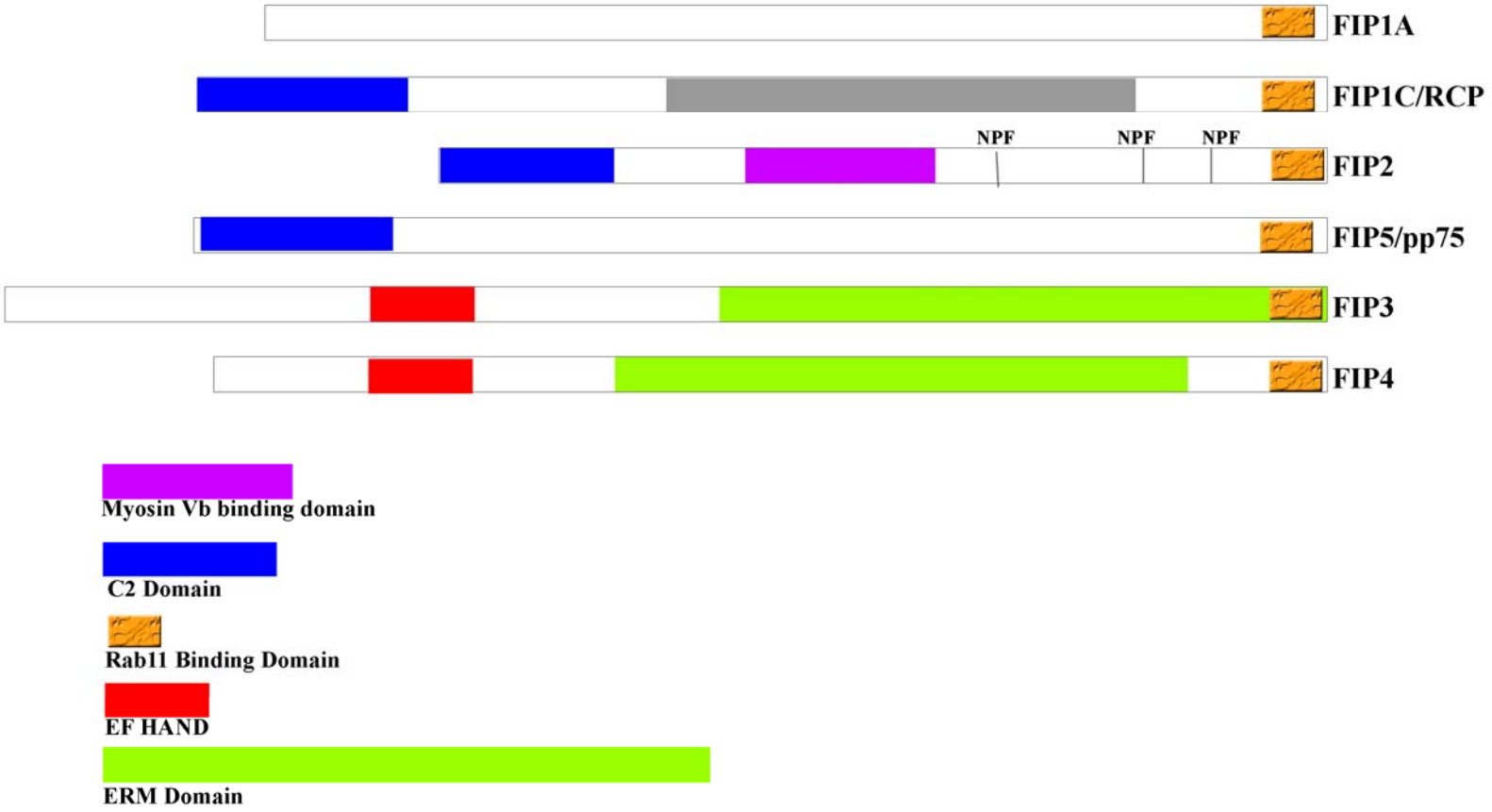

Figure 7: Schematic of Rab11-FIP Proteins

A diagrammatic depiction of the Rab11-FIPs. FIPs are characterized by having a carboxy-terminal Rab11 binding domain (orange). RCP and FIP2 have C2 domains (blue), while FIP3 and FIP4 have EF hand domains (red). FIP2 also has a myosin Vb binding domain (purple) and three NPF motifs.

Rab11-FIP2 Interactions

Rab11-FIP2 binds to other proteins in addition to the Rab11 Family members. Rab11-FIP2 was the only member of the family that was able to bind to the motor protein, myosin Vb (Hales *et al.*, 2001). Therefore, our lab studied this interaction in more detail and found that Rab11-FIP2 interacts with myosin Vb between amino acids 191 and 290 of Rab11-FIP2 (Hales *et al.*, 2002) (Figure 8). The distinction of this domain from the RBD led to the hypothesis that Rab11-FIP2, myosinVb and Rab11a form a ternary complex (Hales *et al.*, 2002).

Another structural feature of Rab11-FIP2 is the presence of three NPF motifs (), which are thought to bind the Eps15 homology domain (EH domains). EH domain proteins contain a pair of EF hand motifs that may or may not bind to calcium. The first Rab11-FIP2 interacting EH domain protein reported was Rep1 (Cullis *et al.*, 2002). This same study reported that Rab11-FIP2 also binds to α-adaptin, a component of the AP-2 complex and suggested that Rab11-FIP2 might be involved in the transition from receptor-mediated endocytosis to the sorting endosomes (Cullis *et al.*, 2002). An additional report suggested that Rab11-FIP2 interacts with EHD1 and EHD3 through its second NPF motif (Naslavsky *et al.*, 2006). However, EHD1-4 have an identity of 70% (Rappoport *et al.*, 2006), and since our lab has not been able to duplicate this interaction, the Rab11-FIP2 interaction may be with EHD2 or EHD4 *in vivo*.

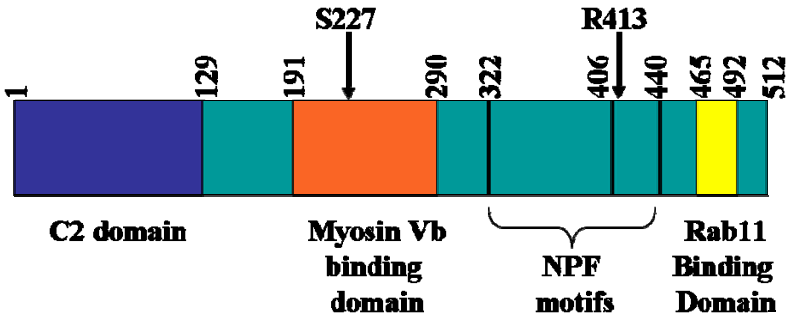

Figure 8: Schematic of Rab11-FIP2 Domains

The amino terminus of Rab11-FIP2 contains a C2 domain from amino acids 1 through 129. Rab11-FIP2 binds to myosin Vb between amino acids 191 and 290. Rab11-FIP2 binds to Rab11a in a carboxy-terminal Rab Binding Domain between residues 465-592. Rab11-FIP2 has three NPF motifs beginning at amino acid 322, 406 and 440. Rab11-FIP2 is phosphorylated on serine 227. Mutation of R413 results in a dominant negative Rab11-FIP2 construct by causing a collapse of the Rab11 positive apical recycling system.

Rab proteins in polarized cells

While the trafficking field was rapidly progressing in non-polarized cells, the pathway in polarized cells was proving to be more complex. In a polarized system, cells have more options for cargo internalization and destination (). The polarized cell includes a more elaborate endosomal structure involving progression through either an apical or basolateral early endosome (EE), sorting or common endosome (CE), and apical recycling endosome (ARE) (Brown *et al.*, 2000) (). Between 1976 and 1978, MDCK cells were established as the model for studying polarity and polarized trafficking (Rodriguez-Boulan *et al.*, 2005).

The apical early endosome (AEE) is a 100-150 nm cup shaped vesicle defined by the presence of Rab5 (Hoekstra *et al.*, 2004). Cargo internalized from the basolateral membrane enters a basolateral early endosome (BEE) also marked by Rab5. Recent work suggests that there are at least two early endosomal populations that are defined based on cargo destination. One population rapidly matures, acquires Rab7 within 30 seconds of

internalization, and is destined for lysosomal degradation. The other endosomal population slowly matures, acquires Rab11 within 100 seconds of internalization, and tubulates during its progression through the recycling pathway (Lakadamyali *et al.*, 2006). In addition, Rab21 moves bidirectionally between the early endosome and the plasma membrane (Pellinen *et al.*, 2006). To add to the complexity, some receptors may utilize different trafficking strategies depending upon the circumstances. For instance, the stimulation of EGFR with a low does of EGF results in EGFR internalized by clathrin-mediated endocytosis and trafficking through the canonical endosomal system. However, if a large amount of EGF is used to stimulate the receptor, it is internalized utilizing raft/caveolin dependent endosome that segregates the receptor for degradation (Polo and Di Fiore, 2006).

Following progression through the early endosome, cargo is delivered to a 60 nm vesicle known as the common endosome (Hoekstra *et al.*, 2004); the analogous compartment in non-polarized cells is the Rab4 positive compartment. However, little work has explored the role of Rab4 in MDCK cells. One report suggests that Rab4 controls the export of transcytotic cargo from the common endosome to the apical membrane (Mohrmann *et al.*, 2002). Additional work suggests that transcytotic cargo enters an ill-defined Rab10 compartment that regulates the exit from the early endosome (Babbey *et al.*, 2006). Rab10 may also be present on the basolateral face of CE (Babbey *et al.*, 2006). In addition, a recent report suggests that Rab11a is localized on vesicles in the basolateral portion of hepatocyotes (Permsin Marbet, 2006), which may actually be the common endosome. However, little work has been done to define this process. Finally, Rab17, a rab specific for epithelial cells (Lutcke *et al.*, 1993), has been

alternatively reported to localize to the CE (Hunziker and Peters, 1998) and the apical recycling endosome (Zacchi *et al.*, 1998). One possibility is that multiple rabs accompany vesicles through the CE, depending upon their origin or destination. However, little work has explored the CE.

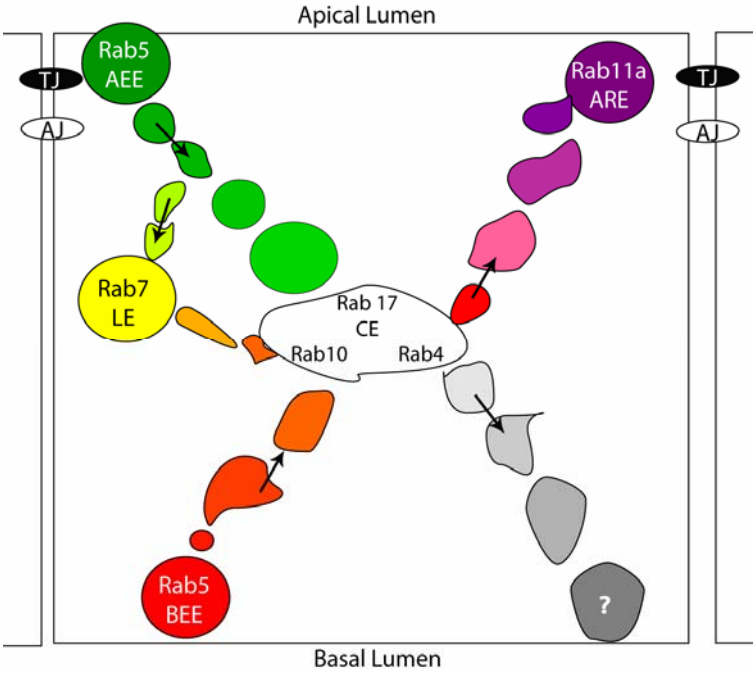

Figure 9: Generalized Model of Trafficking in Polarized Cells

Apical cargo is internalized via a Rab5a positive early endosome (EE). Basolateral cargo is internalized via a Rab5 positive basolateral early endosome (BEE). Both cargos are directed towards a common endosome (CE) or diverted to a Rab7 positive late endosome (LE). If the cargo is destined to the apical plasma membrane, it will be trafficked through a Rab11a positive apical recycling endosome (ARE).Tight junctions (TJ) serve as barriers along the epithelial monolayer while adherens junctions (AJ) serve as a conduit between adjacent cells.

After traversing through the common endosome, apically destined cargo enters the apical recycling endosome (ARE). The ARE consists of a branching tubulovesicular network that begins in the apical region and extends to the cell periphery (Hoekstra *et al.*, 2004). Rab11a containing vesicles localize near the centrosome beneath the apical

membrane in the ARE dependent upon intact microtubules. Destabilization of microtubules with nocodazole causes Rab11a positive vesicles to disperse, while stabilization with taxol causes congregation near tight junctions (Casanova *et al.*, 1999). Rab11 has been seen to remain with the vesicle through fusion with the plasma membrane (Ward *et al.*, 2005) and is suggested to have a role in vesicle fusion or docking since it is often found between two fusing vesicles (Savina *et al.*, 2005).

Endocytic trafficking in polarized cells

In addition to more intricate pathways in polarized cells, recent work suggests that the internalization method of the cargo influences the trafficking pathway followed. There are numerous examples of receptors following the canonical pathway, and yet the details of the internalization process reveal added complexity based on the proteins involved. Cargo internalization occurs via clathrin-coated pits, caveosomes, or clathrin- and caveolae-independent mechanisms (Kirkham and Parton, 2005). Each process has distinct effectors and adaptors (). Of most relevance to this work are proteins specifically related to the recycling endosome.

Transferrin receptor is internalized using a clathrin-coated pit mediated by AP-2. However, while LDL and EGFR also use clathrin-coated pits, they do not use the AP-2 adaptor but instead use Eps 15 and epsin (Perret *et al.*, 2005). The cystic fibrosis transmembrane receptor (CFTR) is internalized via clathrin-coated pits by binding to AP-2 (Gentzsch *et al.*, 2004). Internalized CFTR is recycled back to the plasma membrane along microtubules in a Rab5 and Rab11 dependent manner (Gentzsch *et al.*, 2004). However, integrins utilize the actin cytoskeleton during internalization and an entirely different small GTPase, ARF6 (Powelka *et al.*, 2004). The ARF6 compartment is

internalized in a clathrin-independent manner (Donaldson, 2003) that is also used by LH and beta2-adrenergic receptors. However, recycling cargo from this internalization route also can utilize a Rab11 positive pathway for exit back to the plasma membrane (Powelka *et al.*, 2004). Both Rab11-FIP3 and FIP4 interact with ARF6, creating a potential linking mechanism between this internalization route and the Rab11 recycling endosome (Hickson *et al.*, 2003; Fielding *et al.*, 2005).

Table 1: Proteins and lipids in polarized systems

Proteins associated with the various endocytic processes and compartments in polarized epithelial cells.

Apical Endocytosis	AP-2 (Folsch, 2005) Rab5 family (Bucci *et al.*, 1994)
Basolateral Sorting	AP-1B (Folsch, 2005) AP-4 (Folsch, 2005) Rab8 (Lock and Stow, 2005a) Actin (Rodriguez-Boulan *et al.*, 2004) Rme-1/EHD3 (Babbey *et al.*, 2006)
Endosomal Sorting	AP-1A (Folsch, 2005) AP-3A (Folsch, 2005) AP-4 (Folsch, 2005)
Basolateral to apical transcytosis	Cholesterol (Perret *et al.*, 2005) Sphingolipids (Perret *et al.*, 2005) Caveolin-1 (Rodriguez-Boulan *et al.*, 2004)
Early endosome	PI(3)P (Perret *et al.*, 2005) Rab5 family (Bucci *et al.*, 1994) Rab21 (Simpson *et al.*, 2004) EEA1 (Mu *et al.*, 1995) Rab22 (Magadan *et al.*, 2006)
Recycling endosome	PI(4)P (Perret *et al.*, 2005) Rab11 family (Goldenring *et al.*, 1996) Sec15 (Zhang *et al.*, 2004)
Common Endosome	Rab17 (Hoekstra *et al.*, 2004) Rab4 (Mohrmann *et al.*, 2002)

Even cargo that is internalized together may be destined for separate trafficking pathways. For example, a BEE containing recently internalized transferrin receptor and polymeric IgA receptor (pIgAR) does not deliver its contents to the same compartment. Clathrin-coated vesicles retrieve TfR resulting in a cup-shaped pIgAR-containing vesicle. The pIgAR vesicle uses microtubules to traffic into the sorting endosome (Musch, 2004).

The polarized trafficking field continues to place the components of vesicle machinery on the correct membrane subdomain and/or endosomal structure. The work presented here addressed the hypothesis that Rab11-FIP2 is a critical regulator of plasma membrane recycling. We have uncovered a novel role for Rab11-FIP2 in the re-establishment of polarity regulated in part by phosphorylation by MARK2 (chapter 2). We developed and analyzed a new Rab11-FIP2 mutant, which has differentiable effects on the endosomal structure than previously characterized mutants (chapter 3). Finally, we have identified proteins that interact in complex with Rab11-FIP2 (chapter 4), the results of which will greatly enhance our understanding of the endosomal structure in polarized MDCK cells (chapter 5).

References

Babbey, C.M., Ahktar, N., Wang, E., Chen, C.C., Grant, B.D., and Dunn, K.W. (2006). Rab10 regulates membrane transport through early endosomes of polarized Madin-Darby canine kidney cells. Mol Biol Cell *17*, 3156-3175.

Bhartur, S.G., Calhoun, B.C., Woodrum, J., Kurkjian, J., Iyer, S., Lai, F., and Goldenring, J.R. (2000). Genomic structure of murine Rab11 family members. Biochem Biophys Res Commun *269*, 611-617.

Brown, P.S., Wang, E., Aroeti, B., Chapin, S.J., Mostov, K.E., and Dunn, K.W. (2000). Definition of distinct compartments in polarized Madin-Darby canine kidney (MDCK)

cells for membrane-volume sorting, polarized sorting and apical recycling. Traffic *1*, 124-140.

Bryant, D.M., and Stow, J.L. (2004). The ins and outs of E-cadherin trafficking. Trends Cell Biol *14*, 427-434.

Bucci, C., Wandinger-Ness, A., Lutcke, A., Chiariello, M., Bruni, C.B., and Zerial, M. (1994). Rab5a is a common component of the apical and basolateral endocytic machinery in polarized epithelial cells. Proc Natl Acad Sci U S A *91*, 5061-5065.

Casanova, J.E., Wang, X., Kumar, R., Bhartur, S.G., Navarre, J., Woodrum, J.E., Altschuler, Y., Ray, G.S., and Goldenring, J.R. (1999). Association of Rab25 and Rab11a with the apical recycling system of polarized Madin-Darby canine kidney cells. Mol Biol Cell *10*, 47-61.

Caviston, J.P., and Holzbaur, E.L. (2006). Microtubule motors at the intersection of trafficking and transport. Trends Cell Biol *16*, 530-537.

Chavrier, P., Gorvel, J.-P., Stelzer, E., Simons, K., Gruenberg, J., and Zerial, M. (1991). Hypervariable C-termmal domain of rab proteins acts as a targeting signal *353*, 769-772.

Chavrier, P., Parton, R.G., Hauri, H.P., Simons, K., and Zerial, M. (1990a). Localization of low molecular weight GTP binding proteins to exocytic and endocytic compartments. Cell *62*, 317-329.

Chavrier, P., Vingron, M., Sander, C., Simons, K., and Zerial, M. (1990b). Molecular cloning of YPT1/SEC4-related cDNAs from an epithelial cell line. Mol Cell Biol *10*, 6578-6585.

Chen, D., Ganapathy, P., Zhu, L.J., Xu, X., Li, Q., Bagchi, I.C., and Bagchi, M.K. (1999). Potential regulation of membrane trafficking by estrogen receptor alpha via induction of rab11 in uterine glands during implantation. Mol Endocrinol *13*, 993-1004.

Chen, W., Feng, Y., Chen, D., and Wandinger-Ness, A. (1998). Rab11 is required for trans-golgi network-to-plasma membrane transport and a preferential target for GDP dissociation inhibitor. Mol Biol Cell *9*, 3241-3257.

Cullis, D.N., Philip, B., Baleja, J.D., and Feig, L.A. (2002). Rab11-FIP2, an adaptor protein connecting cellular components involved in internalization and recycling of epidermal growth factor receptors. J Biol Chem *277*, 49158-49166.

Donaldson, J.G. (2003). Multiple Roles for Arf6: Sorting, Structuring, and Signaling at the Plasma Membrane. 10.1074/jbc.R300026200. J. Biol. Chem. *278*, 41573-41576.

Duman, J.G., Tyagarajan, K., Kolsi, M.S., Moore, H.P., and Forte, J.G. (1999). Expression of rab11a N124I in gastric parietal cells inhibits stimulatory recruitment of the H+-K+-ATPase. Am J Physiol *277*, C361-372.

Dumanchin, C., Czech, C., Campion, D., Cuif, M.H., Poyot, T., Martin, C., Charbonnier, F., Goud, B., Pradier, L., and Frebourg, T. (1999). Presenilins interact with Rab11, a small GTPase involved in the regulation of vesicular transport. Hum Mol Genet *8*, 1263-1269.

Fielding, A.B., Schonteich, E., Matheson, J., Wilson, G., Yu, X., Hickson, G.R., Srivastava, S., Baldwin, S.A., Prekeris, R., and Gould, G.W. (2005). Rab11-FIP3 and FIP4 interact with Arf6 and the exocyst to control membrane traffic in cytokinesis. Embo J *24*, 3389-3399.

Folsch, H. (2005). The building blocks for basolateral vesicles in polarized epithelial cells. Trends Cell Biol *15*, 222-228.

Gentzsch, M., Chang, X.-B., Cui, L., Wu, Y., Ozols, V.V., Choudhury, A., Pagano, R.E., and Riordan, J.R. (2004). Endocytic Trafficking Routes of Wild Type and {Delta}F508 Cystic Fibrosis Transmembrane Conductance Regulator. 10.1091/mbc.E04-03-0176. Mol. Biol. Cell *15*, 2684-2696.

Goldenring, J.R., Smith, J., Vaughan, H.D., Cameron, P., Hawkins, W., and Navarre, J. (1996). Rab11 is an apically located small GTP-binding protein in epithelial tissues. Am J Physiol *270*, G515-525.

Goldenring, J.R., Soroka, C.J., Shen, K.R., Tang, L.H., Rodriguez, W., Vaughan, H.D., Stoch, S.A., and Modlin, I.M. (1994). Enrichment of rab11, a small GTP-binding protein, in gastric parietal cells. Am J Physiol *267*, G187-194.

Gomes, A.Q., Ali, B.R., Ramalho, J.S., Godfrey, R.F., Barral, D.C., Hume, A.N., and Seabra, M.C. (2003). Membrane Targeting of Rab GTPases Is Influenced by the Prenylation Motif. Mol. Biol. Cell *14*, 1882-1899.

Green, E.G., Ramm, E., Riley, N.M., Spiro, D.J., Goldenring, J.R., and Wessling-Resnick, M. (1997). Rab11 is associated with transferrin-containing recycling compartments in K562 cells. Biochem Biophys Res Commun *239*, 612-616.

Gumbiner, B.M. (2005). REGULATION OF CADHERIN-MEDIATED ADHESION IN MORPHOGENESIS. Nature Reviews Molecular Cell Biology
Nat Rev Mol Cell Biol *6*, 622-634.

Hales, C.M., Griner, R., Hobdy-Henderson, K.C., Dorn, M.C., Hardy, D., Kumar, R., Navarre, J., Chan, E.K., Lapierre, L.A., and Goldenring, J.R. (2001). Identification and characterization of a family of Rab11-interacting proteins. J Biol Chem *276*, 39067-39075.

Hales, C.M., Vaerman, J.P., and Goldenring, J.R. (2002). Rab11 family interacting protein 2 associates with Myosin Vb and regulates plasma membrane recycling. J Biol Chem *277*, 50415-50421.

Hammer, J.A., 3rd, and Wu, X.S. (2002). Rabs grab motors: defining the connections between Rab GTPases and motor proteins. Curr Opin Cell Biol *14*, 69-75.

Helenius, A., and Marsh, M. (1982). Endocytosis of enveloped animal viruses. Ciba Found Symp, 59-76.

Hickson, G.R., Matheson, J., Riggs, B., Maier, V.H., Fielding, A.B., Prekeris, R., Sullivan, W., Barr, F.A., and Gould, G.W. (2003). Arfophilins are dual Arf/Rab 11 binding proteins that regulate recycling endosome distribution and are related to Drosophila nuclear fallout. Mol Biol Cell *14*, 2908-2920.

Hoekstra, D., Tyteca, D., and van IJzendoorn, S.C.D. (2004). The subapical compartment: a traffic center in membrane polarity development. J Cell Sci *117*, 2183-2192.

Hunziker, W., and Peters, P.J. (1998). Rab17 Localizes to Recycling Endosomes and Regulates Receptor-mediated Transcytosis in Epithelial Cells 10.1074/jbc.273.25.15734. J. Biol. Chem. *273*, 15734-15741.

Ivanov, A., McCall, I., Babbin, B., Samarin, S., Nusrat, A., and Parkos, C. (2006). Microtubules regulate disassembly of epithelial apical junctions. BMC Cell Biology *7*, 12.

Jin, M., and Goldenring, J.R. (2006). The Rab11-FIP1/RCP gene codes for multiple protein transcripts related to the plasma membrane recycling system. Biochim Biophys Acta.

Kahn, R.A., Volpicelli-Daley, L., Bowzard, B., Shrivastava-Ranjan, P., Li, Y., Zhou, C., and Cunningham, L. (2005). Arf family GTPases: roles in membrane traffic and microtubule dynamics. 10.1042/BST20051269. Biochem. Soc. Trans. *33*, 1269-1272.

Khosravi-Far, R., Lutz, R.J., Cox, A.D., Conroy, L., Bourne, J.R., Sinensky, M., Balch, W.E., Buss, J.E., and Der, C.J. (1991). Isoprenoid modification of rab proteins terminating in CC or CXC motifs. Proc Natl Acad Sci U S A *88*, 6264-6268.

Kirkham, M., and Parton, R.G. (2005). Clathrin-independent endocytosis: new insights into caveolae and non-caveolar lipid raft carriers. Biochim Biophys Acta *1746*, 349-363.

Kobayashi, J., Inai, T., and Shibata, Y. (2002). Formation of tight junction strands by expression of claudin-1 mutants in their ZO-1 binding site in MDCK cells. Histochem Cell Biol *117*, 29-39.

Lakadamyali, M., Rust, M.J., and Zhuang, X. (2006). Ligands for clathrin-mediated endocytosis are differentially sorted into distinct populations of early endosomes. Cell *124*, 997-1009.

Lapierre, L.A., Kumar, R., Hales, C.M., Navarre, J., Bhartur, S.G., Burnette, J.O., Provance, D.W., Jr., Mercer, J.A., Bahler, M., and Goldenring, J.R. (2001). Myosin vb is associated with plasma membrane recycling systems. Mol Biol Cell *12*, 1843-1857.

Le, T.L., Yap, A.S., and Stow, J.L. (1999). Recycling of E-Cadherin: A Potential Mechanism for Regulating Cadherin Dynamics. 10.1083/jcb.146.1.219. J. Cell Biol. *146*, 219-232.

Lindsay, A.J., Hendrick, A.G., Cantalupo, G., Senic-Matuglia, F., Goud, B., Bucci, C., and McCaffrey, M.W. (2002). Rab coupling protein (RCP), a novel Rab4 and Rab11 effector protein. J Biol Chem *277*, 12190-12199.

Lock, J.G., and Stow, J.L. (2005a). Rab11 in recycling endosomes regulates the sorting and basolateral transport of E-cadherin. Mol Biol Cell.

Lock, J.G., and Stow, J.L. (2005b). Rab11 in Recycling Endosomes Regulates the Sorting and Basolateral Transport of E-Cadherin 10.1091/mbc.E04-10-0867. Mol. Biol. Cell *16*, 1744-1755.

Lutcke, A., Jansson, S., Parton, R., Chavrier, P., Valencia, A., Huber, L., Lehtonen, E., and Zerial, M. (1993). Rab17, a novel small GTPase, is specific for epithelial cells and is induced during cell polarization. 10.1083/jcb.121.3.553. J. Cell Biol. *121*, 553-564.

Madrid, A.S., and Weis, K. (2006). Nuclear transport is becoming crystal clear. Chromosoma *V115*, 98-109.

Magadan, J.G., Barbieri, M.A., Mesa, R., Stahl, P.D., and Mayorga, L.S. (2006). Rab22a Regulates the Sorting of Transferrin to Recycling Endosomes. Mol. Cell. Biol. *26*, 2595-2614.

Mammoto, A., Ohtsuka, T., Hotta, I., Sasaki, T., and Takai, Y. (1999). Rab11BP/Rabphilin-11, a downstream target of rab11 small G protein implicated in vesicle recycling. J Biol Chem *274*, 25517-25524.

Matter, K., Aijaz, S., Tsapara, A., and Balda, M.S. (2005). Mammalian tight junctions in the regulation of epithelial differentiation and proliferation. Curr Opin Cell Biol *17*, 453-458.

Michel, D., Arsanto, J.-P., Massey-Harroche, D., Beclin, C., Wijnholds, J., and Le Bivic, A. (2005). PATJ connects and stabilizes apical and lateral components of tight junctions in human intestinal cells 10.1242/jcs.02528. J Cell Sci *118*, 4049-4057.

Mohrmann, K., Leijendekker, R., Gerez, L., and van der Sluijs, P. (2002). rab4 Regulates Transport to the Apical Plasma Membrane in Madin-Darby Canine Kidney Cells 10.1074/jbc.M111237200. J. Biol. Chem. *277*, 10474-10481.

Mu, F.-T., Callaghan, J.M., Steele-Mortimer, O., Stenmark, H., Parton, R.G., Campbell, P.L., McCluskey, J., Yeo, J.-P., Tock, E.P.C., and Toh, B.-H. (1995). EEA1, an Early Endosome-Associated Protein. 10.1074/jbc.270.22.13503. J. Biol. Chem. *270*, 13503-13511.

Musch, A. (2004). Microtubule Organization and Function in Epithelial Cells doi:10.1111/j.1600-0854.2003.00149.x. Traffic *5*, 1-9.

Naslavsky, N., Rahajeng, J., Sharma, M., Jovic, M., and Caplan, S. (2006). Interactions between EHD Proteins and Rab11-FIP2: A role for EHD3 in early endosomal transport 10.1091/mbc.E05-05-0466. Mol. Biol. Cell *17*, 163-177.

Nelson, W.J. (2003). Adaptation of core mechanisms to generate cell polarity. Nature *422*, 766-774.

Pellinen, T., Arjonen, A., Vuoriluoto, K., Kallio, K., Fransen, J.A.M., and Ivaska, J. (2006). Small GTPase Rab21 regulates cell adhesion and controls endosomal traffic of {beta}1-integrins. 10.1083/jcb.200509019. J. Cell Biol. *173*, 767-780.

Permsin Marbet, C.R., Bruno Stieger, Lukas Landmann,. (2006). Quantitative microscopy reveals 3D organization and kinetics of endocytosis in rat hepatocytes. Microscopy Research and Technique *69*, 693-707.

Perret, E., Lakkaraju, A., Deborde, S., Schreiner, R., and Rodriguez-Boulan, E. (2005). Evolving endosomes: how many varieties and why? Curr Opin Cell Biol *17*, 423-434.

Pfeffer, S.R. (2001). Rab GTPases: specifying and deciphering organelle identity and function. Trends Cell Biol *11*, 487-491.

Pfeffer, S.R. (2005). Structural Clues to Rab GTPase Functional Diversity 10.1074/jbc.R500003200. J. Biol. Chem. *280*, 15485-15488.

Polo, S., and Di Fiore, P.P. (2006). Endocytosis conducts the cell signaling orchestra. Cell *124*, 897-900.

Powelka, A.M., Sun, J., Li, J., Gao, M., Shaw, L.M., Sonnenberg, A., and Hsu, V.W. (2004). Stimulation-Dependent Recycling of Integrin beta-1 Regulated by ARF6 and Rab11. doi:10.1111/j.1600-0854.2004.00150.x. Traffic *5*, 20-36.

Prekeris, R., Davies, J.M., and Scheller, R.H. (2001). Identification of a novel Rab11/25 binding domain present in Eferin and Rip proteins. J Biol Chem *276*, 38966-38970.

Prekeris, R., Klumperman, J., and Scheller, R.H. (2000). A Rab11/Rip11 protein complex regulates apical membrane trafficking via recycling endosomes. Mol Cell *6*, 1437-1448.

Rappoport, J.Z., Kemal, S., Benmerah, A., and Simon, S.M. (2006). Dynamics of clathrin and adaptor proteins during endocytosis 10.1152/ajpcell.00160.2006. Am J Physiol Cell Physiol *291*, C1072-1081.

Ren, M., Xu, G., Zeng, J., De Lemos-Chiarandini, C., Adesnik, M., and Sabatini, D.D. (1998). Hydrolysis of GTP on rab11 is required for the direct delivery of transferrin from the pericentriolar recycling compartment to the cell surface but not from sorting endosomes. Proc Natl Acad Sci U S A *95*, 6187-6192.

Rink, J., Ghigo, E., Kalaidzidis, Y., and Zerial, M. (2005). Rab conversion as a mechanism of progression from early to late endosomes. Cell *122*, 735-749.

Rodriguez-Boulan, E., Kreitzer, G., and Musch, A. (2005). ORGANIZATION OF VESICULAR TRAFFICKING IN EPITHELIA. Nature Reviews Molecular Cell Biology Nat Rev Mol Cell Biol *6*, 233-247.

Rodriguez-Boulan, E., Musch, A., and Le Bivic, A. (2004). Epithelial trafficking: new routes to familiar places. Current Opinion in Cell Biology *16*, 436-442.

Rybin, V., Ullrich, O., Rubino, M., Alexandrov, K., Simon, I., Seabra, M.C., Goody, R., and Zerial, M. (1996). GTPase activity of Rab5 acts as a timer for endocytic membrane fusion *383*, 266-269.

Savina, A., Fader, C.M., Damiani, M.T., and Colombo, M.I. (2005). Rab11 Promotes Docking and Fusion of Multivesicular Bodies in a Calcium-Dependent Manner doi:10.1111/j.1600-0854.2004.00257.x. Traffic *6*, 131-143.

Schimmoller, F., Simon, I., and Pfeffer, S.R. (1998). Rab GTPases, Directors of Vesicle Docking. 10.1074/jbc.273.35.22161. J. Biol. Chem. *273*, 22161-22164.

Seabra, M.C., and Coudrier, E. (2004). Rab GTPases and myosin motors in organelle motility. Traffic *5*, 393-399.

Seabra, M.C., and Wasmeier, C. (2004). Controlling the location and activation of Rab GTPases. Current Opinion in Cell Biology *16*, 451-457.

Segev, N. (2001). Ypt/Rab GTPases: Regulators of Protein Trafficking 10.1126/stke.2001.100.re11. Sci. STKE *2001*, re11-.

Shin, K., Straight, S., and Margolis, B. (2005). PATJ regulates tight junction formation and polarity in mammalian epithelial cells. 10.1083/jcb.200408064. J. Cell Biol. *168*, 705-711.

Simpson, J.C., Griffiths, G., Wessling-Resnick, M., Fransen, J.A.M., Bennett, H., and Jones, A.T. (2004). A role for the small GTPase Rab21 in the early endocytic pathway 10.1242/jcs.01560. J Cell Sci *117*, 6297-6311.

Sonnichsen, B., De Renzis, S., Nielsen, E., Rietdorf, J., and Zerial, M. (2000). Distinct membrane domains on endosomes in the recycling pathway visualized by multicolor imaging of Rab4, Rab5, and Rab11. J Cell Biol *149*, 901-914.

Stenmark, H., and Olkkonen, V.M. (2001). The Rab GTPase family. Genome Biol *2*, REVIEWS3007.

Stevenson, B.R., and Keon, B.H. (1998). THE TIGHT JUNCTION: Morphology to Molecules. doi:10.1146/annurev.cellbio.14.1.89. Annual Review of Cell and Developmental Biology *14*, 89-109.

Takei, K., and Haucke, V. (2001). Clathrin-mediated endocytosis: membrane factors pull the trigger. Trends Cell Biol *11*, 385-391.

Touchot, N., Chardin, P., and Tavitian, A. (1987). Four additional members of the ras gene superfamily isolated by an oligonucleotide strategy: molecular cloning of YPT-related cDNAs from a rat brain library. Proc Natl Acad Sci U S A *84*, 8210-8214.

Tunggal, J.A., Helfrich, I., Schmitz, A., Schwarz, H., Gunzel, D., Fromm, M., Kemler, R., Krieg, T., and Niessen, C.M. (2005). E-cadherin is essential for in vivo epidermal barrier function by regulating tight junctions. Embo J *24*, 1146-1156.

Ullrich, O., Reinsch, S., Urbe, S., Zerial, M., and Parton, R.G. (1996). Rab11 regulates recycling through the pericentriolar recycling endosome. J Cell Biol *135*, 913-924.

Wallace, D.M., Lindsay, A.J., Hendrick, A.G., and McCaffrey, M.W. (2002). Rab11-FIP4 interacts with Rab11 in a GTP-dependent manner and its overexpression condenses the Rab11 positive compartment in HeLa cells. Biochem Biophys Res Commun *299*, 770-779.

Ward, E.S., Martinez, C., Vaccaro, C., Zhou, J., Tang, Q., and Ober, R.J. (2005). From Sorting Endosomes to Exocytosis: Association of Rab4 and Rab11 GTPases with the Fc Receptor, FcRn, during Recycling
10.1091/mbc.E04-08-0735. Mol. Biol. Cell *16*, 2028-2038.

Wennerberg, K., and Der, C.J. (2004). Rho-family GTPases: it's not only Rac and Rho (and I like it). 10.1242/jcs.01118. J Cell Sci *117*, 1301-1312.

Woodman, P. (1998). Vesicle transport : More work for the Rabs? Current Biology *8*, R199-R201.

Zacchi, P., Stenmark, H., Parton, R.G., Orioli, D., Lim, F., Giner, A., Mellman, I., Zerial, M., and Murphy, C. (1998). Rab17 Regulates Membrane Trafficking through Apical Recycling Endosomes in Polarized Epithelial Cells. 10.1083/jcb.140.5.1039. J. Cell Biol. *140*, 1039-1053.

Zeng, J., Ren, M., Gravotta, D., De Lemos-Chiarandini, C., Lui, M., Erdjument-Bromage, H., Tempst, P., Xu, G., Shen, T.H., Morimoto, T., Adesnik, M., and Sabatini, D.D. (1999). Identification of a putative effector protein for rab11 that participates in transferrin recycling. Proc Natl Acad Sci U S A *96*, 2840-2845.

Zhang, X.-M., Ellis, S., Sriratana, A., Mitchell, C.A., and Rowe, T. (2004). Sec15 Is an Effector for the Rab11 GTPase in Mammalian Cells 10.1074/jbc.M402264200. J. Biol. Chem. *279*, 43027-43034.

CHAPTER II

MARK2 PHOSPHORYLATION OF RAB11-FIP2 IS NECESSARY FOR THE TIMELY ESTABLISHMENT OF POLARITY IN MDCK CELLS

Nicole A. Ducharme, Chadwick M. Hales,[*] Lynne A. Lapierre, Amy-Joan L. Ham, [†]

Asli Oztan, [‡] Gerard Apodaca,[‡] and James R. Goldenring

From the Departments of Surgery and Cell & Developmental Biology, [†]Department of Biochemistry and Mass Spectrometry Research Center, Vanderbilt University School of Medicine, Vanderbilt-Ingram Cancer Center and the Nashville VA Medical Center, Nashville, TN 37232. *Institute of Molecular Medicine, Medical College of Georgia, Augusta, GA 30912. [‡]Cell Biology & Physiology, University of Pittsburgh School of Medicine, Pittsburgh, PA 15261.

Running Title: MARK2 Phosphorylation of Rab11-FIP2

Published in Molecular Biology of the Cell.

Abstract

Rab11a, myosin Vb and the Rab11-Family of Interacting Protein 2 (FIP2) regulate plasma membrane recycling in epithelial cells. This study sought to characterize more fully Rab11-FIP2 function by identifying kinase activities modifying Rab11-FIP2. We have found that gastric microsomal membrane extracts phosphorylate Rab11-FIP2 on serine 227. We identified the kinase that phosphorylated Rab11-FIP2 as MARK2/EMK1/Par-1Bα (MARK2), and recombinant MARK2 phosphorylated Rab11-FIP2 only on serine 227. We created stable MDCK cell lines expressing EGFP-Rab11-FIP2 wild type or a non-phosphorylatable mutant (Rab11-FIP2(S227A)). Analysis of these cell lines demonstrates a new role for Rab11-FIP2 in addition to that in the plasma membrane recycling system. In calcium switch assays, cells expressing Rab11-FIP2(S227A) showed a defect in the timely reestablishment of p120-containing junctional complexes. However, Rab11-FIP2(S227A) did not affect localization with recycling system components or the normal function of apical recycling and transcytosis pathways. These results indicate that phosphorylation of Rab11-FIP2 on serine 227 by MARK2 regulates an alternative pathway modulating the establishment of epithelial polarity.

Introduction

The establishment of polarity is an intricately regulated process in epithelial cells. The apical and basolateral domains must remain separated by the tight junctions to segregate membrane proteins. For example, while the apical domain of MDCK cells

contains GP-135 (Ojakian and Schwimmer, 1988), the basolateral domain expresses Na/K-ATPase (Louvard, 1980). The tight junction serves as a physical barrier between the two protein pools and is characterized by the expression of ZO-1, claudins and occludin in an epithelial monolayer. An adherens junction facilitates cell-cell contact which is regulated in part by E-cadherin and p120 (reviewed in (Miyoshi and Takai, 2005)). Each of these proteins must be trafficked to the correct domain of the cell for the epithelial monolayer to function appropriately. These diverse destinations require intricate trafficking pathways to ensure their accuracy. Recently, Rab11a has been implicated in the trafficking of E-cadherin to the adherens junction (Lock and Stow, 2005a), suggesting that the Rab11a pathway may be important in the establishment of polarized domains.

Rab11a, a member of the Rab11 sub-family of small GTPases, is well-established as a participant in the regulation of recycling endosomal trafficking. Rab11a is associated with vesicles in the apical portion of epithelial cells near the centrosome and beneath the apical plasma membrane (Casanova et al., 1999). Plasma membrane recycling is critical in maintaining proper membrane protein expression in response to stimuli for such diverse events as nutrient internalization and the recycling of ion channels and receptors (Takei and Haucke, 2001; Volpicelli *et al.*, 2002; Fan *et al.*, 2003; Fan *et al.*, 2004). However, recent work has begun to connect the recycling system to the trafficking pathways of junctional proteins (Le *et al.*, 1999a; Lock and Stow, 2005a).

The family of small GTPases, including Rab11a, interacts with and is regulated by specific interacting proteins. Numerous binding partners have been elucidated for Rab11a including: 1) myosin Vb (Lapierre et al., 2001), 2) rabphillin11/Rab11-binding

protein (Mammoto et al., 1999; Zeng et al., 1999), and 3) a family of Rab11-interacting proteins (FIPs): Rab11-FIP1, Rab11-FIP2, Rab11-FIP3 (Hales et al., 2001), Rab11-FIP4 (Wallace et al., 2002), Rab11-FIP5 (pp75/Rip11) (Prekeris et al., 2000), and RCP (Lindsay et al., 2002). The Rab11-FIP proteins each interact with Rab11 family members (Rab11a, Rab11b and Rab25) at their carboxyl-termini through predicted coiled-coil regions containing an amphipathic alpha helical Rab binding domain (Hales et al., 2001; Prekeris et al., 2001). The diversity of multiple Rab11-FIP proteins, all of which bind to Rab11 with similar helices, suggests that each Rab11-FIP may be important in a spatially restricted manner or in separate trafficking processes.

In particular, Rab11-FIP2 appears to form a ternary complex with both Rab11a and myosin Vb (Hales et al., 2002). A truncation of Rab11-FIP2 lacking its amino terminal C2 domain (Rab11-FIP2(129-512)) strongly inhibits plasma membrane recycling (Hales et al., 2002). Nevertheless, studies in non-polarized cells have also implicated Rab11-FIP2 in the regulation of endocytosis through interaction with the early endosomal protein Reps1 (Cullis et al., 2002).

In this study, we describe the involvement of Rab11-FIP2 in the establishment of polarity. We have biochemically purified a kinase activity, which phosphorylated Rab11-FIP2 on serine 227 and was identified by mass spectrometry as MARK2/EMK1/Par-1Bα (MARK2). Previous studies have associated MARK2 with changes in aspects of polarity (Cohen et al., 2004). Disruption of the junctional integrity with low calcium followed by reestablishment of normal extracellular calcium (calcium switch) showed that phosphorylation of Rab11-FIP2 is important for the timely re-establishment of polarity.

The results indicate that phosphorylation of Rab11-FIP2 by MARK2 serves as an important regulatory mechanism for the establishment of epithelial cell polarity.

Materials and Methods

Materials: Rabbit anti-Rab11a (VU57) antibodies were developed against the amino terminus of human Rab11a and were specific for Rab11a versus Rab11b and Rab25 (Lapierre, manuscript in preparation). The other antibodies used were rat anti-ZO-1 (Chemicon), mouse anti-ZO-1 (Zymed), mouse pan anti-cadherin (Sigma), mouse anti-p120 catenin (BD), mouse monoclonal anti-ezrin (4A5, Chemicon), rabbit anti-occludin (8 ug/ml, Zymed), anti-GFP mouse monoclonal (8362-1, BD), and anti-GFP rabbit (AB290, AbCam). All secondary antibodies were from Jackson Immuno Research. Dr. Roy Zent of Vanderbilt University kindly provided mouse monoclonal anti-GP135.

Database searches and alignment: Rab11-FIP2 homologs were identified through GenBank searches using the Rab11 binding domain. FlyBase, JGI Xenopus, UCSC Genscan were also used to identify homologs. Alignments were performed using ClustalW.

Site directed mutagenesis: All site-directed mutagenesis of Rab11-FIP2 was performed using Pfu Turbo polymerase according to the QuikChange Site-Directed Mutagenesis Kit from Stratagene (La Jolla, CA) with a 16 minute extension time. Primers were synthesized (Invitrogen) with one nucleotide change per oligonucleotide sequence. The TCA encoding for amino acid 227 was changed to GCA for the S227A mutant. All

constructs were created in pEGFP-C2 (Clontech) and subsequently recloned into pET-30a (Novagen) with EcoRI and SalI restriction sites.

Protein Production: For recombinant protein production constructs in pET-30a vectors were retransformed into BL21(DE3)pLysS bacteria. Bacteria were grown to log phase and then induced with IPTG (400 ng/ml) for 3 hours at 37°C. To harvest protein, bacteria were pelleted at 2,000 g and then resuspended in lysis buffer (50 mM sodium phosphate buffer, pH 8.0, 300 mM NaCl with protease inhibitors (protein buffer) and 10 mM imidazole). Protein was harvested according to the manufacturer's protocol (Novagen). Briefly, the bacteria were then sonicated 4 times for 20 seconds at maximum potency on ice. The lysate was extracted with 0.1% Triton X-100 for 5 minutes on ice. The extracted lysate was cleared by centrifugation at 15,000 g, and the resulting supernate was incubated with nickel-affinity resin at 4°C (His-Bind, Novagen). The beads and protein were washed in protein buffer with 20 mM imidazole. The bound protein was eluted overnight at 4°C with elution buffer (protein buffer with 250 mM imidazole). Recombinat MARK2 was purchased from Upstate (14-544).

Rabbit Gastric Tubulovesicle Preparation: Fractions of rabbit gastric mucosal microsomes were prepared as previously described from the fundic mucosa of New Zealand White rabbits (Basson et al., 1991). The rabbit gastric mucosa tissue was homogenized in five volumes of 15 mM HEPES, 300 mM sucrose buffer, pH 7.4 with protease inhibitors (Sigma) with a Potter homogenizer at 1000 rpm. The homogenate was sequentially centrifuged at 500g for 10 min, 5000g for 10 min, 17,000g for 20 min, and 100,000g for 60 min, and the 100,000 g pellet was resuspended in the homogenization buffer and frozen at -80°C until use.

Kinase Identification: The 100,000g microsomal pellet from rabbit gastric mucosa was thawed on ice and then extracted for 30 minutes with 1% Triton-X 100. The solubilized microsomes were centrifuged at 100,000 g for 1 hour at 4°C. The supernatant from this spin was diluted 1:10 with Buffer A (5mM sodium phosphate, pH 7.2, 0.1% Triton-X100) for protein purification. The diluted homogenate was loaded on a HiTrap Q FF column, (2 ml, Amersham) pre-equilibrated in Buffer A at 1 ml/min. The Rab11-FIP2 kinase activity which voided the column was collected and then further purified over a ceramic hydroxylapatite column (Econo-Pac CHT-I 1 ml cartridge, BioRad) preequilibrated in Buffer A. The void fraction was collected and the bound protein was eluted in a gradient from 0 to 500 mM sodium phosphate, pH 7.2, 0.1% Triton-X100. The Rab11-FIP2 kinase activity eluted at approximately 250 mM sodium phosphate. The fractions with the highest activity were pooled, diluted 1:1 in Buffer A, and chromatographed over MONO-S resin (5 ml) (Pharmacia-Biotech). The bound protein was eluted with a continuous salt gradient from 0 to 1M NaCl in Buffer A. The Rab11-FIP2 kinase activity eluted at 400 mM NaCl. The fractions with the highest activity were pooled and further purified over a Cibachrome-Blue affinity column (HiTrap Blue, 1ml, Amersham). The proteins were eluted with a continuous gradient to 2 M NaCl in Buffer A. Kinase activity eluted at approximately 500 mM NaCl. Finally, the fractions with the highest activity were loaded onto a 10% to 40% glycerol gradient and centrifuged for 24 hours at 160,000g. The Rab11-FIP2 kinase activity peaked at approximately 17% glycerol. Each step was monitored by the *in vitro* kinase activity assay.

The fraction from the glycerol gradient that contained the greatest amount of kinase activity was subjected to trypsin digestion and the resulting peptides were

analyzed by LC-MS/MS for protein identification. Prior to trypsin digestion, the samples were cleaned up using a 10 KD Ultrafree MC regenerated cellulose filter (Millipore) and the proteins were subsequently digested directly off of the filter as previously described (Manza, 2005).

LC-MS analysis of the resulting peptides was performed using a ThermoFinnigan LTQ ion trap mass spectrometer equipped with a Thermo MicroAS autosampler and Thermo Surveyor HPLC pump, Nanospray source, and Xcalibur 1.4 instrument control. The peptides were separated on a packed capillary tip, 100 μm x 11 cm, with C_{18} resin (Monitor C_{18}, 5 micron, 100 angstrom, Column Engineering, Ontario CA) using an inline solid phase extraction column that was 100μm x 6cm packed with the same C18 resin (using a frit generated with liquid silicate Kasil 1 (Cortes et al., 1987)) similar to that previously described (Licklider et al., 2002), except the flow from the HPLC pump was split prior to the injection valve. The flow rate during the solid phase extraction phase of the gradient was 1 μL/min and during the separation phase was 700 nL/min. Mobile phase A was 0.1% formic acid, mobile phase B was acetonitrile with 0.1% formic acid. A 95 min gradient was performed with a 15 min washing period (100 % A for the first 10 min followed by a gradient to 98% A at 15 min) to allow for solid phase extraction and removal of any residual salts. After the initial washing period, a 60 minute gradient was performed where the first 35 min was a slow, linear gradient from 98% A to 75 % A, followed by a faster gradient to 10 % A at 65 min and an isocratic phase at 10 % A to 75 min. The MS/MS spectra of the peptides was performed using data-dependent scanning in which one full MS spectra, using a full mass range of 400-2000 amu, was followed by 3 MS/MS spectra. Proteins were identified using the SEQUEST algorithm (Yates et al.,

1995) and the SEQUEST Browser software in the Bioworks 3.1 software package (Thermo Electron, San Jose, CA), using the non-redundant database from NCBI.

For phosphorylation mapping experiments, the Rab11-FIP2 band was excised from a one-dimensional-SDS-PAGE gel and either trypsin or chymotrysin digestion was performed in-gel. The samples were then analyzed using data-dependent analysis similar to that described above with the addition of a neutral loss scan to scan for neutral loss of phosphoric acid (loss of 98) in the top three ions. If a neutral loss ion was found, it was fragmented and an MS/MS/MS spectrum was collected. In addition to using the SEQUEST algorithm to search for phosphorylations on serines, threonines or tyrosines, the data were searched for modifications using the PMOD algorithm (Hansen et al., 2005).

In vitro kinase activity assay during purification: The chromatographic fractions were added to the substrate (Rab11-FIP2(190-383)) in a 50 mM Tris buffer containing 5 mM $MgCl_2$, EGTA (1mM), protease inhibitors (1:100) and 25 μM dithiothreitol on ice. [^{32}P]-γ-ATP was added and the reaction was incubated at 35° C for 10 minutes. The reactions were terminated with the addition of SDS buffer (final concentrations, 300 mM Tris, pH 7.5, 1% SDS, 20 mM EDTA, 17.5 mM sucrose) and incubated at 70° C for 10 minutes. The samples were resolved on 12% SDS-PAGE gels, stained with colloidal Coomassie (GelCode Blue, Pierce, Rockford IL) for protein detection, dried under vacuum and analyzed with Phosphorimaging (Molecular Dynamics) for [^{32}P]-phosphate incorporation.

In situ phosphorylation: We utilized [^{32}P]-orthophosphate incorporation to assess phosphorylation *in situ.* MDCK cells were plated on 60 mm Transwell filters (Corning)

and allowed to polarize at confluence for 3 days. MDCK cells stably expressing EGFP-Rab11-FIP2 or EGFP-Rab11-FIP2(S227A) constructs were incubated with [^{32}P]-orthophosphate in phosphate-free DMEM supplemented with 2 mg/ml bovine serum albumin for 2 hours. The cells were solubilized in lysis buffer (30mm Tris, pH 8.5, 150 mM NaCl, 20 mM magnesium acetate, 1% CHAPS with protease inhibitors and phosphatase inhibitors), extracted on ice for 20 minutes, and centrifuged for 20 min at 15,000g to pellet the insoluble material.

For immunoprecipitation, anti-rabbit IgG Dynabeads (Dynal) were loaded with either 5 μl of anti-GFP antibody AB290 serum (AbCam) or control rabbit serum for two hours at 4°C. Beads were washed 3 times with TBS. Lysate was diluted in immunoprecipitation buffer (final concentration 30 mM Tris pH 7.5, 150 mM NaCl, 20 mM magnesium acetate, protease inhibitors and phosphatase inhibitors) and incubated with the beads overnight at 4°C. The beads were washed twice for 20 minutes with immunoprecipitation buffer with 0.1% CHAPS and then once with 30 mM Tris, pH 7.5. The beads were eluted in 1% SDS buffer and proteins were resolved on 10% SDS-PAGE gels which were either dried and visualized by a phosphoryimaging screen (Molecular Dynamics) for [^{32}P]-phosphoproteins or transferred to nitrocellulose for anti-GFP immunoblotting.

Immunoblotting: Protein samples were resolved on 10% SDS–polyacrylamide gels following a standard Laemmli protocol (Laemmli, 1970). All incubations were performed at room temperature. Proteins were transferred to nitrocellulose. Blots were blocked for 1 h with 5% DMP/TBS-T (5% dry milk powder, Tris-buffered saline, 0.05% Tween-20). The blots were incubated with primary antibody diluted in 2.5% DMP/TBS-T for 1.5 h

(mouse monoclonal anti-GFP 1:2000, washed three times for 10 min in TBS-T, and incubated for 1 h with horseradish perioxidase-labeled anti-mouse secondary (Jackson Immunological) diluted in 1% DMP/TBS-T. The blots were then washed three times with TBS-T followed by one time with TBS and specific labeling was detected by enhanced chemiluminescence (Supersignal, Pierce) with autoradiography using Kodak BioMax ML film.

Cell Culture: Parental T23 MDCKs (Barth *et al.*, 1997) as well as the stably transfected cell lines were grown in D-MEM supplemented with 10% fetal bovine serum (Gibco), penicillin-streptomycin, 2mM L-glutamine, and 0.1 mM MEM non-essential amino acids (Gibco/BRL). Media for cell lines also contained 0.5mg/ml G418 sulfate (Cellgro), and 0.25ng/ml hygromycin (Invitrogen). In the stable cell lines, expression of the EGFP chimeras was inhibited with doxycycline (20ng /ml) (Calbiochem). To examine EGFP protein expression, cells were grown on 0.4 μm Transwell filters (Costar) without doxycycline in tetracycline screened fetal bovine serum (HyClone) media for 2-4 days.

GFP constructs and transfections: Doxycycline-inhibitable expression vectors were generated by excising the EGFP-Rab11-FIP2 wild type and mutant sequences from pEGFP-vectors with NheI and SmaI and ligating into a pTRE2hyg vector (Clontech) cut with NheI and EcoRV. Transfection was performed using Effectene (Qiagen) following the manufactures protocol. One μg of vector was transfected into a 60 mm plate of T23 MDCK cells in normal media. The following day, the cells were trypsinized and replated in serial dilutions including 0.25 ng/ml hygromycin for selection and 20ng/ml doxycycline for suppression of EGFP expression. Multiple colonies were selected, expanded for 10 days, and then screened for EGFP expression in media with tetracycline

screened serum. Multiple clones were initially characterized, all of which showed the same expression pattern and level of the EGFP construct. One clone was selected for each construct to use as the tetracycline-repressible stable cell lines (expressing EGFP-Rab11-FIP2 wild type or EGFP-Rab11-FIP2(S227A)).

Polymeric Immunoglobin A (pIgA) Trafficking in MDCK Cells Labeling of pIgA and trafficking experiments were done as previously described (Hales *et al.*, 2002) except that we used the cell culture media described above. Cells were loaded from the apical side and fixed at time 0 following a 30 minute loading.

Analysis of [^{125}I]IgA Postendocytotic Fate: [^{125}I]IgA was iodinated using the ICl method to a specific activity of 1.0-2.0 x 107 cpm/µg (Breitfeld et al., 1989). The postendocytotic fate of a preinternalized cohort of [^{125}I]IgA (at 5-10 µg/ml) was analyzed as described previously (Apodaca et al., 1994). In brief, filter-grown MDCK cells expressing the various FIP2 constructs and wild-type pIgR were cultured in the presence or absence of doxycycline, and [^{125}I]IgA internalized from the basolateral cell surface of the cells for 10 min at 37˚ C. The basal surface of the cells were rapidly washed three-times, the apical and basolateral medium aspirated, and replaced with fresh medium. The cells were then incubated for 3 min at 37˚ C. This wash procedure takes 5 min at 37˚ C. Fresh medium was added to the cells and they were chased for up to 2 h at 37˚ C. At the designated time points, the apical and basolateral media (0.5 ml) were collected and replaced with fresh media. After the final time point, filters were cut out of the insert and the amount of [^{125}I]IgA quantified with a gamma counter. The media samples were precipitated with 10% trichloroacetic acid (TCA) for 30 min on ice, and then centrifuged in a microfuge

for 15 min at 4˚ C. The amount of [^{125}I]IgA in the TCA-soluble (degraded) and insoluble fractions (intact) was quantified with a gamma counter.

Calcium Switch: Cells were grown to confluencey on filters in regular media with or without doxycycline. Cells were washed with low calcium media (MEM, Cellgro 15-015-CV, 10% dialyzed FBS, penicillin-streptomycin, 2mM L-glutamine, and 0.1 mM MEM non-essential amino acids (Gibco/BRL)). The cells were incubated in low calcium media overnight with or without doxycycline. Calcium was added to the top and bottom of the filter to a final concentration of 1.8 mM. The cells were collected at the indicated timepoints.

Laminin Replating Assay: Cells were trypsinized and replated on 24-well plate 0.45 micron laminin coated filters (BD Biosciences). The cells were collected at the indicated timepoints.

Immunofluorescence for calcium switch and replating experiments: Cells were washed one time with PBS and then pre-extracted on ice in 0.2% Triton X-100 in PBS. Cells were fixed for 30 minutes in 3% paraformaldehyde at room temperature. Cells were permeabilized with 0.05% Trition X-100 in PBS for 5 minutes on ice. Cells were incubated with anti-p120 and ZO-1 antibodies in PBS for one hour on ice. Cells were washed one time with PBS. Cells were incubated with species-specific cy3-anti mouse IgG and cy5-anti-rat IgG in PBS for 30 minutes at room temperature. Cells were washed first with PBS and then with 50mM sodium phosphate. Finally cells were stained with DAPI in sodium phosphate. Filters were cut out of the transwells and mounted with Prolong Anitfade solution (Molecular Probes). Cells were imaged on a Zess LSM510 confocal microscope using a 100X lens. Z-sections were 0.3 microns.

Additional Immunofluorescence: Cells were washed three times with PBS and then fixed in 4% paraformaldehyde for 15 minutes at room temperature. The cells were washed twice with PBS and stored at 4° in PBS until staining. Cells were blocked with extraction buffer (10% normal donkey serum, 150 mM NaCl, 20 mM sodium phosphate, pH 7.4, 0.3% TritonX-10) for twenty minutes. Primary antibody was immediately added in antibody buffer (10% normal donkey serum, 150 mM NaCl, 20 mM sodium phosphate, pH 7.4, 0.05% Tween-20) for 2 hours. The cells were washed with PBS three times. Secondary species-specific Cy dye-labeled anti-IgGs were added for 1 hour in antibody buffer. After washing with PBS two times, the cells were washed with 50 mM sodium phosphate once and then stained with DAPI in sodium phosphate. Filters were cut out of the transwells and mounted with Prolong Antifade solution (Molecular Probes). Cells were imaged on a Zeiss LSM510 confocal microscope using a 100X lens. Z-sections were 0.5 microns.

Results

Phosphorylation of Rab11-FIP2

While previous investigations have noted potential phosphorylation sites on Rab11-FIP2, no discrete kinase activities phosphorylating the protein have been identified. We sought to identify potential phosphorylating activities for Rab11-FIP2 by assaying phosphorylation of recombinant Rab11-FIP2 *in vitro* using extracts from rabbit 100,000g gastric microsomes that are enriched in parietal cell tubulovesicles (H/K-ATPase containing apical recycling membranes).

Extracts of rabbit gastric microsomes solubilized in 1% Triton X-100 strongly phosphorylated recombinant Rab11-FIP2 (Figure 10A). Phosphoamino acid analysis indicated that Rab11-FIP2 was primarily phosphorylated on serine residues (Figure 10B). Two-dimensional tryptic phosphopeptide mapping revealed that Rab11-FIP2 was phosphorylated on a major site (80%) and a minor site (20%) (data not shown). Carboxyl and amino terminal recombinant truncations narrowed the region of phosphorylation to amino acids 187-356. A further truncation to amino acids 227-356 was not phosphorylated. We therefore performed site directed mutagenesis on high probability serine residues between 187 and 230. Mutation of serine 227 to alanine led to a greater than 80% reduction in the *in vitro* phosphorylation by gastric microsomal extracts (Figure 10A). Serine to alanine mutations at serines 223, 224 and 229 had no effect on phosphorylation (data not shown).

Since we had no evidence for the phosphorylation of Rab11-FIP2 by the more common characterized protein kinases, and since serine 227 did not fall into any canonical consensus sites for known kinases, we sought to isolate the Rab11-FIP2 kinase activity from rabbit gastric microsomes. The 100,000g microsomal membrane fraction from rabbit gastric mucosa was used to isolate the kinase activity that phosphorylated Rab11-FIP2 on serine 227. Microsomal proteins were extracted with 1% Triton X-100 and proteins were resolved sequentially on Mono-Q, hydroxylapatite, Mono-S, and Cibachrome Blue resins followed by resolution on continuous glycerol gradients (see Materials and Methods). The fractions with the highest activity from column chromatography and the final glycerol gradient fraction containing serine 227 Rab11-

FIP2 kinase activity were submitted for proteomic analysis by total trypsin digestion and analysis of peptides by LC-MS/MS (Vanderbilt University Proteomics Laboratory, Mass Spectrometry Research Center). Only one kinase was identified consistently in these fractions from two different sample preparations: Par-1Bα/MARK2/EMK1 (MARK2) (5.5% - 14.7% coverage by amino acid). Seven separate peptides were identified matching either rat or human sequences (Table 2).

Table 2: Peptides Obtained from Mass Spectrometry for R ab11-FIP2 Kinase Identification

Peptide sequences of MARK2 identified in Rab11-FIP2 kinase preparations by Mass Spectrometry. Xcorr - Cross Correlation Score as identified by SEQUEST {Link et al.,1999}; z - charge state of peptide

Peptide Match	*Xcorr*	*z*
AENLLLDADMNIK	4.54	2
KYDGPEVDVWSLGVILYTLVSGSLPFDGQNLK	3.73	3
LFEVIETEK	2.59	2
PSADLTNSSAPSPSHK	2.44	3
TQLNSSSLQK	2.59	2
FLILNPSK	1.94	2
VLNHPNIVK	1.42	2

To verify MARK2 as a Rab11-FIP2 kinase, we assessed the ability of recombinant activated MARK2 to phosphorylate recombinant Rab11-FIP2 *in vitro*. While recombinant MARK2 strongly phosphorylated recombinant Rab11-FIP2, we observed little phosphorylation of Rab11-FIP2(S227A) (Figure 10C). In addition, we examined by LC/MS tandem mass spectrometry phosphorylation sites in recombinant Rab11-FIP2 when the protein was phosphorylated by MARK2 and found that Serine 227 was phosphorylated in peptides produced

from both trypsin and chymotrypsin digestions. In addition, spectra of the peptides from both digests contained a neutral loss of 98 (NL98) ion, indicative of a phosphorylation site, and an MS/MS/MS spectrum of the NL98 ion in the tryptic peptide confirmed that the ion resulted from neutral loss of phosphoric acid resulting from the phosphorylation.

Upon inspection of the available genomic databases using the Rab11 binding domain, we found that the serine 227 site is an evolutionarily conserved residue in putative Rab11-FIPs from numerous species including *Drosophilia melanogaster* and *Danio rerio* (Figure 10D). Interestingly, this phosphorylation site, the first serine residue of SMSxL, is a non-canoncial site for MARK2. Previous studies have suggested that MARK2 phosphorylates KxGS sites (Drewes et al., 1997). This non-canonical site is also present in two other human Rab11-interacting proteins, RCP and Rab11-FIP1. Activated recombinant MARK2 phosphorylated both RCP and Rab11-FIP1 *in vitro* (data not shown).

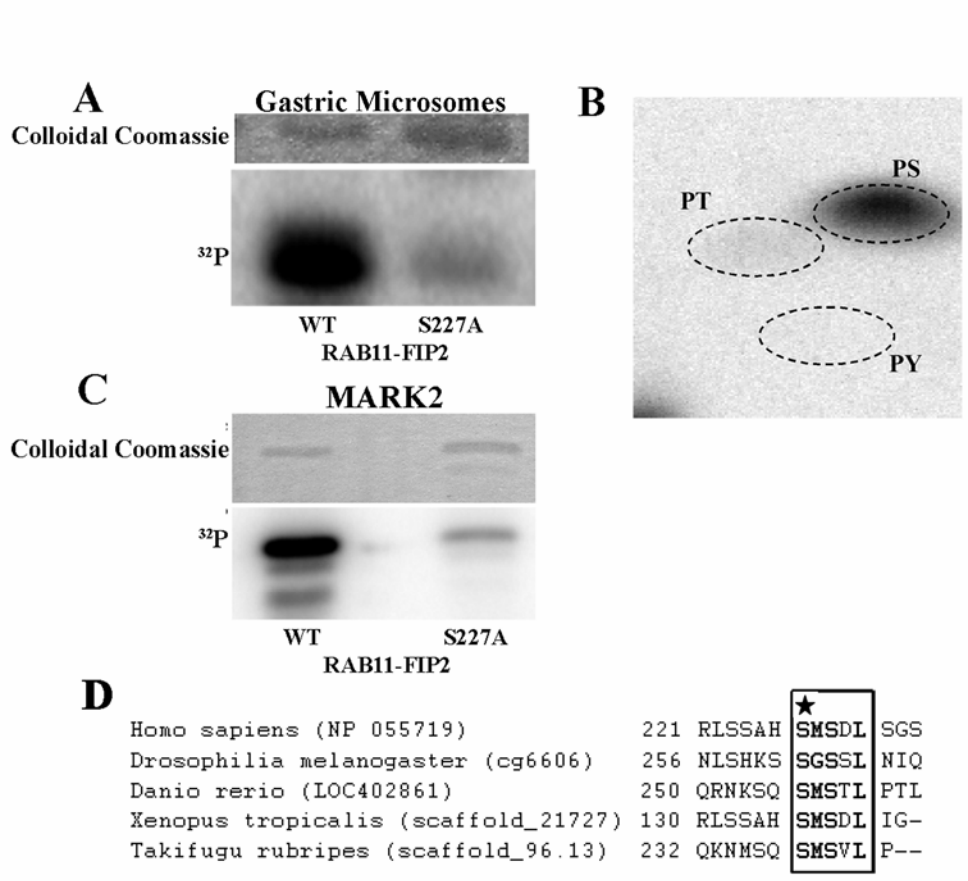

Figure 10: Rab11-FIP2 kinase activities.

A: A kinase activity associated with rabbit gastric microsomes phosphorylates Rab11-FIP2 on serine 227. Top: coomassie stain for protein levels; bottom: phosphorimage. B: Phosphoamino acid analysis demonstrates phosphorylation of Rab11-FIP2 is on serine resdiues. Positions of phosphoamino acid standards are shown by dotted lines. PS is phosphoserine. PT is phosphothreonine. PY is phosphotyrosine. C: Rab11-FIP2 is phosphorylated by recombinant activated MARK2 in vitro on serine 227 of Rab11-FIP2 wild type by not Rab11-FIP2(S227A). Top blot coomassie stain for protein levels; bottom blot, phosphorimage. D: Amino acid alignment of the putative Rab11-FIP2 sequences. The conserved phosphorylation site is boxed and in bold font. The phosphorylated serine is marked by a star.

Rab11-FIP2 is phosphorylated *in situ*

To assess the importance of Rab11-FIP2 phosphorylation *in situ*, we generated MDCK T23 cell lines with tetracycline-repressible expression of EGFP-Rab11-FIP2 wild type and non-phosphorylatable EGFP-Rab11-FIP2(S227A). EGFP-Rab11-FIP2 and EGFP-Rab11-FIP2(S227A) expressing cells were grown on permeable filters and labeled

for 2 hours with [32P]-orthophosphate, followed by lysis and immunoprecipitiation of GFP-Rab11-FIP2 proteins with anti-GFP antibodies. An immunoblot using anti-GFP showed that the amount of protein immunoprecipitated was similar between the two conditions. However, while the wild-type Rab11-FIP2 was strongly phosphorylated *in situ*, Rab11-FIP2(S227A) demonstrated far less *in situ* phosphorylation (Figure 11). We consistently observed a phosphorylated breakdown product in the EGFP-Rab11-FIP2 wild type cell line that was not present in the EGFP-Rab11-FIP2(S227A) line. This breakdown was also apparent in recombinant protein preparations, suggesting that Rab11-FIP2 is readily degraded by an as yet unknown mechanism.

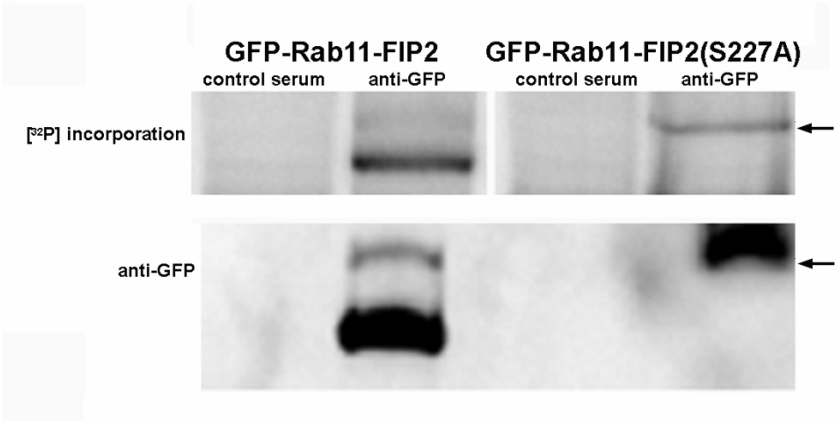

Figure 11: EGFP-Rab11-FIP2 is phosphorylated in situ.

Upper blot: Phosphorimage of phosphorylation of immunoprecipitated EGFP-Rab11-FIP2 from MDCK cell lines stably expressing either EGFP-Rab11-FIP2 or EGFP-Rab11-FIP2(S227A). Cells were loaded with [32P]-orthophosphate, lysed and immunoprecipitated with an anti-GFP antibody and proteins were resolved on SDS-PAGE gels. Lower blot: Immunoblot probing for GFP of immunoprecipitated lysates. Full length EGFP-Rab11-FIP2 is 75 kd (depicted with an arrow), but is consistently broken down by an as yet unknown mechanism.

Recently, PEST sequences have been implicated in the degradation of RCP, a member of the Rab11-FIPs (Marie et al., 2005). While, Rab11-FIP2 does not have PEST sequences, degradation may be a prominent regulatory mechanism in this family. Although mutation

of the phosphorylation site appears to stabilize the protein, we have no evidence that phosphorylated Rab11-FIP2 binds 14-3-3 proteins (data not shown). These results establish the presence of Rab11-FIP2 phosphorylation on serine 227 in polarized MDCK cells.

Overexpression of cargo alters Rab11-FIP2 morphology

During the characterization of the tetracycline-repressible stable MDCK T23 cell lines, we noticed two morphologies apparent in each of 10 lines cloned of EGFP-Rab11-FIP2 wild type. One morphology was similar to the EGFP-Rab11-FIP2 distribution previously reported by our lab in transiently transfected MDCK cells (Hales *et al.*, 2001) and others in A431 cells (Lindsay and McCaffrey, 2004), maintaining an apical vesicular appearance traditionally attributed to the apical recycling endosome. In the second morphology, EGFP-Rab11-FIP2 localized on smaller vesicles and along the lateral membrane. One publication has reported this alternate morphology in A431 cells in response to treatment with EGF (Lindsay and McCaffrey, 2004). Because we isolated multiple individual clones that exhibited both morphologies, we sought to understand the implications of this diversity. One difference between this and our previous study (Hales *et al.*, 2001), was the use of T23 MDCK cells as the parental line (Barth *et al.*, 1997) instead of MDCK II cells. The T23 clone incorporates both the stable expression of polymeric IgA receptor (pIgR) and the tetracycline-repressible transactivator tTA into MDCK II cells. When we compared MDCK II cells transiently expressing EGFP-Rab11-FIP2 to T23 cells expressing EGFP-Rab11-FIP2, the difference in distribution was apparent. The transiently transfected MDCK II cells displayed our previously published distribution for EGFP-Rab11-FIP2, while the T23 cells stably expressing EGFP-Rab11-

FIP2 displayed both morphologies (Figure 12A). Upon initiation of pIgA trafficking, the cells changed to the more traditional apical recycling endosomal morphology (Figure 12B). These dynamic localizations suggest an additional new role for Rab11-FIP2 beyond the recycling pathway.

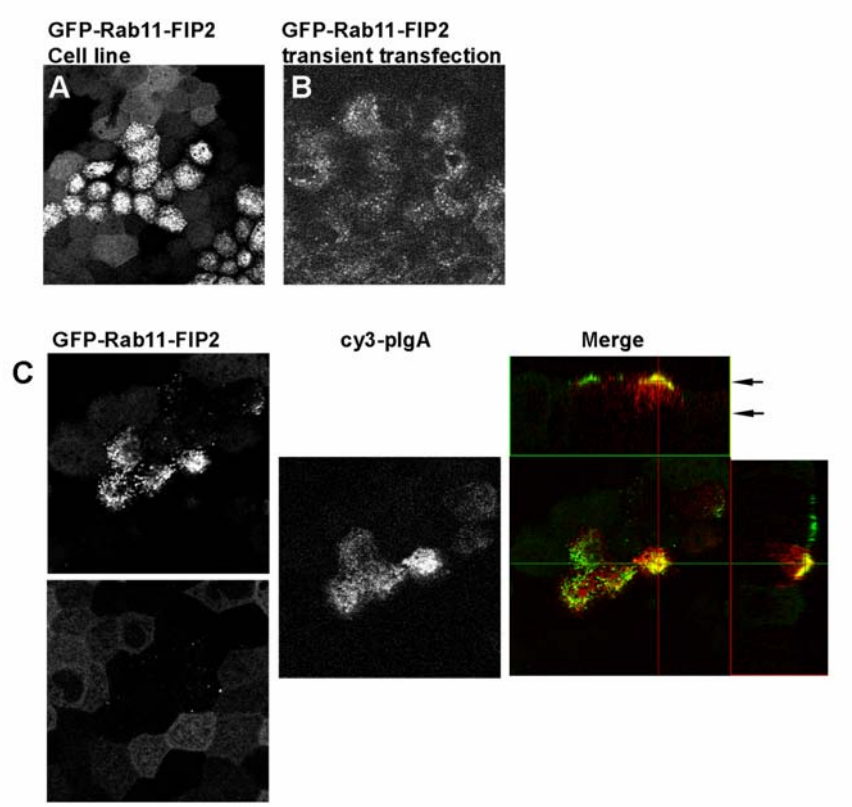

Figure 12: Distribution of EGFP-Rab11-FIP2 in stably overexpressing cell lines.

A) T23 cells stably expressing EGFP-Rab11-FIP2 exhibit two different morphologies. B) Transiently transfected MDCK II cells show only a punctuate subapical distribution of EGFP-Rab11-FIP2. C) T23 cells expressing EGFP-Rab11-FIP2 in the presence or absence of pIgA (red in merge). Upon induction of trafficking, the EGFP-Rab11-FIP2 exhibits dynamic relocalization to the more traditional recycling system. EGFP images are from two different z positions in the same confocal stack, as indicated in the XY orthogonal view, to enhance the visualization of both morphologies.

Manipulation of Rab11-FIP2 phosphorylation alters its apical distribution.

Rab11-FIP2 was initially characterized as an interacting protein for Rab11a (Hales et al., 2001). Rab11a has traditionally been associated with trafficking through the plasma membrane (Casanova et al., 1999). Therefore, we examined the general effect of overexpression of EGFP-Rab11-FIP2 and it nonphosphorylatable mutant on the distribution of the recycling system components in our inducible cell lines. The phenotype observed in each of these lines was most prominent in polarized cells grown on filters and was difficult to discern in non-polarized cells grown on glass (data not shown).

In both cell lines, EGFP-Rab11-FIP2 and EGFP-Rab11-FIP2(S227A) showed overlapping localization with Rab11a (data not shown). The EGFP-Rab11-FIP2 in the wild type cell line localized near the apical membrane as shown by comparison with the apical marker GP135 (

Figure 13). A portion of the EGFP-Rab11-FIP2 was interspersed with the GP135 staining while the remainder was immediately subapical to the membrane. The non-phosphorylatable EGFP-Rab11-FIP2(S227A) population of vesicles extended further below the plasma membrane as shown by comparison with both GP135 (

Figure 13). Similar results were seen comparing the distribution of EGFP-Rab11-FIP2 proteins with that of ezrin (data not shown).

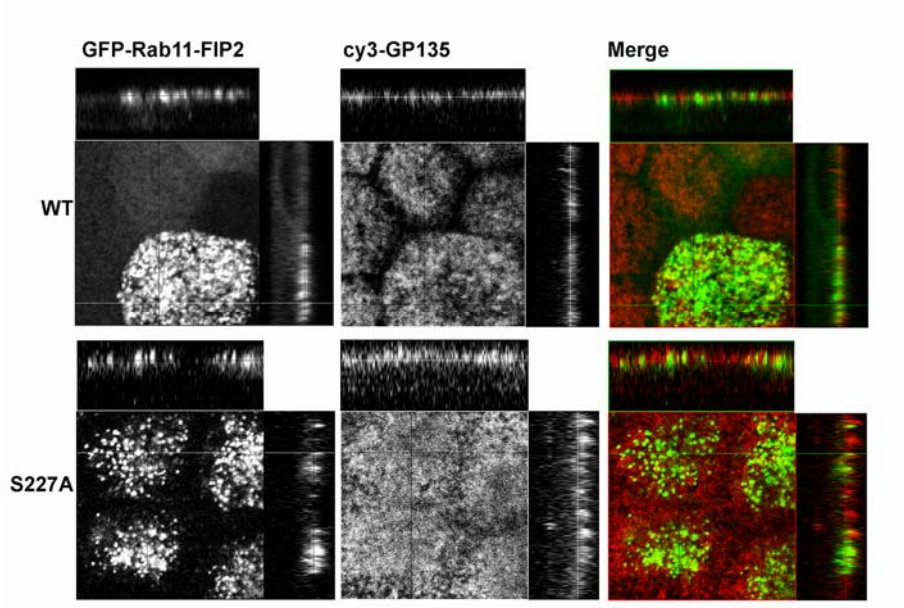

Figure 13: Subapical distribution of EGFP-Rab11-FIP2 in stably expressing cell lines.

Localization of the apical maker GP135 with EGFP-Rab11-FIP2 and EGFP-Rab11-FIP2(S227A) was compared in stable cell lines. Confocal immunofluorescence imaging of the EGFP-Rab11-FIP2 constructs with GP135 showed that EGFP-Rab11-FIP2 partially colocalized and interspersed with the apical marker GP135 (red in merge). EGFP-Rab11-FIP2(S227A) was also partially colocalized with and partially beneath the apical marker GP135 (red in merge). The x-y planes are optical sections taken 2.5 microns apart.

Effects of phosphorylation site mutations on Rab11-FIP2 recycling system interactions

Next, we analyzed the interaction of Rab11-FIP2(S227A) with known apical recycling system components including association with myosin Vb and Rab11a as well as Rab11-FIP2 dimerization by far western analysis (Ducharme *et al.*, 2005). All three interactions were maintained regardless of the mutated state of Rab11-FIP2 (data not shown). These interactions were confirmed by yeast two hybrid analyses, which revealed that phosphorylation of S227 did not affect Rab11a or myosin Vb interactions with Rab11-FIP2 or Rab11-FIP2 – Rab11-FIP2 dimerization (data not shown). We have previously demonstrated that

expression of myosin Vb tail causes compaction of the Rab11a-containing apical recycling system and marked inhibition of both apical recycling and transcytosis (Lapierre et al., 2001). Transfection of EGFP- Rab11-FIP2 or EGFP-Rab11-FIP2(S227A) expressing cell lines with DsRed2-myosin Vb tail elicited colocalization of both EGFP-Rab11-FIP2 proteins with myosin Vb tail and Rab11a in a collapsed recycling system (Figure 14) further indicating that phosphorylation state does not affect association with myosin Vb. We also examined the effects of over-expression of wild type EGFP-Rab11-FIP2 or EGFP-Rab11-FIP2(S227A) on trafficking of polymeric IgA in the tetracycline repressible cell lines. Both transcytosis and apical

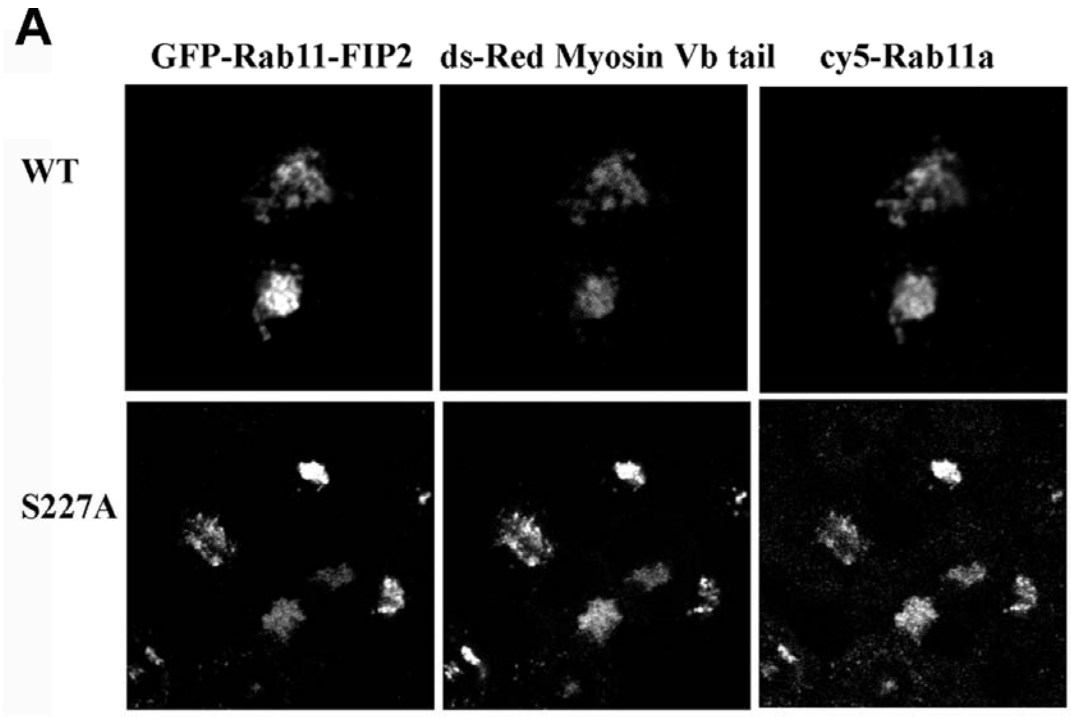

Figure 14: Phosphorylation of Rab11-FIP2 does not alter interaction with myosin Vb tail.

The phosphorylation state of Rab11-FIP2 does not affect known interactions with myosin Vb. Stable EGFP-RAB11-FIP2 cells lines were transiently transfected with Ds-Red2 myosin Vb tail.

Rab11-FIP2 wildtype and Rab11-FIP2(S227A) as well as Rab11a were pulled into the myosin Vb tail collapsed recycling system as expected

recycling of pIgA, well characterized functions of the Rab11a containing recycling system, were unaffected by the overexpression of wild type or mutant EGFP-Rab11-FIP2 proteins (Figure 15).

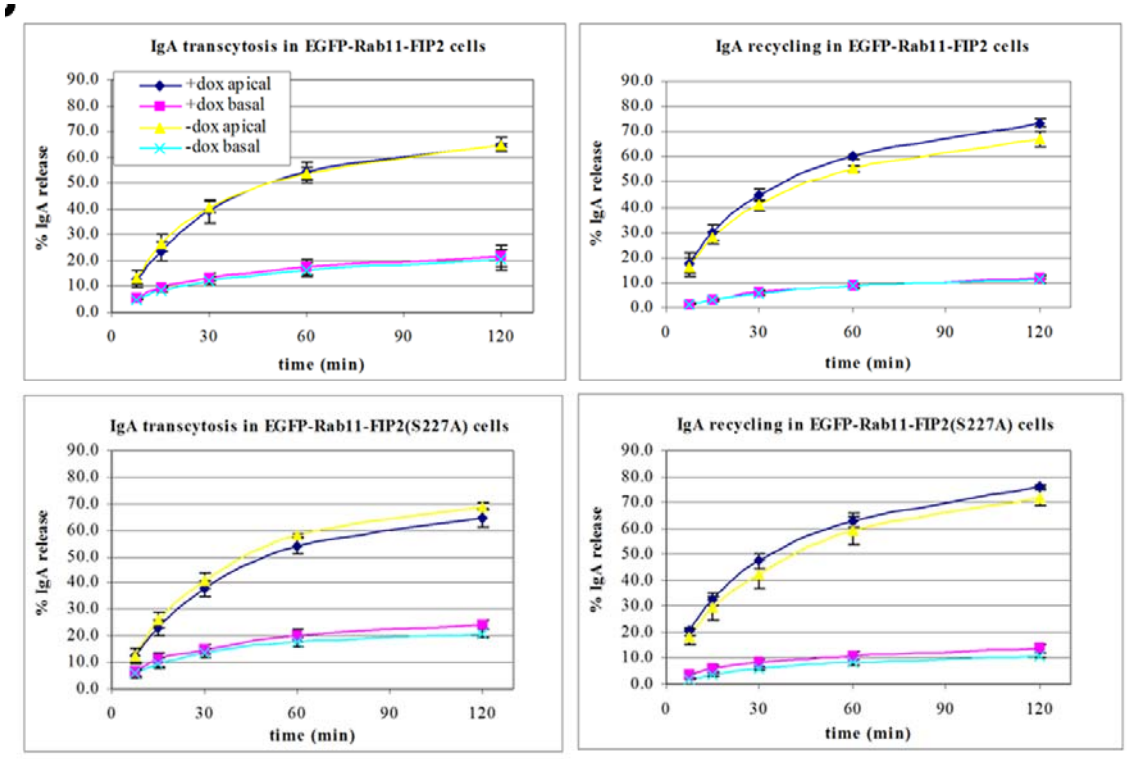

Figure 15: Phosphorylation of Rab11-FIP2 does not alter apical recycling or transcytosis

Recycling functions of Rab11-FIP2 are not affected by phosphorylation on serine 227. Apical recycling and transcytosis of [125I]IgA were assessed in stable transfected cell lines in the presence or absence of doxycycline. Neither apical recycling nor transcytosis were affected by the phosphorylation state of Rab11-FIP2. Top graphs are EGFP-Rab11-FIP2 wild type. Bottom graphs are EGFP-Rab11-FIP2(S227A). Left hand side shows data from transcytosis assays, while the right hand side shows results from apical recycling assays. Dark blue and pink lines indicate that doxycycline was present in the media (inhibiting expression of the EGFP-chimera). Yellow and light blue lines indicate that the cells were incubated in doxycycline-free media allowing for expression of EGFP-chimera proteins. Dark blue and yellow lines indicate media was collected from the apical side of the transwell. Pink and light blue lines indicate media was

collected from the basal side of the transwell. The results show no effects of EGFP-Rab11-FIP2 expression on either transcytosis or apical recycling.

Rab11-FIP2 phosphorylation is important for the formation of calcium dependent junctions.

MARK2 has previously been implicated in the proper establishment of polarity in both *C. elegans* embryos (Guo and Kemphues, 1995) and MDCK cells (Bohm et al., 1997; Cohen and Musch, 2003). Thus, we hypothesized that Rab11-FIP2 phosphorylation may also impact on polarity. We assessed the effect of Rab11-FIP2 phosphorylation mutants on the re-establishment of polarity following calcium switch. Cell polarity was disrupted by switching confluent cells to calcium free media overnight. Cells were then fixed at indicated time intervals following re-addition of 1.8 mM calcium. These cells were stained for ZO-1 and p120 catenin to assess the re-establishment of tight and adherens junctions, respectively.

EGFP-Rab11-FIP2 wild type exhibited dynamic movements during the re-establishment of polarity. After incubation overnight in calcium free media, EGFP-Rab11-FIP2 localized along the lateral membrane and in perinuclear pools. Following re-addition of calcium, Rab11-FIP2 initially moved to perincular pools where it colocalized with Rab11a (data not shown). Over time, EGFP-Rab11-FIP2 redistributed near the apical membrane, a pattern similar to that in cells that did not undergo a calcium switch (Figure 16). These cells did reform proper junctions as measured by immunofluorescence staining for both p120 catenin and ZO-1 localization by 6 hours and 3 hours, respectively, after re-establishment of normal extracellular calcium (Figures Figure 17A and B). Similar

results were seen with the tight junction marker occludin as well as adherens junction proteins beta-catenin and E-cadherin (data not shown).

Interestingly, the EGFP-Rab11-FIP2(S227A) did not exhibit the same dynamic movement during the establishment of polarity. The EGFP-Rab11-FIP2(S227A) initially localized along the apical and lateral membranes following incubation with calcium free media, often appearing as subapical rings. Moreover, after re-addition of calcium, EGFP-Rab11-FIP2(S227A) was less compacted in the internal pools compared with EGFP-Rab11-FIP2. Finally, 1.5 hours after the re-addition of calcium, the non-phosphorylatable mutant localized diffusely near the apical surface exclusively (Figure 16). EGFP-Rab11-FIP2(S227A) expressing cells did not re-establish proper adherens junctions as assessed by a lack of p120 catenin localization to the lateral junctions by 6 hours after the re-addition of calcium (Figure 17A). This cell line did re-localize ZO-1 by 3 hours after calcium addition (Figure 17B). When calcium switch was performed in the presence of doxycycline to block expression of EGFP-Rab11-FIP2(S227A), both p120 catenin and ZO-1 re-localized to their junctions after re-addition of calcium by 3 hours (Figure 17A and B), as seen previously (Gumbiner et al., 1988; Straight et al., 2004).

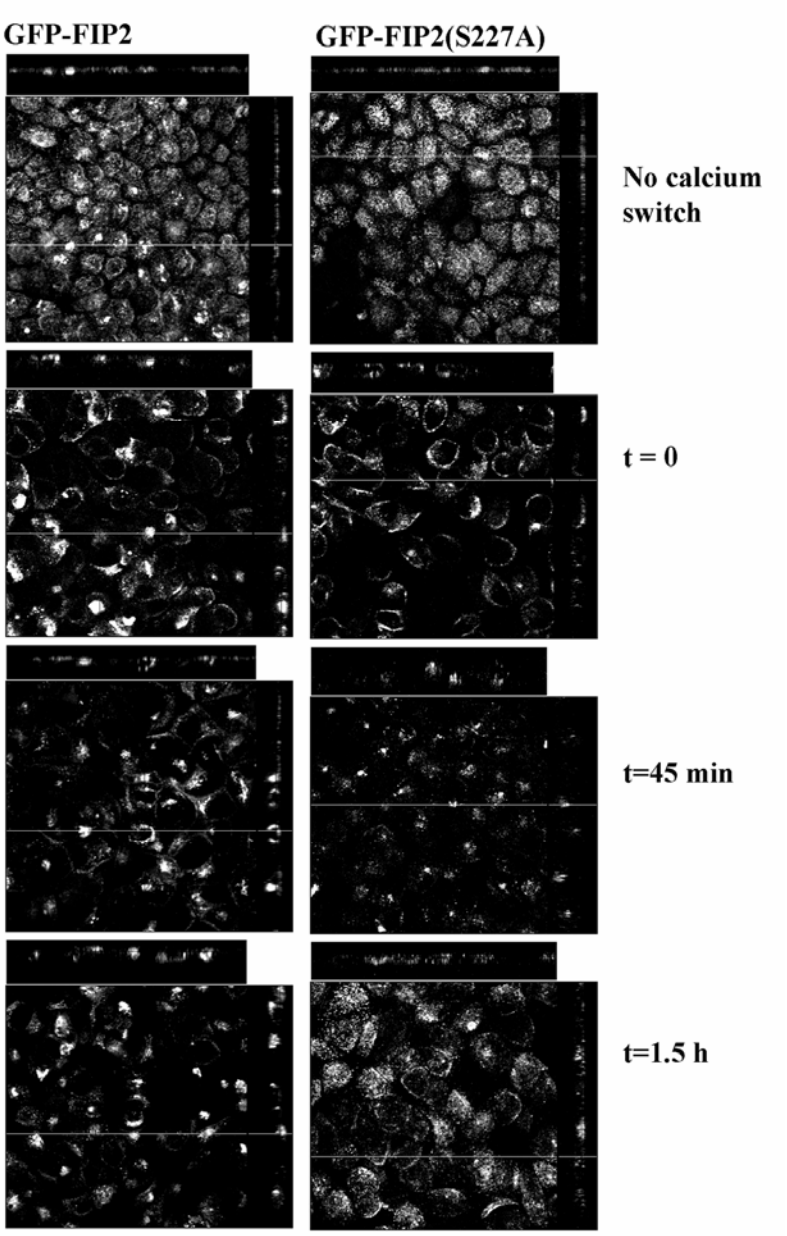

Figure 16: Distribution of EGFP-Rab11-FIP2 during calcium switch.

Cell lines expressing EGFP-Rab11-FIP2 or its phosphorylation mutant were subjected to the calcium switch protocol and fixed at the indicated time points following readdition of extracellular calcium. The EGFP-Rab11-FIP2 initially moved to a lateral membrane before accumulating in a tight spot internally. As the junctions reformed, the construct localized to the apical membrane as seen for those cells not subject to the switch. EGFP-Rab11-FIP2(S227A) initially localized in sub-apical rings. As the junctions reformed, the construct was less compact and became diffusely apical. The x-y planes are compiled stacks of optical sections taken 2.5 microns apart.

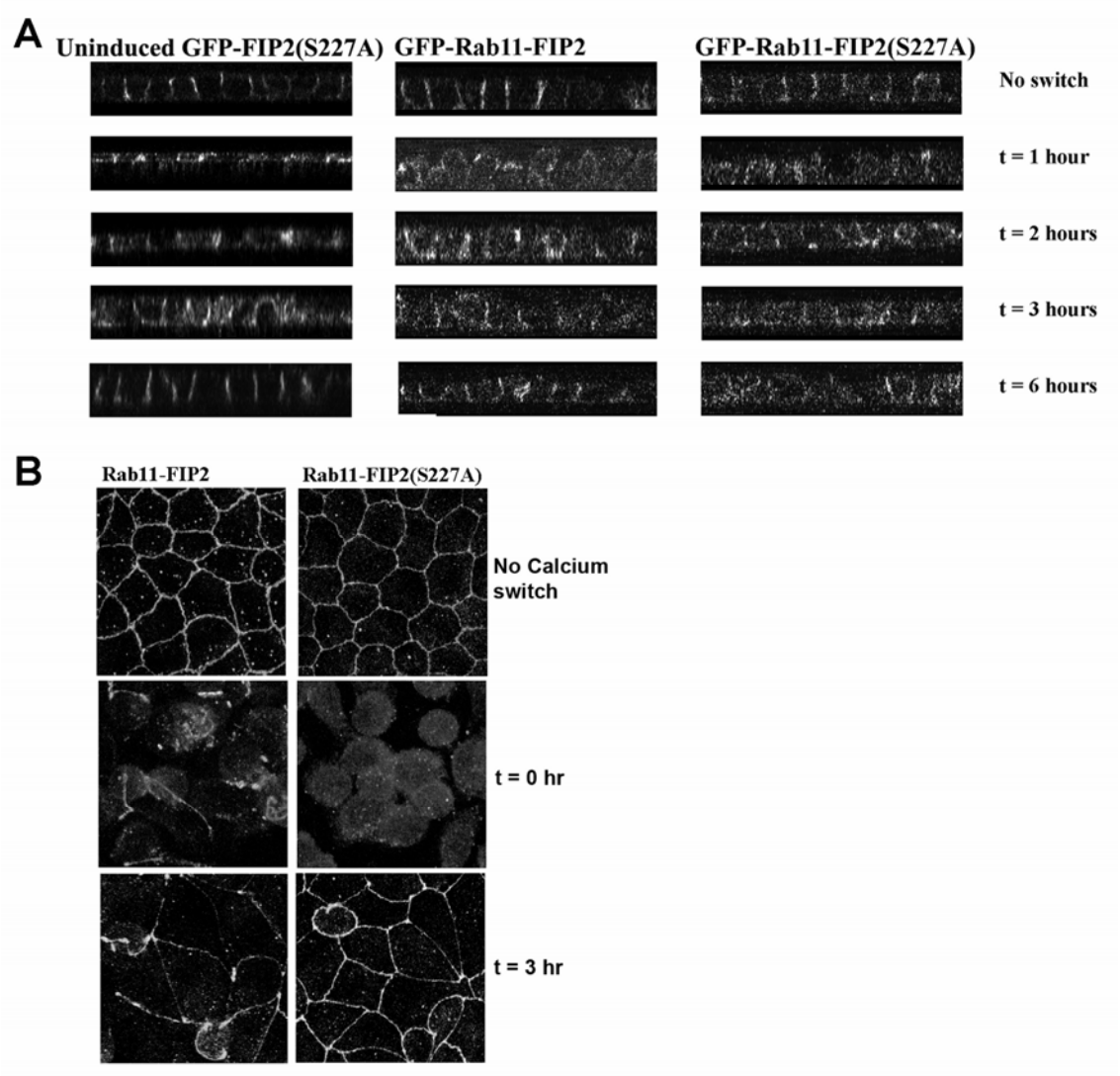

Figure 17: Phosphorylation of Rab11-FIP2 is necessary for the proper reestablishment of p120 at adherens junctions, but not ZO-1 at tight junctions.

Cell lines expressing EGFP-Rab11-FIP2 or its phosphorylation mutant were subjected to the calcium switch protocol and fixed at the indicated time points. A) Z sections from cells in the calcium switch experiment stained for p120 catenin. Note the delayed establishment of p120 localization in Rab11-FIP2(S227A) compared to wild type. p120 staining showed a normal re-establishment at the adherens junction in EGFP-Rab11-FIP2 cells grown in the presence of doxycycline (uninduced). B) Projections of z-stacks from ZO-1 staining during the calcium switch experiment demonstrate the normal reestablishment of ZO-1 at tight junctions in all cell lines.

A recent report suggests that the Rab11a pathway is involved in the trafficking of newly synthesized E-cadherin (Lock and Stow, 2005a). Therefore, it was possible that the Rab11a pathway was involved in the internalization or

recycling of junctional constituents. Nevertheless, we did not observe colocalization of any junctional protein with Rab11-FIP2 during the calcium switch assay. We therefore examined the localization of junctional makers in cells expressing the previously characterized dominant negative recycling system trafficking mutants EGFP-myosin Vb tail (Figure 18A) and EGFP-Rab11-FIP2(129-512) (data not shown). Neither dominant negative construct showed colocalization with p120 or ZO-1. To confirm that a Rab11a-dependent pathway utilizing Rab11-FIP2 pathway was not involved during trafficking, we examined the effects of these dominant negative mutants in the calcium switch assay. No p120 was observed in myosin Vb tail or Rab11-FIP2(129-512) containing collapsed recycling systems (Figure 18B). Furthermore, throughout the timecourse of the calcium add-back, we did not observe localization of any junctional marker within the inhibited recycling system (data not shown).

As an independent method of assessing junction formation, we trypsinized cells and replated them at high density on laminin-coated filters. We examined the cells at fixed time points to assess the establishment of junctions by staining for p120 and ZO-1. Cells overexpressing EGFP-Rab11-FIP2 wild type reestablished normal junctions by 4 hours after replating, while the EGFP-Rab11-FIP2(S227A) expressing cells did not (Figure 19). ZO-1 localization was reestablished similarly in both lines by 4 hours. Thus, the inability to phosphorylate serine 227 of Rab11-FIP2 delays adherens junction formation in multiple assays.

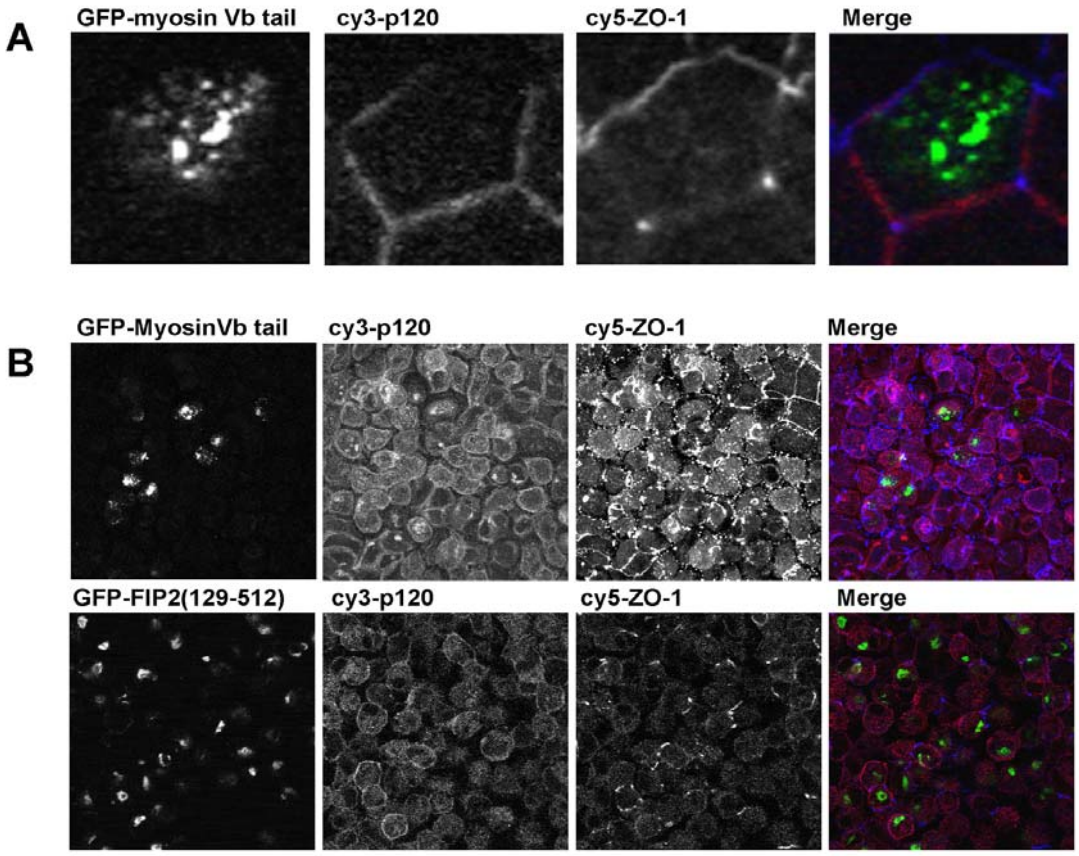

Figure 18: Dominant negative Rab11a recycling system trafficking mutants do not co-localize with junctional proteins p120 or ZO-1.

A) X-Y confocal sections showing dual labeling of p120 catenin (cy 3, pseudo colored red) and ZO-1 (cy5, pseudo colored blue) in EGFP-myosin Vb tail cells. No colocalization was found between the junctional markers and EGFP-myosin Vb tail. B) Projections showing dual labeling of p120 catenin (cy 3, pseudo colored red) and ZO-1 (cy5, pseudo colored blue) in EGFP-Rab11-FIP2(129-512) and EGFP-myosin Vb tail cells following calcium switch at t = 0. Junctional markers do not colocalize with the dominant negative inhibitors of the Rab11a apical recycling system. No localization with the collapsed recycling system was seen at any time point following reestablishment of extracellular calcium

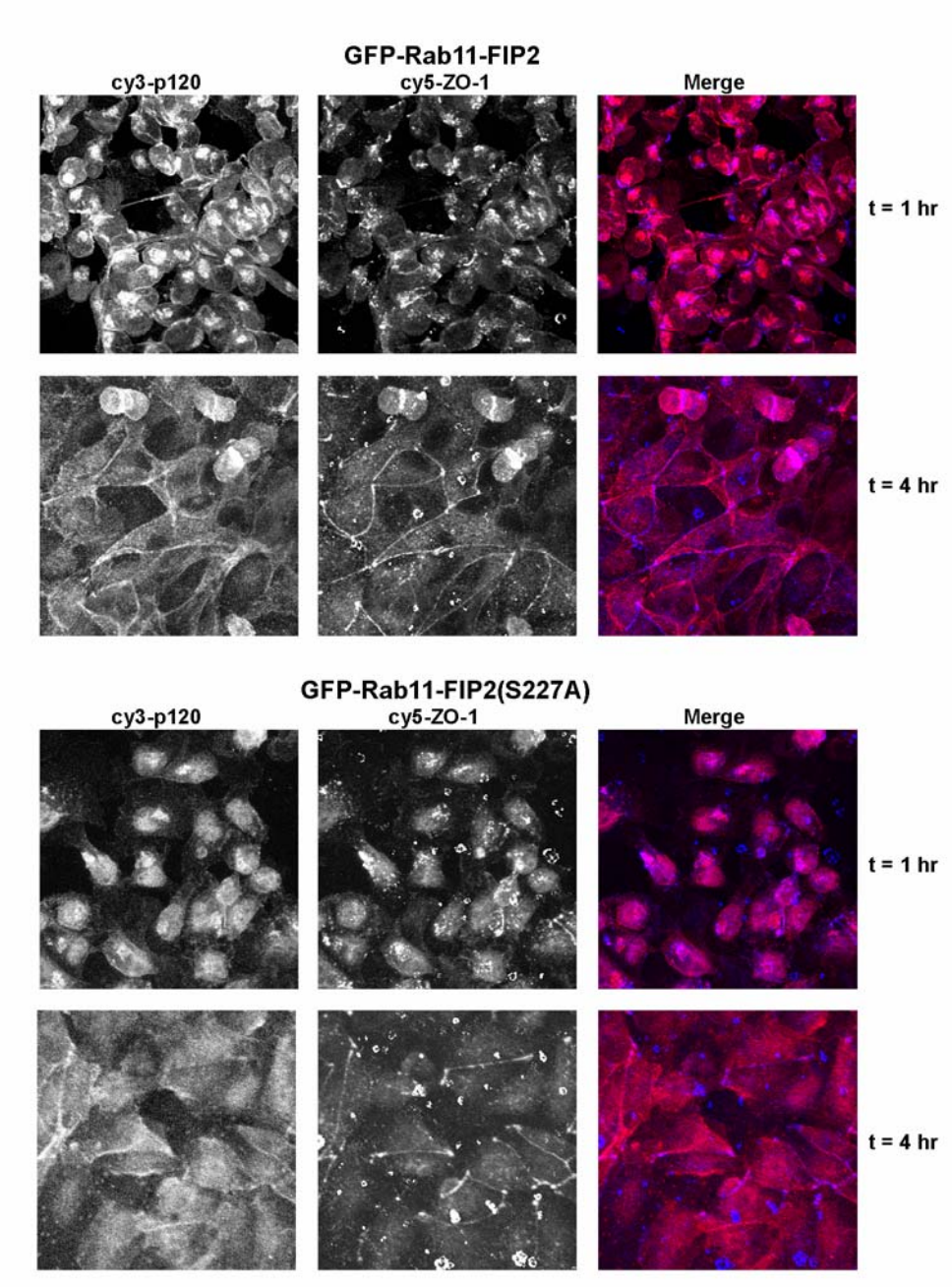

Figure 19: Phosphorylation of Rab11-FIP2 is necessary for the proper reestablishment of polarity in a replating assay.

Cell lines expressing EGFP-Rab11-FIP2 or EGFP-Rab11-FIP2(S227A) were trypsinzied and replated on laminin-coated filters. The cells were fixed at the indicated time points and stained with p120 (pseudo colored red) and ZO-1 (pseudo colored blue). These overlays show x-y planes following replating. While ZO-1 was reestablished at tight junctions in both lines, EGFP-Rab11-FIP2(S227A) expressing cells demonstrated a deficit in p120 localization four hours after replating.

Discussion

Traditionally, the apical recycling system is marked by the presence of Rab11a. Rab11a and its known family of interacting proteins (Rab11-FIPs) regulate trafficking through the apical recycling system. For example, removal of the C2 domain from Rab11-FIP2 causes a disruption of the trafficking of pIgA through the apical recycling system (Hales et al., 2002). In addition, we have shown that myosin Vb associates with the Rab11a and Rab11-FIP2 to form a ternary regulatory complex for apical recycling (Hales et al., 2002). However, Rab11-FIP2 also has a role in cellular function beyond apical recycling. We and others have previously shown that a subset of the Rab11-FIP2 is not with the recycling system in quiescent cells (Hales *et al.*, 2001; Cullis *et al.*, 2002). Rab11-FIP2 associates with EH domain proteins such as Reps1, assisting in receptor mediated endocytosis (Cullis *et al.*, 2002). In the initial characterization of Rab11-FIP2, we found that not all Rab11-FIP2 colocalized with Rab11a. This was apparent particularly when cells were treated with the microtubule-stabilizing drug, taxol. Taxol treatment of polarized cells caused Rab11a containing recycling vesicles to relocate to apical corners near the tight junction complex (Casanova et al., 1999). However, taxol treatment of cells caused Rab11-FIP2 to localize at both the apical corner and laterally (Hales et al., 2001), suggesting that not all of Rab11-FIP2 was involved in the Rab11a-containing recycling pathway. This lateral localization is similar to that seen after the removal of calcium in the EGFP-Rab11-FIP2(S227A) cells. Importantly, in these studies, we have demonstrated that phosphorylation of Rab11-FIP2 on serine 227 by MARK2 is not involved in the traditional apical recycling pathway, but is instead involved in the establishment of epithelial cell polarity.

The recycling system is a dynamic tubular network with multiple regulators and signaling pathways. Present models suggest that the assembly of multiple proteins associating with Rab11a regulates trafficking through the recycling system. While few of the Rab proteins are directly regulated by protein phosphorylation (van der Sluijs et al., 1992), phosphorylation of Rab interacting proteins has emerged as an important regulatory mechanism. Thus, the Rab3 interacting protein, rabphilin-3, is phosphorylated both by protein kinase A and calmodulin-dependent kinase II (Kato et al., 1994; Numata et al., 1994). Rabphilin-3 phosphorylation reduces its affinity for membranes (Foletti et al., 2001; Lonart and Sudhof, 2001). Rab11-FIP5 (pp75/Rip11) was originally described as an autoantigen phosphoprotein, and as in the case of rabphilin-3, phosphorylation appeared to alter subcellular localization (Wang *et al.*, 1999; Prekeris *et al.*, 2000). The kinase activity responsible for Rab11-FIP5 phosphorylation is unclear, although we have not found phosphorylation of Rab11-FIP5 by MARK2 (data not shown). In the present report, we have found that MARK2 can phosphorylate Rab11-FIP2. Nevertheless, mutation of serine 227 does not alter apical membrane recycling or transcytosis. Thus, MARK2 appears to regulate Rab11-FIP2 functions distinct from its role in the recycling system.

MARK2 is a member of the PAR (partitioning-defect) family originally characterized as PAR1 in *C. elegans* (Kemphues et al., 1988). Since that time, the majority of the work on this kinase has related to phosphorylation of Tau, MAP2C and MAP4 on their microtubule binding domains which results in disruption of the microtubule network (Drewes *et al.*, 1995; Drewes *et al.*, 1997; Ebneth *et al.*, 1999). In *Drosophila*, MARK2 regulates the density, stability and apicobasal organization of

microtubules by regulating the microtubule plus ends (Doerflinger et al., 2003). While MARK2 phosphorylation of Rab11-FIP2 does not appear to affect the traditional Rab11a trafficking pathway, it previous studies have implicated MARK2 in the breakdown of the microtubule network. MARK2 phosphorylation events may also be regulating the movement of vesicles along the microtubule network.

The *S. pombe* family MARK2 member, kin1, is necessary to establish the rod shaped morphology and for progression of cytokinesis (Drewes and Nurse, 2003). This kinase also plays a role in the establishment of polarity. MARK2 is essential for epithelial specific microtubule arrays in polarized cells (Cohen et al., 2004). Overexpression of the kinase inhibits apical/basolateral polarization in MDCK cells partially by altering apical protein transport. Interestingly, cells overexpressing MARK2 form a polarity axis parallel to the substratum (Cohen and Musch, 2003). Recently, the yeast homolog was reported to interact with components of the exocytic machinery including the yeast Rab family member, Sec4 (Elbert et al., 2005), thus establishing a precedent for the involvement of this kinase family in Rab related trafficking. The results presented here indicate that phosphorylation of Rab11-FIP2 by MARK2 is necessary for the proper localization of junctional proteins. The importance of the phosphorylation site was most obvious when manipulating the system through a calcium switch assay. The re-establishment of polarity was grossly delayed in cells overexpressing EGFP-Rab11-FIP2(S227A). p120 catenin did not organize into junctions when cells were examined up to eight hours after the addition of normal media. Similar defects in the establishment of polarity in EGFP-Rab11-FIP2(S227A) expressing cells were also observed in replating assays. Nevertheless, we did not observe any difference in trans-epithelial resistance (TER) between cells

expressing EGFP-Rab11-FIP2, EGFP-Rab11-FIP2(S227A) or uninduced cell lines (data not shown). However, cells that have ZO-1 knocked out also do not have reduced TER, suggesting that other junctional proteins such as ZO-2 can compensate for a lack of junctional ZO-1 (Umeda *et al.*, 2004).

Previous work by Parkos and colleagues demonstrated that junctional proteins including cadherin, p120 and ZO-1 are internalized in response to calcium depletion (Ivanov et al., 2004). During *Drosophila* cellularization, cadherin is initially localized along the entire lateral membrane and then becomes sequestered into both apical lateral and basal lateral compartments, finally restricted to the apically oriented adherens junction (Le Bivic, 2005). This dual localization found during mid-cellularization is reminiscent of the localization of p120 observed in cells overexpressing EGFP-Rab11-FIP2(S227A), suggesting that these cells may never achieve proper adherens junctions. The role of Rab11-FIP2 in adherens junction protein trafficking is supported by a recent study by Stow and colleague demonstrating that newly synthesized cadherin requires functional Rab11 for proper localization (Lock and Stow, 2005a). However, our work suggests that establishment of junctions is not blocked by expression of previously characterized inhibitors of the apical recycling system, Rab11-FIP2(129-512) and Myosin Vb tail. Another Rab11-FIP, Rab Coupling Protein (RCP), was also recently found to relocalize with Rab11a to the lateral membrane in the presence of calpeptin, a potent blocker of calcium mediated calpain actions (Marie et al., 2005). In the presence of calpain inhibitor, RCP relocalized in a pattern similar to that for Rab11-FIP2 during the initial stages of junctional reformation following readdition of calcium. Interestingly, RCP also has the MARK2 phosphorylation site and is phosphorylated by MARK2 *in*

vitro, suggesting a possible common regulatory mechanism for both RCP and Rab11-FIP2 in response to calcium.

In summary, the present studies have defined a novel consensus site for phosphorylation by MARK2 of Rab11-FIP2. Manipulation of the serine 227 phosphorylation site in Rab11-FIP2 alters the establishment of polarity in polarized MDCK cells but does not affect traditional recycling system trafficking pathways. These studies demonstrate that Rab11-FIP2 plays an important role in regulating epithelial cell polarity, distinct from its function in the Rab11a-containing recycling pathways.

Acknowledgments

This work was supported by grants to JRG from NIH NIDDK (DK48370 and DK43405) and GA from NIH NIDDK (RO1DK51970). We thank Dr. Roy Zent for the gift of antibody reagents. Confocal fluorescence imaging was performed in part through the use of the VUMC Cell Imaging Shared Resource, (supported by NIH grants CA68485, DK20593, DK58404 and HD15052). The authors also thank Vanderbilt University for institutional support of the Proteomics Laboratory in the Mass Spectrometry Research Center through the Academic Venture Capital Fund. We thank Kenya Avant, Cathy Caldwell, Salisha Hill, Dr. Karen Hobdy-Henderson, Dr. Joseph Roland and Dr. Min Jin for support of these studies.

Nicole A. Ducharme drafted the manuscript and performed the experiments relating to figures 9A, C and D, figures 10-13 and figures 15-18. Chadwick M. Hales identified the

phosphorylation site. Lynne A. Lapierre assisted in experimental interpretation and manuscript editing. Amy-Joan L. Ham supervised the mass spectrometry components of the project. Asli Oztan and Gerard Apodaca did the quantified pIgA trafficking experiments relating to figure 14. James R. Goldenring was involved in guiding the experimental design with Nicole Ducharme.

References

Apodaca, G., Katz, L.A., and Mostov, K.E. (1994). Receptor-mediated transcytosis of IgA in MDCK cells is via apical recycling endosomes. J Cell Biol *125*, 67-86.

Barth, A.I.M., Pollack, A.L., Altschuler, Y., Mostov, K.E., and Nelson, W.J. (1997). NH2-terminal deletion of beta -catenin results in stable colocalization of mutant beta -catenin with adenomatous polyposis coli protein and altered MDCK cell adhesion. J. Cell Biol. *136*, 693-706.

Basson, M.D., Goldenring, J.R., Tang, L.H., Lewis, J.J., Padfield, P., Jamieson, J.D., and Modlin, I.M. (1991). Redistribution of 23 kDa tubulovesicle-associated GTP-binding proteins during parietal cell stimulation. Biochem J *279 (Pt 1)*, 43-48.

Bohm, H., Brinkmann, V., Drab, M., Henske, A., and Kurzchalia, T.V. (1997). Mammalian homologues of C. elegans PAR-1 are asymmetrically localized in epithelial cells and may influence their polarity. Curr Biol *7*, 603-606.

Breitfeld, P.P., Casanova, J.E., Harris, J.M., Simister, N.E., and Mostov, K.E. (1989). Expression and analysis of the polymeric immunoglobulin receptor in Madin-Darby canine kidney cells using retroviral vectors. Methods Cell Biol *32*, 329-337.

Casanova, J.E., Wang, X., Kumar, R., Bhartur, S.G., Navarre, J., Woodrum, J.E., Altschuler, Y., Ray, G.S., and Goldenring, J.R. (1999). Association of Rab25 and Rab11a with the apical recycling system of polarized Madin-Darby canine kidney cells. Mol Biol Cell *10*, 47-61.

Cohen, D., Brennwald, P.J., Rodriguez-Boulan, E., and Musch, A. (2004). Mammalian PAR-1 determines epithelial lumen polarity by organizing the microtubule cytoskeleton. J Cell Biol *164*, 717-727.

Cohen, D., and Musch, A. (2003). Apical surface formation in MDCK cells: regulation by the serine/threonine kinase EMK1. Methods *30*, 269-276.

Cortes, H.J., Pfeiffer, C.D., Richter, B.E., and Stevens, T. (1987). Porous ceramic bed supports for fused silica packed capillary columns used in liquid chromatography. Journal of High Resolution Chromatography and Chromatography Communications *10*, 446-448.

Cullis, D.N., Philip, B., Baleja, J.D., and Feig, L.A. (2002). Rab11-FIP2, an adaptor protein connecting cellular components involved in internalization and recycling of epidermal growth factor receptors. J Biol Chem *277*, 49158-49166.

Doerflinger, H., Benton, R., Shulman, J.M., and St Johnston, D. (2003). The role of PAR-1 in regulating the polarised microtubule cytoskeleton in the Drosophila follicular epithelium. Development *130*, 3965-3975.

Drewes, G., Ebneth, A., Preuss, U., Mandelkow, E.M., and Mandelkow, E. (1997). MARK, a novel family of protein kinases that phosphorylate microtubule-associated proteins and trigger microtubule disruption. Cell *89*, 297-308.

Drewes, G., and Nurse, P. (2003). The protein kinase kin1, the fission yeast orthologue of mammalian MARK/PAR-1, localises to new cell ends after mitosis and is important for bipolar growth. FEBS Lett *554*, 45-49.

Drewes, G., Trinczek, B., Illenberger, S., Biernat, J., Schmitt-Ulms, G., Meyer, H.E., Mandelkow, E.M., and Mandelkow, E. (1995). Microtubule-associated protein/microtubule affinity-regulating kinase (p110mark). A novel protein kinase that regulates tau-microtubule interactions and dynamic instability by phosphorylation at the Alzheimer-specific site serine 262. J Biol Chem *270*, 7679-7688.

Ducharme, N.A., Jin, M., Lapierre, L.A., and Goldenring, J.R. (2005). Assessment of Rab11-FIP2 interacting proteins in vitro. Methods in Enzymology. In: GTPases Regulating Membrane Targeting and Fusion, ed. C.J.D. William E. Balch, and Alan Hall: Academic Press, 706-715.

Ebneth, A., Drewes, G., Mandelkow, E.M., and Mandelkow, E. (1999). Phosphorylation of MAP2c and MAP4 by MARK kinases leads to the destabilization of microtubules in cells. Cell Motil Cytoskeleton *44*, 209-224.

Elbert, M., Rossi, G., and Brennwald, P. (2005). The yeast par-1 homologs kin1 and kin2 show genetic and physical interactions with components of the exocytic machinery. Mol Biol Cell *16*, 532-549.

Fan, G.H., Lapierre, L.A., Goldenring, J.R., and Richmond, A. (2003). Differential regulation of CXCR2 trafficking by Rab GTPases. Blood *101*, 2115-2124.

Fan, G.-H., Lapierre, L.A., Goldenring, J.R., Sai, J., and Richmond, A. (2004). Rab11-Family Interacting Protein 2 and Myosin Vb are required for CXCR2 recycling and receptor-mediated chemotaxis. Mol. Biol. Cell *15*, 2456-2469.

Foletti, D.L., Blitzer, J.T., and Scheller, R.H. (2001). Physiological modulation of rabphilin phosphorylation. J Neurosci *21*, 5473-5483.

Gumbiner, B., Stevenson, B., and Grimaldi, A. (1988). The role of the cell adhesion molecule uvomorulin in the formation and maintenance of the epithelial junctional complex. J. Cell Biol. *107*, 1575-1587.

Guo, S., and Kemphues, K.J. (1995). par-1, a gene required for establishing polarity in C. elegans embryos, encodes a putative Ser/Thr kinase that is asymmetrically distributed. Cell *81*, 611-620.

Hales, C.M., Griner, R., Hobdy-Henderson, K.C., Dorn, M.C., Hardy, D., Kumar, R., Navarre, J., Chan, E.K., Lapierre, L.A., and Goldenring, J.R. (2001). Identification and characterization of a family of Rab11-interacting proteins. J Biol Chem *276*, 39067-39075.

Hales, C.M., Vaerman, J.P., and Goldenring, J.R. (2002). Rab11 family interacting protein 2 associates with Myosin Vb and regulates plasma membrane recycling. J Biol Chem *277*, 50415-50421.

Hansen, B.T., Davey, S.W., Ham, A.J., and Liebler, D.C. (2005). P-Mod: an algorithm and software to map modifications to peptide sequences using tandem MS data. J Proteome Res *4*, 358-368.

Ivanov, A.I., Nusrat, A., and Parkos, C.A. (2004). Endocytosis of epithelial apical junctional proteins by a clathrin-mediated pathway into a unique storage compartment. Mol Biol Cell *15*, 176-188.

Kato, M., Sasaki, T., Imazumi, K., Takahashi, K., Araki, K., Shirataki, H., Matsuura, Y., Ishida, A., Fujisawa, H., and Takai, Y. (1994). Phosphorylation of Rabphilin-3A by calmodulin-dependent protein kinase II. Biochem Biophys Res Commun *205*, 1776-1784.

Kemphues, K.J., Priess, J.R., Morton, D.G., and Cheng, N.S. (1988). Identification of genes required for cytoplasmic localization in early C. elegans embryos. Cell *52*, 311-320.

Laemmli, U.K. (1970). Cleavage of structural proteins during the assembly of the head of bacteriophage T4. Nature *227*, 680-685.

Lapierre, L.A., Kumar, R., Hales, C.M., Navarre, J., Bhartur, S.G., Burnette, J.O., Provance, D.W., Jr., Mercer, J.A., Bahler, M., and Goldenring, J.R. (2001). Myosin vb is associated with plasma membrane recycling systems. Mol Biol Cell *12*, 1843-1857.

Le Bivic, A. (2005). E-cadherin-mediated adhesion is not the founding event of epithelial cell polarity in Drosophila. Trends Cell Biol *15*, 237-240.

Le, T.L., Yap, A.S., and Stow, J.L. (1999). Recycling of E-Cadherin: A potential mechanism for regulating cadherin dynamics. J. Cell Biol. *146*, 219-232.

Licklider, L.J., Thoreen, C.C., Peng, J., and Gygi, S.P. (2002). Automation of nanoscale microcapillary liquid chromatography-tandem mass spectrometry with a vented column. Anal Chem *74*, 3076-3083.

Lindsay, A.J., Hendrick, A.G., Cantalupo, G., Senic-Matuglia, F., Goud, B., Bucci, C., and McCaffrey, M.W. (2002). Rab coupling protein (RCP), a novel Rab4 and Rab11 effector protein. J Biol Chem *277*, 12190-12199.

Lindsay, A.J., and McCaffrey, M.W. (2004). The C2 domains of the class I Rab11 family of interacting proteins target recycling vesicles to the plasma membrane 10.1242/jcs.01280. J Cell Sci *117*, 4365-4375.

Link, A.J., Eng, J., Schieltz, D.M., Carmack, E., Mize, G.J., Morris, D.R., Garvik, B.M., and Yates, J.R., 3rd. (1999). Direct analysis of protein complexes using mass spectrometry. Nat Biotechnol *17*, 676-682.

Lock, J.G., and Stow, J.L. (2005). Rab11 in recycling endosomes regulates the sorting and basolateral transport of E-cadherin. Mol Biol Cell.

Lonart, G., and Sudhof, T.C. (2001). Characterization of rabphilin phosphorylation using phospho-specific antibodies. Neuropharmacology *41*, 643-649.

Louvard, D. (1980). Apical membrane aminopeptidase appears at site of cell-cell contact in cultured kidney epithelial cells. Proc Natl Acad Sci U S A *77*, 4132-4136.

Mammoto, A., Ohtsuka, T., Hotta, I., Sasaki, T., and Takai, Y. (1999). Rab11BP/Rabphilin-11, a downstream target of rab11 small G protein implicated in vesicle recycling. J Biol Chem *274*, 25517-25524.

Manza, L.L., Stamer, S.L., Ham, A.-J.L., Codreanu, S.G., and Liebler, D.C. (2005). Sample Preparation and Digestion for Proteomic Analysis Using Spin Filters. Proteomics *In press*.

Marie, N., Lindsay, A.J., and McCaffrey, M.W. (2005). Rab coupling protein is selectively degraded by calpain in Ca 2+-dependent manner. Biochem J.

Miyoshi, J., and Takai, Y. (2005). Molecular perspective on tight-junction assembly and epithelial polarity. Advanced Drug Delivery Reviews *57*, 815-855.

Numata, S., Shirataki, H., Hagi, S., Yamamoto, T., and Takai, Y. (1994). Phosphorylation of Rabphilin-3A, a putative target protein for Rab3A, by cyclic AMP-dependent protein kinase.
Biochem Biophys Res Commun *203*, 1927-1934.

Ojakian, G., and Schwimmer, R. (1988). The polarized distribution of an apical cell surface glycoprotein is maintained by interactions with the cytoskeleton of Madin-Darby canine kidney cells. J. Cell Biol. *107*, 2377-2387.

Prekeris, R., Davies, J.M., and Scheller, R.H. (2001). Identification of a novel Rab11/25 binding domain present in Eferin and Rip proteins. J Biol Chem *276*, 38966-38970.

Prekeris, R., Klumperman, J., and Scheller, R.H. (2000). A Rab11/Rip11 protein complex regulates apical membrane trafficking via recycling endosomes. Mol Cell *6*, 1437-1448.

Straight, S.W., Shin, K., Fogg, V.C., Fan, S., Liu, C.-J., Roh, M., and Margolis, B. (2004). Loss of PALS1 Expression Leads to Tight Junction and Polarity Defects. Mol. Biol. Cell *15*, 1981-1990.

Takei, K., and Haucke, V. (2001). Clathrin-mediated endocytosis: membrane factors pull the trigger. Trends Cell Biol *11*, 385-391.

Umeda, K., Matsui, T., Nakayama, M., Furuse, K., Sasaki, H., Furuse, M., and Tsukita, S. (2004). Establishment and characterization of cultured epithelial cells lacking expression of ZO-1. J. Biol. Chem. *279*, 44785-44794.

van der Sluijs, P., Hull, M., Huber, L.A., Male, P., Goud, B., and Mellman, I. (1992). Reversible phosphorylation--dephosphorylation determines the localization of rab4 during the cell cycle. Embo J *11*, 4379-4389.

Volpicelli, L.A., Lah, J.J., Fang, G., Goldenring, J.R., and Levey, A.I. (2002). Rab11a and myosin Vb regulate recycling of the M4 muscarinic acetylcholine receptor. J Neurosci *22*, 9776-9784.

Wallace, D.M., Lindsay, A.J., Hendrick, A.G., and McCaffrey, M.W. (2002). Rab11-FIP4 interacts with Rab11 in a GTP-dependent manner and its overexpression condenses the Rab11 positive compartment in HeLa cells. Biochem Biophys Res Commun *299*, 770-779.

Wang, D., Buyon, J.P., Zhu, W., and Chan, E.K. (1999). Defining a novel 75-kDa phosphoprotein associated with SS-A/Ro and identification of distinct human autoantibodies. J Clin Invest *104*, 1265-1275.

Yates, J.R., 3rd, Eng, J.K., McCormack, A.L., and Schieltz, D. (1995). Method to correlate tandem mass spectra of modified peptides to amino acid sequences in the protein database. Anal Chem *67*, 1426-1436.

Zeng, J., Ren, M., Gravotta, D., De Lemos-Chiarandini, C., Lui, M., Erdjument-Bromage, H., Tempst, P., Xu, G., Shen, T.H., Morimoto, T., Adesnik, M., and Sabatini, D.D. (1999). Identification of a putative effector protein for rab11 that participates in transferrin recycling. Proc Natl Acad Sci U S A *96*, 2840-2845.

CHAPTER III

DOMINANT NEGATIVE RAB11-FIP2 MUTANTS UNCOVER DIFFERENTIABLE STEPS IN TRANSCYTOSIS

Nicole A Ducharme, Janice A Williams, Asli Oztan,[‡] Gerard Apodaca,[‡] and James R Goldenring

From the Departments of Surgery and Cell & Developmental Biology, Vanderbilt University School of Medicine, Vanderbilt-Ingram Cancer Center and the Nashville VA Medical Center, Nashville, TN 37232. [‡]Cell Biology & Physiology, University of Pittsburgh School of Medicine, Pittsburgh, PA 15261.

Running Title: Dominant negative Rab11-FIP2 Mutants

Key Words: Rab11-FIP2, Rab11a, IgA, trafficking, transcytosis, apical recycling, GP135, early endosome, EEA1, EHD3

Submitted for Publication to American Journal of Physiology – Cell Physiology.

Abstract

Transcytosis through the apical recycling system of polarized cells is regulated by Rab11a and a series of Rab11a-interacting proteins. We have identified a point mutant in Rab11 Family Interacting Protein 2 (Rab11-FIP2) which alters the function of Rab11a-containing trafficking systems. Rab11-FIP2(S229A/R413G) or Rab11-FIP2(R413G) cause the formation of a tubular cisternal structure containing Rab11a and decrease the rate of polymeric IgA transcytosis. The R413G mutation does not alter Rab11-FIP interactions with any known binding partners. Overexpression of Rab11-FIP2(S229A/R413G) alters the localization of a sub-population of the apical membrane protein GP135. In contrast, Rab11-FIP2(129-512) alters the localization of early endosome protein EEA1. Both Rab11-FIP2(S229A/R413G) and Rab11-FIP2(129-512) cause an uncoupling of Rab11a-containing membranes from the microtubule and actin cytoskeletons. The results indicate that Rab11-FIP2 regulates trafficking at multiple points within the apical recycling system.

Introduction

The interaction of cells with their environment is dependent upon their repertoire of plasma membrane proteins including ion channels, ion pumps, and receptors. Regulation of the expression or activity of these proteins at the cell surface can influence cell physiology. Recent studies have focused increasing attention on protein

internalization and recycling as modulators of cell function. In particular, Rab11a, a member of the Rab11 sub-family of small GTPases, is well-established as a regulator of the recycling system. Rab11a is associated with vesicles in the apical portion of epithelial cells near the centrosome and beneath the apical plasma membrane (1).

Rab11a interacts with and is regulated by specific interacting proteins. The exit of cargo from the recycling endosome is dependent upon interaction of Rab11a with the actin motor protein, myosin Vb (2), as well as with a group of proteins, the Rab11 Family Interacting Proteins (Rab11-FIPs). The growing family of Rab11-FIPs currently include: four Rab11-FIP1 proteins (3-5), Rab11-FIP2, Rab11-FIP3 (4), Rab11-FIP4 (6), and Rab11-FIP5 (pp75/Rip11) (7, 8). The Rab11-FIP proteins each interact with Rab11 family members (Rab11a, Rab11b and Rab25) at their carboxyl-termini through predicted coiled-coil regions containing an amphipathic alpha helical Rab binding domain (4, 9). The diversity of multiple Rab11-FIP proteins, all of which bind to Rab11 with similar helices, suggests that each Rab11-FIP may be important in distinct trafficking processes.

In particular, Rab11-FIP2 (FIP2) appears to form a ternary complex with both Rab11a and myosin Vb (10). In addition, FIP2 and Rab11a were redistributed when the microtubule architecture was modified with either taxol or nocodazole, demonstrating a link between the microtubule network and the recycling system (4). FIP2 has an amino terminal C2 domain as well as a carboxy terminal Rab11 binding domain (4). A truncation of FIP2 lacking its amino terminal C2 domain (FIP2(ΔC2)) strongly inhibits plasma membrane recycling, (10). This mutant has been used by us and others to assess proteins utilizing the Rab11a recycling pathway (10-13). Similarly, a mutant myosin Vb

lacking the motor domain, myosin Vb-tail, also acts as a dominant negative mutant and has proven useful in the assessment of trafficking through the Rab11a trafficking pathway (14-17). However, we recently have reported that FIP2 also has a role in the establishment of cell polarity (18). In this study, we sought to confirm our initial hypothesis that FIP2 is involved in the recycling pathway (4) utilizing a newly identified dominant negative mutant of FIP2. Unexpectedly, this mutant has differentiable effects from the previously characterized FIP2 mutant FIP2(ΔC2). The availability of multiple mutants for manipulation of the Rab11a pathway allows a greater appreciation of the complexity of the steps required for trafficking through the apical recycling system.

Materials and Methods

Materials: Rabbit anti-Rab11a (VU57) antibodies were developed against the amino terminus of human Rab11a and were specific for Rab11a versus Rab11b and Rab25 (Lapierre, submitted). The other antibodies used were rat anti-ZO-1 ([1:200]; Chemicon), mouse anti-G97 ([1:1000]; CDF4, Invitrogen), and mouse anti-EEA1 ([1:100]; 610457, BD Transduction). All secondary antibodies were from Jackson Immuno Research. Dr. Roy Zent of Vanderbilt University kindly provided mouse monoclonal anti-GP135 [1:100]. The cytoskeletal manipulation drug were Cytochalasin D and Nocodazole (Calbiochem). EHD1 and EHD3 cDNA sequences were a gift of Dr. Steven Caplan.

Site directed mutagenesis: All site-directed mutagenesis of Rab11-FIP2 was performed using Pfu Turbo polymerase according to the QuikChange Site-Directed Mutagenesis Kit from Stratagene (La Jolla, CA) with a 16 minute extension time. Primers were

synthesized (Invitrogen) with one nucleotide change per oligonucleotide sequence. All site-directed mutants were created in pEGFP-C2 (Clontech) and subsequently recloned into pET-30a (Novagen) with EcoRI and SalI restriction sites.

Cell Culture: Parental T23 MDCKs (19) as well as the stably transfected cell lines were grown in D-MEM supplemented with 10% fetal bovine serum (Gibco), penicillin-streptomycin, 2mM L-glutamine, and 0.1 mM MEM non-essential amino acids (Gibco/BRL). Media for cell lines also contained 0.5mg/ml G418 sulfate (Cellgro), and 0.25ng/ml hygromycin (Invitrogen). In the stable cell lines, expression of the EGFP chimeras was inhibited with doxycycline ([20ng/ml]; Calbiochem). To examine EGFP protein expression, cells were grown on 0.4 μm Transwell filters (Costar) without doxycycline in tetracycline screened fetal bovine serum (HyClone) media for 2-4 days.

GFP constructs and transfections: Doxycycline-inhibitable expression vectors were generated by excising the FIP2 wild type and mutant sequences from pEGFP-vectors with NheI and SmaI and ligating into a pTRE2hyg vector (Clontech) cut with NheI and EcoRV. Transfection was performed using Effectene (Qiagen) following the manufactures protocol. One μg of vector was transfected into a 60 mm plate of T23 MDCK cells in normal media. The following day, the cells were trypsinized and replated in serial dilutions including 0.25 ng/ml hygromycin for selection and 20ng/ml doxycycline for suppression of EGFP expression. Multiple colonies were selected, expanded for 10 days, and then screened for EGFP expression in media with tetracycline screened serum. Multiple clones were initially characterized, all of which showed similar expression patterns and levels of the EGFP construct. One clone was selected for each

construct to use as the tetracycline-repressible stable cell lines (expressing FIP2 wild type, FIP2(ΔC2), FIP2(S229A), FIP2(R413G) or EGFP-Rab11FIP2(SARG)).

Electron microscopy procedures: Cells were plated on Costar clear Transwell filters and allowed to polarize for 4-5 days. The cells were washed twice in PBS prior to fixing in 4% gluteraldyhe, 0.1 M Cacodylate buffer and PBS for 1 hour on ice. Following fixation, the cells were washed twice in 0.1 M Cacodylate buffer and 1XPBS. After washing, the filters with the cells were excised from the Transwell and rolled into a cylindrical tube and tied with a strand of hair to prevent unraveling. Once rolled into tubes, the filters were transferred to 1.5ml eppendorf tubes and fixed for 2 hours on ice in 1% osmium tetraoxide and 0.1 M Cacodylate buffer. Next, the cells were washed once with 0.1 M Cacodylate buffer followed by an ethanol dehydration series with 10-minute incubations on ice. Following the final 100% ethanol dehydration, the samples were rocked and incubated in equal volumes of 100% ethanol and Spurrs resin for at least 8 hours, then incubated in a 1:2 ratio of 100% ethanol and Spurrs resin for another 8-16 hours before undergoing two 8 hour pure resin incubations. Transwell filters were then transferred to molds with fresh resin and allowed to polymerize 24-48 hours at 65°C. 50-100 nm thick sections were then taken of each filter of cells and collected on 200 nm copper grids. Grids of sections were then stained for 12 minutes in 1% depleted uranyl acetate and washed for 1 minute. After the grids air-dried, they were counter stained with saturated lead citrate for 10 minutes, followed by a 2 minute water wash. The sections were imaged using a Philips CM12 electron microscope.

Fluorescent Polymeric Immunoglobin A (pIgA) Trafficking in MDCK Cells: Fluorescent labeling of pIgA and trafficking experiments were done as previously described described

(10) except that we used the cell culture media described above. Cells were loaded from the basolateral side and fixed at times 0 and 40 minutes following a 15 minute loading incubation.

Analysis of [^{125}I]IgA Postendocytotic Fate: [^{125}I]IgA was iodinated using the ICl method to a specific activity of 1.0-2.0 x 10^7 cpm/μg (20). The postendocytotic fate of a preinternalized cohort of [^{125}I]IgA (at 5-10 μg/ml) that was transcytosed was analyzed as described previously (21). In brief, filter-grown MDCK cells expressing the various Rab11-FIP2 constructs and wild-type pIgR were cultured in the presence or absence of doxycycline, and [^{125}I]IgA internalized from the basolateral cell surface of the cells for 10 min at 37˚ C. The basal surface of the cells were rapidly washed three-times, the apical and basolateral medium aspirated, and replaced with fresh medium. The cells were then incubated for 3 min at 37˚ C. This wash procedure takes 5 min at 37˚ C. Fresh medium was added to the cells and they were chased for up to 2 h at 37˚ C. At the designated time points, the apical and basolateral media (0.5 ml) were collected and replaced with fresh media. After the final time point, filters were cut out of the insert and the amount of [^{125}I]IgA quantified with a gamma counter.

The postendocytic fate of apically internalized [^{125}I]IgA was essentially as described above. However, following ligand internalization the apical surface of the cells were treated three times for 10 min with 100 μg/ml trypsin at 4 °C to strip surface bound ligand. The cells were then treated with 125 μg/ml soybean trypsin inhibitor for 10 min at 4 C (22). The postendocytic fate was determined as described above.

Statistical Significance: Two-way ANOVA with a Bonferroni post-hoc test was performed using GraphPad Prism version 4 for Macintosh, GraphPad Software, San

Diego, California USA, www.graphpad.com. The quantified trafficking numbers were assessed for statistically significant differences between each cell line with and without doxycycline in the media for either apical and basolateral media collection. If a statistically significant difference was found by ANOVA between the two conditions, the differences at each individual time point were assessed using the post-hoc test.

Immunofluorescence: Cells grown on Transwell filters were washed three times with PBS and then fixed in 4% paraformaldehyde for 15 minutes at room temperature. The cells were washed twice with PBS and stored at 4° in PBS until staining. Cells were blocked with extraction buffer (10% normal donkey serum, 150 mM NaCl, 20 mM sodium phosphate, pH 7.4, 0.3% TritonX-10) for twenty minutes. Primary antibody was added in antibody buffer (10% normal donkey serum, 150 mM NaCl, 20 mM sodium phosphate, pH 7.4, 0.05% Tween-20) for 2 hours. Secondary species-specific Cy dye-labeled anti-IgGs were added for 1 hour in antibody buffer. After washing with PBS two times, filters were cut out of the Transwells. These filters were washed once more in PBS and mounted with Prolong Antifade solution (Molecular Probes). Cells were imaged on a Zeiss LSM510 confocal microscope using a 100X lens. Z-sections were 0.5 microns.

Manipulations of the cytoskeleton: Manipulations of the microtubule cytoskeleton (1) were performed as previously described. Briefly, for assessment of the microtubule network, polarized cells were incubated at 4˚ C for 30 minutes. Nocodazole was added in a final concentration of 33µM for 30 minutes at 4˚ C. The cells were then moved to 37˚ C for an hour prior to fixation. For manipulation of the actin network, cells were incubated with cytochalasin D at a final concentration of 2 µM for 2 hours at 37˚ C.

Results

Isolation of a new Rab11-FIP2 mutant

We isolated a mutant FIP2 construct, FIP2(S229A/R413G) (hereafter referred to as SARG), through a spontaneous mutation at R413 when constructing FIP2(S229A) as a control for previous studies (18). FIP2(SARG) was accumulated in pleomorphic tubular cisternae which were acentrically located in the subapical region (Figure 20A). This tubular structure was in contrast to our previously characterized dominant negative FIP2 mutant, FIP2(ΔC2), a FIP2 construct lacking the C2 domain (10), which localizes as a central subapical ring. Following identification of the double mutant, we assessed the effects of each single mutant in stable cell lines. FIP2(S229A) has no discernible effect on the morphology of the recycling system, with EGFP labeled vesicles scattered throughout the subapical region as we have previously seen with overexpression of wild type FIP2 (Figure 20A) (4, 18). In contrast, FIP2(R413G) had a severe phenotype with collection of the EGFP in tubular cisternae. These results suggested that the FIP2(R413G) mutation was responsible for the altered morphology seen in the double mutant. The cells expressing FIP2(R413G) were difficult to maintain in a uniform monolayer in culture on Transwell filters. Therefore, we utilized the more uniform pattern found in the double mutant FIP2(SARG) cell line for our further studies (Figure 20A).

Next, we looked specifically at the EGFP patterns of the FIP2(SARG) and FIP2(ΔC2) in the Z axis. The FIP2(SARG) pattern is a long tubular structure that localizes from the apical membrane down towards the nucleus of the cells. In contrast, the FIP2(ΔC2) localizes in a centrally expansive tangle of tubules reminiscent of a donut

shape above the nucleus (Figure 20 B,C). In multiple cloned cell lines expressing Rab11-FIP2(SARG), the size of polarized cells was smaller than in cells expressing Rab11-FIP2(ΔC2). We have previously observed a similar enlarged cell phenotype in MDCK cells overexpressing the constitutively GTP-bound form of Rab11a, Rab11a(S20V) (23).

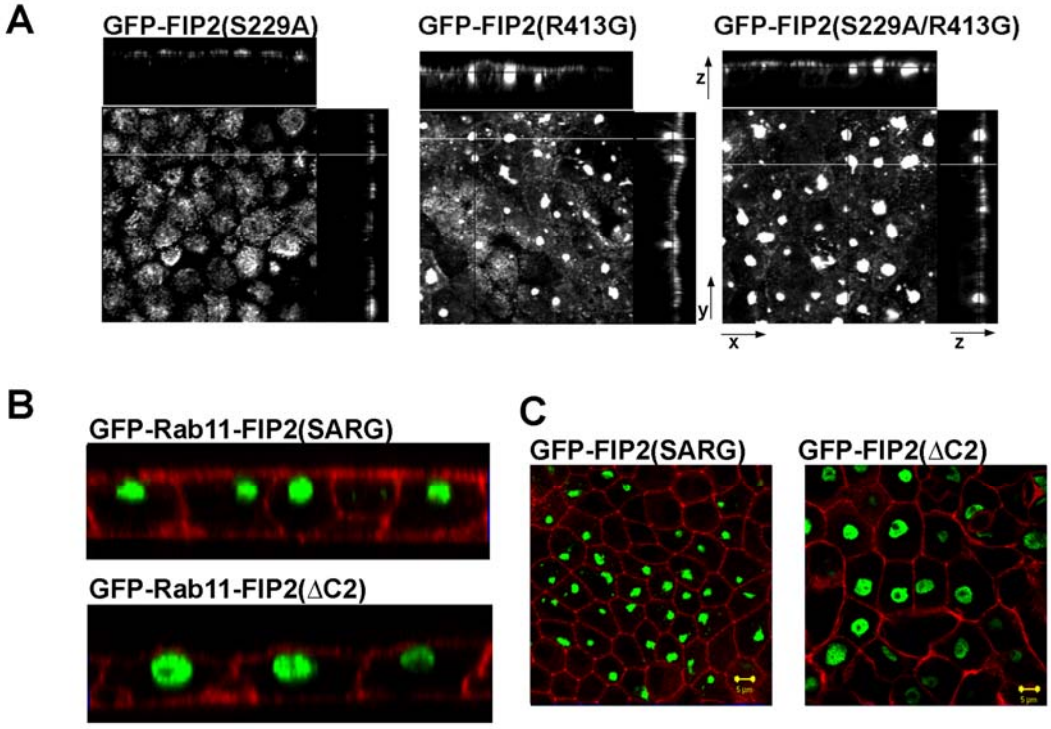

Figure 20: Localization of FIP2 mutants.

A) T23 cells stably expressing each of the mutants (FIP2(S229A), (R413G), (SARG) and (ΔC2)) were imaged by confocal microscopy in the X-Y plane. FIP2(S229A) is indistinguishable from wild type localization. FIP2(R413G) localizes in tight tubular cisternae, but has a non-uniform morphology. FIP2(SARG) always leans towards one corner as tubular cisternae. All images are 100X. B) The FIP2(SARG) and FIP2(ΔC2) cells visualized along the z-axis. 644-phalloidin was pseudo colored red for ease of visualization. Images were taken with a 100x lens with a 3X zoom. C) The relative cell size of the Rab11-FIP2(SARG) mutant was smaller than that of Rab11-FIP2(ΔC2). 644-phalloidin was pseudo colored red for ease of visualization. Images were taken with a 100X objective. Scale bars are 5 μm.

To gain a better understanding of the morphological features of the Rab11-FIP2 mutants, we analyzed the FIP2(ΔC2), FIP2(SARG), and FIP2 wild type cell lines using

transmission electron microscopy (Figure 21). Electron microscopic images demonstrated that both Rab11-FIP2 mutants induced extensive tubular systems within the apical region of the cells. While vesicular elements were always observed throughout the apical region of MDCK cells expressing wild type Rab11-FIP2, no extensive tubular elements were observed.

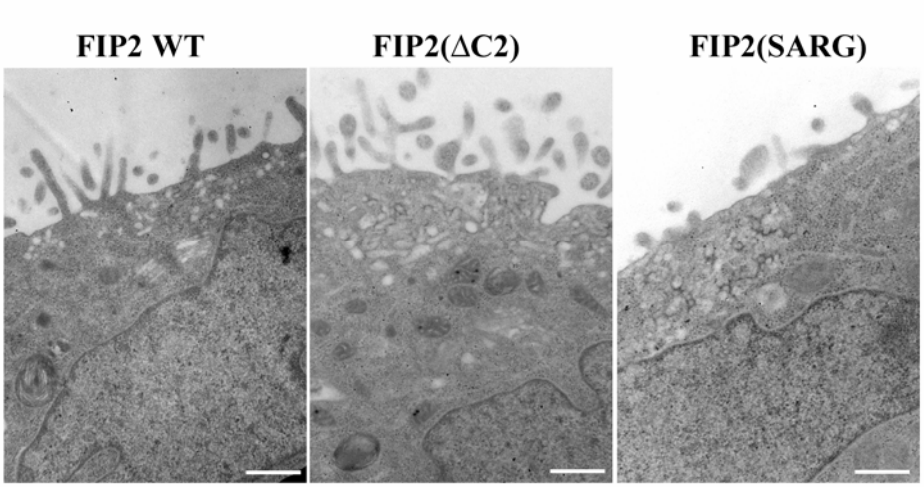

Figure 21: FIP2 mutants show a tangle of tubules by electron microscopy.

T23 cells stably expressing wild type FIP2, FIP2(SARG), or FIP2(ΔC2) were imaged by transmission electron microscopy. Both mutants showed a complex tubular system in the apical region of the cells compared to the wild type cells. Scale bars are 500 nm.

FIP2(SARG) alters localization of traditional components of the recycling system

One potential mechanism to explain the dominant negative phenotype of the FIP2(SARG) mutations is an uncoupling from the other components of the recycling system such as Rab11a. However, we observed that Rab11a colocalized in the tubular cisternae with FIP2(SARG) (Figure 22) and FIP2(R413G) (data not shown). We also observed colocalization of endogenous Rab11-FIP1A and Rab11-FIP5 with FIP2(R413) (data not shown). To assess whether the R413G mutation could alter the interaction of FIP2 with either Rab11a or myosin Vb, we performed yeast two-hybrid binary assays

with both FIP2(R413G) and FIP2(SARG). We observed no differences in interactions with either Rab11a or the tail of myosin Vb (data not shown).

Others have reported that Rab11a localizes at the Golgi apparatus in non-polarized CHO cells but not in MDCK cells (24). In order to assess if FIP2(SARG) accentuated this Golgi associated population of Rab11, we assessed potential colocalization with Golgin-97. However, FIP2(SARG) did not associate with the Golgi population marked by Golgin-97 (Figure 22). Thus, the FIP2(SARG) construct does not cause a collapse of the recycling endosome into the Golgi apparatus.

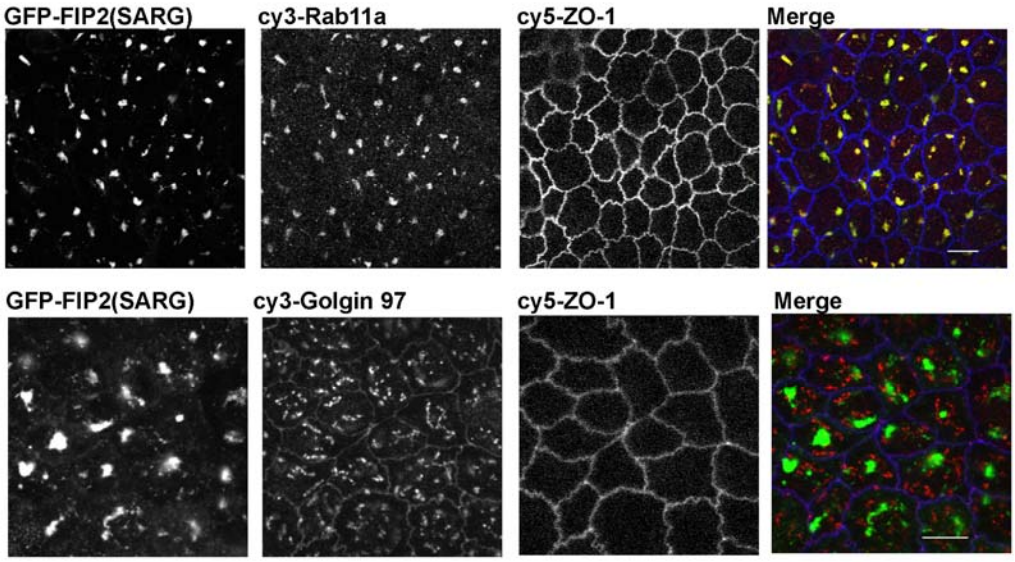

Figure 22: Localization of FIP2(SARG) in relationship to cell markers.

T23 cells stably expressing FIP2(SARG) were stained with antibodies to ZO-1 and either Rab11a (A) or Golgin 97 (B) for immunofluorescence analysis and imaged by confocal microscopy in the X-Y plane. A) Extensive colocalization was seen in T23 cells stably expressing FIP2(SARG) stained for endogenous Rab11a (pseudo-colored red). B) No colocalization of FIP2(SARG) was observed with the Golgi apparatus marker golgin 97 (pseudo-colored red). Expression of the Rab11-FIP2 mutant had no effect on the morphology of the Golgi apparatus. Scale bars are 5 μm.

FIP2(SARG) and FIP2(R413G) decrease the rate of transcytosis

In previous studies, a collapsed cisternal phenotype was associated with decreases in transcytosis. We therefore assessed whether the tubular cisternae of FIP2(SARG) affected the efficiency of trafficking. We examined the ability of the two single and the double Rab11-FIP2 mutants to traffic pIgA. Expression of the FIP2(R413G) mutant resulted in a reproducible decrease in transcytosis (Figure 23). FIP2(SARG) also induced a marked delay in transcytosis through the plasma membrane recycling system (Figure 23). The effects of the two mutants were similar to the inhibition of transcytosis observed in cells expressing FIP2(ΔC2). In addition, expression of FIP2(ΔC2) also appeared to promote basolateral recycling of pIgA. Expression of FIP2(S229A) had no effect on transcytosis. FIP2(R413G) had a slight, but significant decrease on apical recycling. The other three FIP2 mutants did not elicit any apparent effects on the apical recycling of pIgA (Figure 23).

To gain further insights into the inhibition of transcytosis, we visualized IgA trafficking by incubating cells with Alexa568-labeled fluorescent polymeric IgA (Figure 24). When cells were allowed to internalize the fluorescent-IgA from the basolateral medium and then chased for up to 60 minutes, we observed accumulation of IgA containing vesicles in apposition with the EGFP-labeled tubular cisternae in cells expressing either Rab11-FIP2(ΔC2) or Rab11-FIP2(SARG). While in cells expressing Rab11-FIP2(ΔC2), pIgA was present in small vesicles in Rab11-FIP2(SARG) expressing cells, pIgA was present in more tubular structures. These results suggested an alteration of trafficking into or out of the recycling system.

Figure 23: FIP2 mutants (R413G) and (SARG) cause a delay in pIgA transcytosis.

*Graphs showing two representative trials in triplicate of transcytosis of [^{125}I]IgA assessed in stable transfected cell lines in the presence or absence of doxycycline. Transcytosis was delayed in cells overexpressing FIP2(R413G) (right, second graph) or (SARG) (right, third graph) but not in cells overexpressing FIP2(S229A) (right, top graph). FIP2(R413G) had a small, but significant effect on apical recycling (left, second graph). The other three lines showed no effects of FIP2 expression on apical recycling. Close symbols indicated the presence of doxycycline in the media (inhibiting expression of the EGFP-chimera). Open symbols indicate that the cells were incubated in doxycycline-free media allowing for expression of EGFP-chimera proteins. Squares indicate media was collected from the apical side of the transwell. Circles indicate media was collected from the basal side of the transwell. Data was mean +/- SD (n=2, performed in triplicate). Error bars are included for each data point showing +/- one standard deviation. Statistical significance was assessed with two-way ANOVA tests between each cell line with and without doxycycline at each time point as described in materials and methods. * indicates $p<0.05$; ** indicates $p<0.01$; *** indicates $p<0.001$*

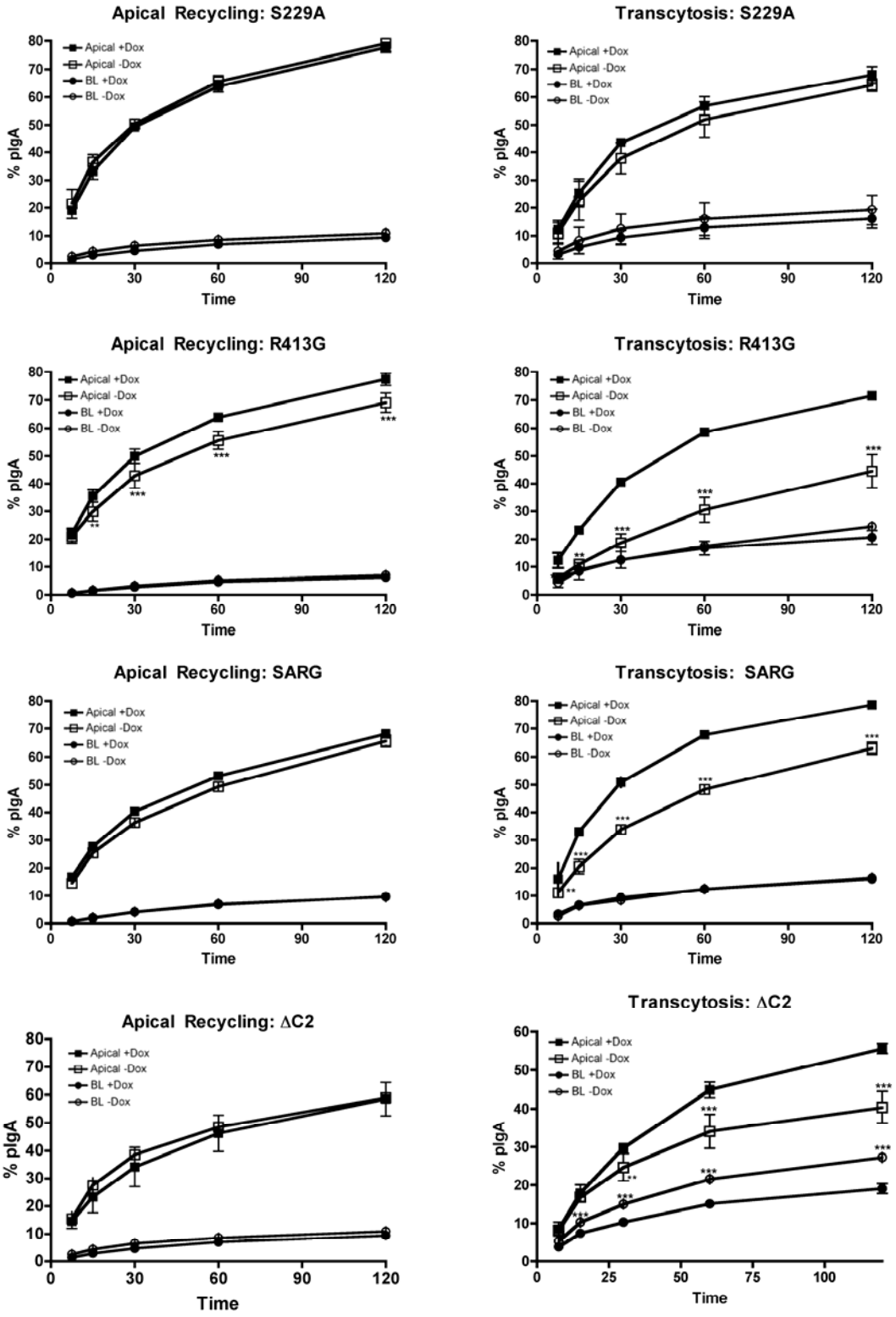

Figure 23: FIP2 mutants (R413G) and (SARG) cause a delay in pIgA transcytosis

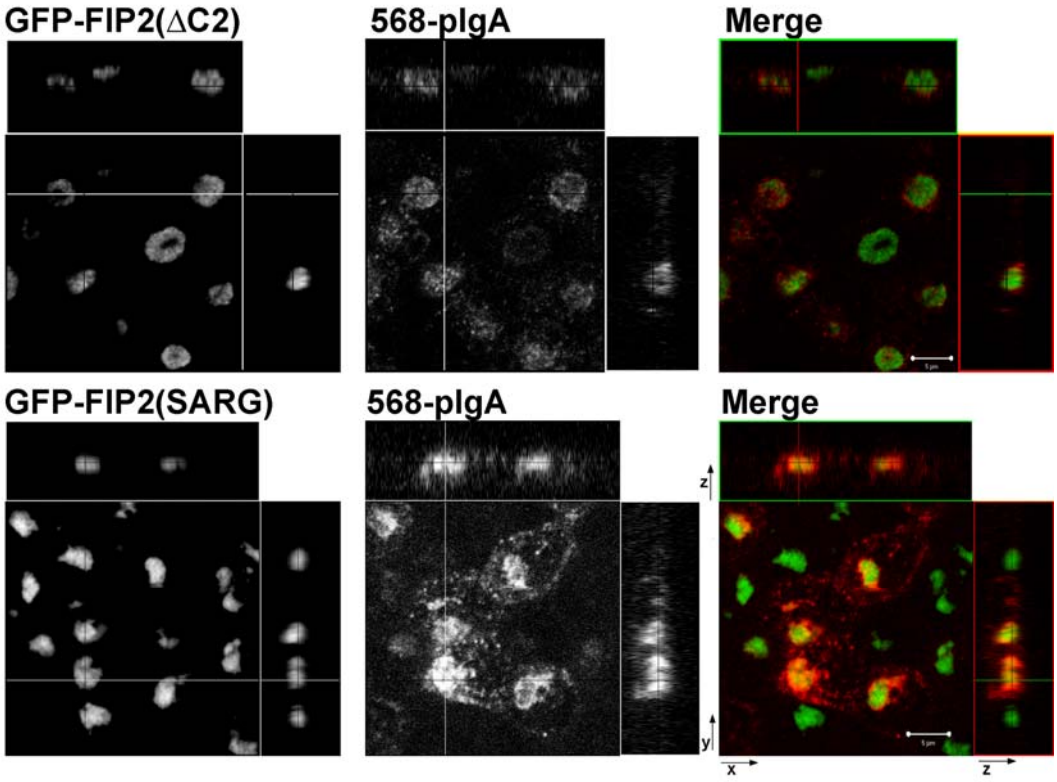

Figure 24: FIP2 mutants (ΔC2) and (SARG) cause an aggregation of pIgA containing vesicles.

Alexa568-pIgA was loaded into stably transfected cell lines expressing FIP2(SARG) or FIP2(ΔC2). The presence of both mutants delayed transcytosis as evidenced by the localization with pIgA containing vesicles around the tubular cisternae after a 30 minute chase. Images were taken with a 100X objective lens with a 3X zoom. Scale bars are 5 μm.

Differentiable effects of FIP2(SARG) from previously characterized dominant negative mutants.

We and others have used the dominant negative construct FIP2(ΔC2) to investigate regulators of cargoes within the apical recycling pathway. The FIP2(SARG) mutant has effects on the recycling system that are distinctly separate from the FIP2(ΔC2) mutant. Figure 25 demonstrates that FIP2(ΔC2) alters the morphology of the early endosomal system marked by the Rab5 interacting protein, EEA1. EEA1 does not colocalize with FIP2(ΔC2), but the EEA1 containing early endosomes appear more

centrally clustered around the EGFP-labeled tubular cisternae. However, this alteration was not seen in FIP2(SARG) cells, thus providing additional evidence that this mutant is not simply causing a collapse of the entire endosomal pathway.

We also compared the effects of Rab11-FIP2 trafficking mutants on apical membrane trafficking. GP135 is a traditional marker for the apical membrane in MDCK cells (25). FIP2(SARG) expressing cells demonstrated a partial accumulation of GP135 within the tubular cisternae. No accumulation of GP135 was seen in FIP2(ΔC2) expressing cells (Figure 26). These results indicate that Rab11-FIP2(SARG), but not Rab11-FIP2(ΔC2), can alter either recycling or de novo trafficking of GP135.

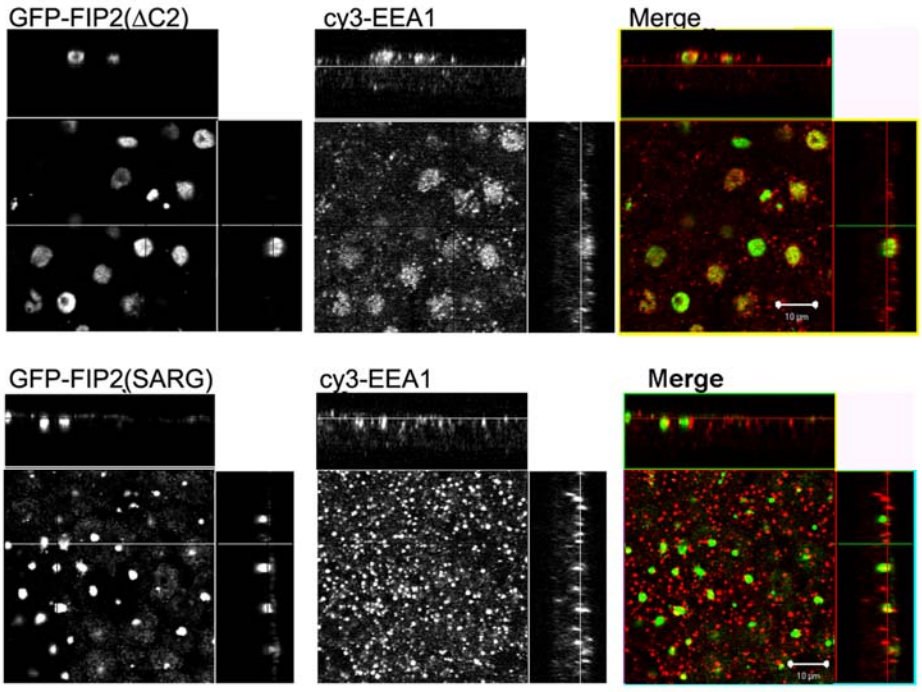

Figure 25: FIP2(ΔC2) causes an aggregation of EEA1 that does not occur in FIP2(SARG).

T23 cells stably expressing FIP2(SARG) and FIP2(ΔC2) were stained with antibodies to EEA1 for immunofluorescence analysis and imaged by confocal microscopy in the X-Y plane.. The EEA1 positive early endosomes (pseudo colored red) showed a collapse towards the FIP2 containing cisternae in cells over-expressing FIP2(ΔC2) but not in cells expressing FIP2(SARG). Scale bars are 10 μm

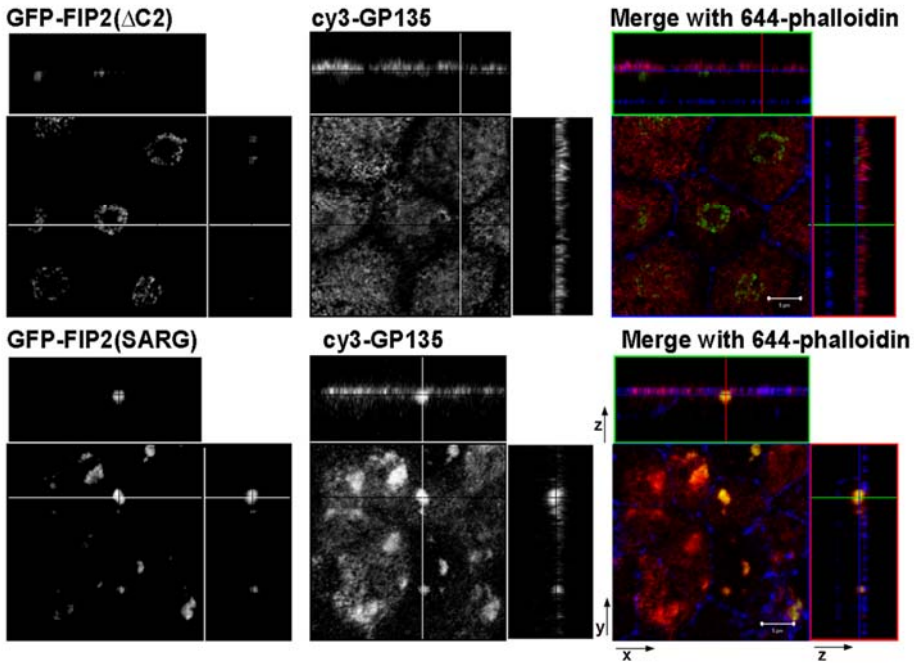

Figure 26: GP135 Accumulates with FIP2(SARG) but not the previously characterized dominant negative FIP2 mutant, ΔC2.

T23 cells stably expressing FIP2(SARG) and FIP2(ΔC2) were stained with antibodies GP135 for immunofluorescence analysis and imaged by confocal microscopy in the X-Y plane. Endogenous GP135 (pseudo colored red) was partially accumulated into the sub-apical extension of the FIP2(SARG) containing structure, but not into the FIP2(ΔC2) collapsed structures. 644-phalloidin was included in the merge image to highlight relative localization within the cell. Scale bars are 5 μm. Images were taken with a 100X lens with a 3X zoom.

FIP2(SARG) is uncoupled from the microtubule and actin cytoskeletal networks

To understand more fully the mechanism behind the reduced efficiency of transcytosis, we assessed the effects of manipulation of the cytoskeleton on the FIP2(SARG) tubular cisternae and on the FIP2(ΔC2) collapsed recycling system. Previous studies had shown that stabilization of microtubules with taxol causes relocation of the Rab11a-containg recycling endosomes to one subapical corner of polarized MDCK cells (2). However, taxol did not alter localization of either FIP2(SARG) or FIP2(ΔC2) (data not shown). Furthermore, disruption of microtubules with nocodazole treatment did

not affect the localization of either FIP2(SARG) or FIP2(ΔC2) (Figure 27). In contrast, the localization of FIP2 wild type in cells was affected by both treatments as we have previously reported (data not shown) (4).

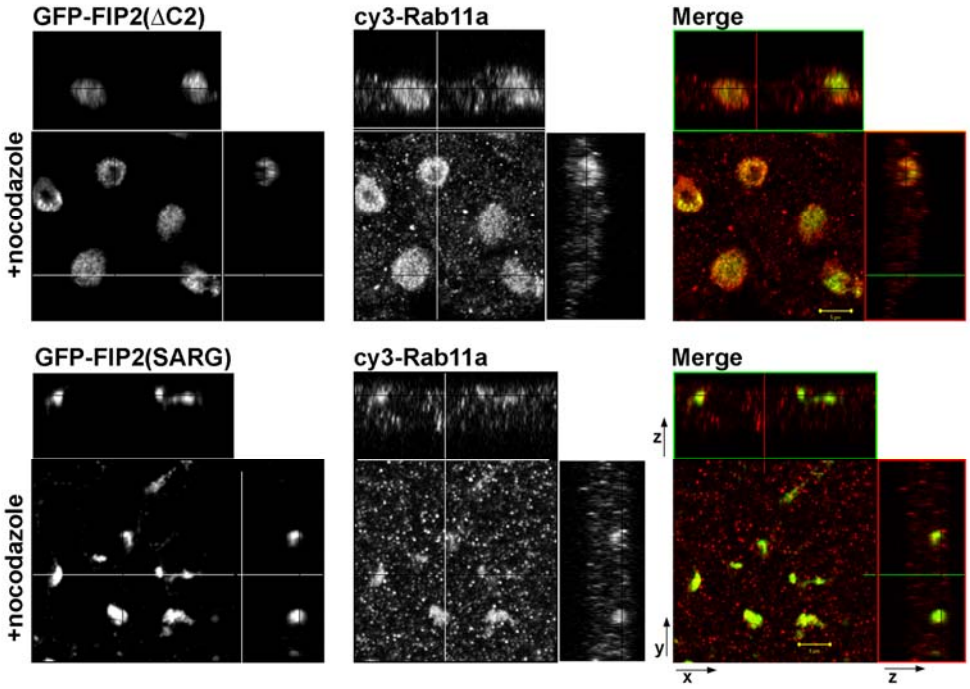

Figure 27: FIP2(SARG) and FIP2(ΔC2) are uncoupled from the microtubule network.

T23 cells stably expressing FIP2(SARG) and FIP2(ΔC2) were treated with nocodazole and stained with antibodies to Rab11a for immunofluorescence analysis imaged by confocal microscopy in the X-Y plane. Disruption of the microtubule network with nocodazole did not alter localization of the FIP2 mutants. Endogenous Rab11a (pseudo-colored red) is also maintained in the EGFP-FIP2 structures. Images were taken with a 100X lens with a 3X zoom. Scale bars are 5 μm.

Because Rab11-FIP2 associates in a ternary complex with the actin motor myosin Vb and Rab11a, we examined the potential dependence of FIP2(SARG) localization on the actin microfilament network. Neither treatment with cytochalasin D (Figure 28) nor treatment with latrunculin B (data not shown) altered localization of the FIP2(SARG)

tubular cisternae. This independence from the actin cytoskeleton was also apparent in the FIP2(ΔC2)-expressing cell line (Figure 28). To confirm that the actin cytoskeleton was affected, we stained with phalloidin and saw the expected disruption of the network (data not shown). We also analyzed the localization of Rab11-FIP1 and Rab11-FIP5. Both Rab11-FIP2 mutants maintained their localization with these other Rab11-FIPs despite manipulation of the cytoskeletal networks (data not shown). Thus, expression of either FIP2(SARG) or FIP2(ΔC2) uncoupled the complex from both the actin and microtubule networks.

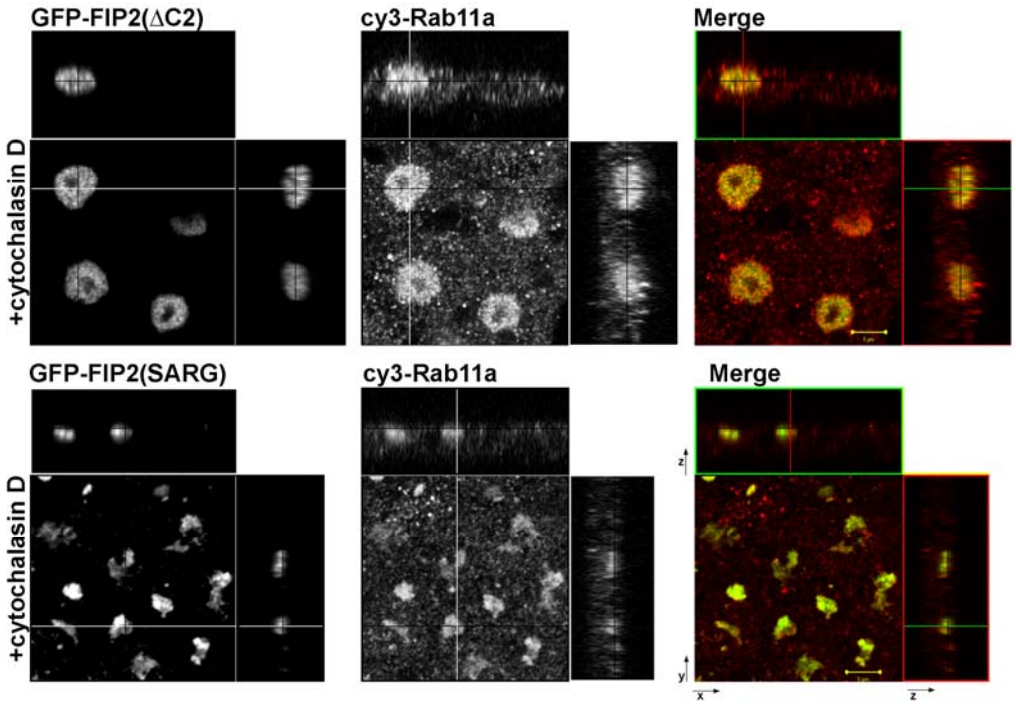

Figure 28: FIP2(SARG) and FIP2(ΔC2) are uncoupled from the actin network.

T23 cells stably expressing FIP2(SARG) and FIP2(ΔC2) were treated with cytochalasin for two hours and stained with antibodies to Rab11a for immunofluorescence analysis and imaged by confocal microscopy in the X-Y plane. Disruption of the actin cytoskeleton with cytochalasin did not alter localization of the FIP2 mutants or their association with Rab11a (pseudo-colored red). Images were taken with a 100X lens with a 3X zoom. Scale bars are 5 μm.

FIP2(SARG) does not alter interactions with EHD proteins

Galperin *et al* have suggested that Eps15 homology domain 3 protein (EHD3) containing vesicles may regulate vesicular microtubule-dependent movement (26). Since previous studies have reported that Rab11-FIP2 interacts with the Eps15 homology domain containing proteins EHD1 and EHD3 (27) and we observed an uncoupling of FIP2(SARG) from the microtubules, we examined the effect of the FIP2(SARG) mutant on these interactions. We found that FIP2(SARG) is able to associate with endogenous EHD1 by immunoprecipitation (data not shown). We visualized associations with EHD proteins through transfection into FIP2(SARG) and FIP2(ΔC2) expressing cells (Figure 29). EHD1 showed extensive colocalization with the cisternal accumulations in both Rab11-FIP2 mutant cell lines (data not shown). In addition, a portion of the overexpressed EHD3 population accumulated in the FIP2(SARG) and FIP2(ΔC2) tubular structures (Figure 29).

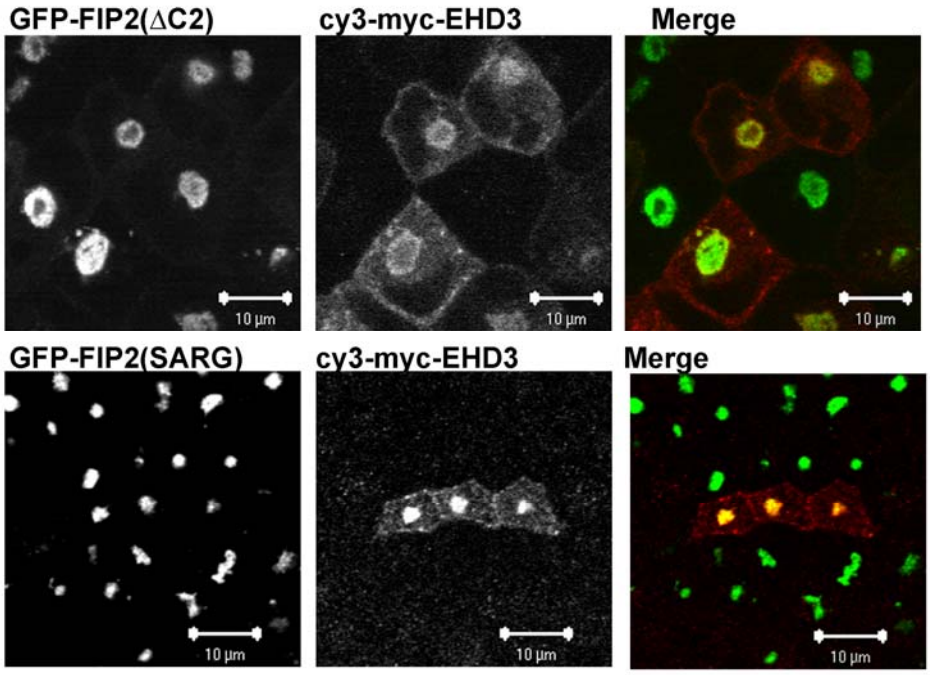

Figure 29: Dominant negative FIP2 mutants do not alter association with EHD3.

Cell stably expressing EGFP-tagged mutants were co-transfected with myc-EHD3 (pseudo-colored red). A portion of the EHD3 population localizes with the collapsed EGFP-mutant structures. Images were taken with a 100X lens. Scale bars are 10 µm

Discussion

Mutations of key proteins within trafficking pathways have led to important insights into the processes of intracellular trafficking in systems ranging from yeast to mammalian cells (2, 28, 29). We have serendipitously isolated a novel FIP2 mutant, FIP2(SARG), which acts as a dominant negative inhibitor of trafficking through the recycling system. Previous reports have noted dominant negative trafficking inhibitors including the truncation of myosin Vb and various carboxyl terminal Rab11-FIP truncations for expression of the Rab11-binding domain helix. All of these truncations of Rab11-interacting proteins have elicited phenotypes with varying levels collapse of the

recycling system into perinuclear tubular cisternae. Nevertheless, the morphologies induced by these trafficking inhibitors, especially in polarized MDCK cells are phenotypically distinct, suggesting differentiable effects on the process of plasma membrane recycling. Thus, the FIP2(SARG) and FIP2(R413G) mutants cause the formation of an eccentrically located and pleomorphic tubular structure. In contrast with previous truncated versions of FIP2, which might have also had effects on general Rab11-FIP function due to the over-expression of Rab11-binding domains, the point mutants of FIP2 are likely specific for FIP2 function. Over-expression of wild type FIP2 does not cause a collapsed or inhibited recycling system phenotype. Thus, the differential effects of the R413G mutation in FIP2 demonstrate the importance of this protein in regulating transcytotic trafficking in polarized MDCK cells.

The inhibitory effects on FIP2 action appear to accrue from the Rab11-FIP2(R413G) mutation. We have utilized the cell lines expressing the dual S229A/Rab11-FIP2(R413G) mutant for a number of our studies on apical recycling system morphology, since the cell lines expressing the single mutation demonstrated significant cell shape alterations over time. Both of these point mutants have a pronounced inhibitory effect on trafficking of pIgA in transcytosis assays, a critical Rab11a-directed pathway (4). While the FIP2(SARG) double mutant exhibited a somewhat lower level of inhibition compared to the single R413G mutant, all of the effects on the morphology of the recycling system were similar. This collapsed cisternal structure displayed differentiable characteristics compared with the previously characterized FIP2(ΔC2) mutant cell lines. While the FIP2(SARG) localization was a tighter, more junctionally-located tubular structure, the FIP2(ΔC2) localized in a donut

shape near the middle of the subapical region. Electron microscopy confirmed that these structures were tubular tangles and not multi-vesicular bodies. The altered shapes of these two inhibited recycling systems suggest that the mutants result in different levels of membrane retention within the recycling endosomes.

FIP2(SARG) has effects on the plasma membrane recycling system that are separable from those of FIP2(ΔC2) (10) or myosin Vb tail (2), two previously characterized dominant negative Rab11a trafficking mutants. In direct comparison with FIP2(ΔC2), we noticed that the stages of the pathway affected appeared morphologically distinct. The ring shape of FIP2(ΔC2) is different from the tight cisternal tubules seen with FIP2(SARG). The stage of the pathway affected by these mutants was also distinguishable by the localization of the EEA1 positive early endosomes. Cells expressing FIP2(ΔC2) showed a redistribution of EEA1 positive early endosomes that was not apparent in FIP2(SARG) expressing cells, suggesting that these two mutants affect different aspects of the FIP2 pathway. The FIP2(ΔC2) mutant appears to alter a broader range of steps in the Rab11a pathway, while the FIP2(SARG) mutant may impact later events in the pathway. Nevertheless, it is important to note that both overexpressed FIP2(ΔC2) and FIP2 mutants carrying the R413G mutation appear to inhibit transcytosis by inhibiting passage of trafficking vesicles through the recycling system. Thus, IgAR containing vesicles accumulate in apposition with the tubular system containing Rab11a. This failure of membranes to move into and through the recycling system may reflect the general uncoupling of recycling system membranes from the cytoskeleton. Thus, treatment with either nocodazole or cytochalasin had no effect on the morphology of FIP2(SARG) or FIP2(ΔC2)-containing tubular cisternae. The inhibition of trafficking

therefore accrues either through blockade of trafficking into Rab11a-containing membranes or a sequestration of Rab11a and Rab11a-dependent effectors with the FIP2 mutants.

Analysis of the data presented here suggests that FIP2 is involved in multiple stages in passage through the Rab11a associated recycling system. The alteration of the early endosomes with the FIP2(ΔC2) mutant suggests that FIP2 may be involved in an early hand off stage. In contrast, the accumulation of GP135 with FIP2(SARG) but not with FIP2(ΔC2) suggests that some recycling cargoes may enter the recycling system at different points within the tubular recycling system. Multiple points of entry into the Rab11a/ FIP2 recycling system may be exploited depending upon the origin of the protein and possibly, its destination. This model supports a dynamic vision of the recycling system trafficking. The R413G mutant of FIP2 had a small but significant effect on apical recycling. While we have previously reported that cells over-expressing FIP2(ΔC2) showed a small decrease in apical recycling, in the present studies, using more quantitative methods here, we were unable to demonstrate a significant effect on apical recycling across the entire time of trafficking. However, it is important to note that the presence of IgAR in the apical recycling pathway in MDCK is an ectopic scenario and may not be analogous to all apical recycling pathways for endogenous cargoes. The FIP2(ΔC2) mutant can inhibit apical recycling of aquaporin-2 in collecting duct cells (30). Therefore, processing through apical recycling systems is likely cell and cargo dependent.

The precise mechanism responsible for inhibition of transcytosis by FIP2(R413G) mutants remains unclear. The FIP2(R413G) and FIP2(SARG) mutants retain their ability

to bind Rab11a and myosin Vb, as assessed by yeast two hybrid analysis. EHD1 and EHD3 both previously regulate plasma membrane recycling and can interact with FIP2 (26, 27, 31). However, FIP2 mutants can still alter the distribution of EHD1 and EHD3. We have found that both FIP2(ΔC2) and FIP2(SARG) are uncoupled from both the actin and microtubule cytoskeletal networks. Thus, disruption of microtubules or actin filaments did not alter the morphology of the collapsed recycling system. Given these findings it is tempting to speculate that FIP2(R413G) causes stabilization of protein complexes regulating apical recycling system trafficking. Similar inhibition of plasma membrane through stabilization of complexes was recently suggested for overexpression of a combination of cytLEK1 and SNAP25 (15). A number of studies including this work have suggested that trafficking through the recycling system may be regulated by multiple handoffs between regulatory complexes defining discrete subdomains within the plasma membrane recycling system (5). Thus stabilization of regulatory complexes may be a potent mechanism for inhibition of trafficking through the complex tubular recycling system.

Acknowledgments

We thank Dr. Roy Zent for the gift of antibody reagents and Dr. Steven Caplan for the gift of EHD1 and EHD3 cDNAs. Confocal images were generated through the use of the VUMC Cell Imaging Shared Resource (supported by NIH grants CA68485, DK20593, DK58404, HD15052, DK59637 and EY08126). This work was supported by NIH National Institute of Diabetes and Digestive and Kidney Diseases (NIDDK) Grants DK-

070856, DK-48370 and DK-43405 (to J.R.G.) and by NIH NIDDK Grants R01 DK-51970 and R37 DK54425 (to G. A.).

Nicole A Ducharme drafted the manuscript and performed the experiments relating to figures 19, 21, 22 and 24-29 as well as the statistical analysis for figure 23. Janice A Williams performed the electron microscopy for figure 20. Asli Oztan and Gerard Apodaca collected the data for the quantified trafficking experiments in figure 23. James R. Goldenring was involved in guiding the experimental design with Nicole Ducharme.

References

1. Casanova JE, Wang X, Kumar R, Bhartur SG, Navarre J, Woodrum JE, et al. Association of Rab25 and Rab11a with the apical recycling system of polarized Madin-Darby canine kidney cells. Mol Biol Cell 1999;10(1):47-61.

2. Lapierre LA, Kumar R, Hales CM, Navarre J, Bhartur SG, Burnette JO, et al. Myosin vb is associated with plasma membrane recycling systems. Mol Biol Cell 2001;12(6):1843-57.

3. Lindsay AJ, Hendrick AG, Cantalupo G, Senic-Matuglia F, Goud B, Bucci C, et al. Rab coupling protein (RCP), a novel Rab4 and Rab11 effector protein. J Biol Chem 2002;277(14):12190-9.

4. Hales CM, Griner R, Hobdy-Henderson KC, Dorn MC, Hardy D, Kumar R, et al. Identification and characterization of a family of Rab11-interacting proteins. J Biol Chem 2001;276(42):39067-75.

5. Jin M, Goldenring JR. The Rab11-FIP1/RCP gene codes for multiple protein transcripts related to the plasma membrane recycling system. Biochim Biophys Acta 2006.

6. Wallace DM, Lindsay AJ, Hendrick AG, McCaffrey MW. Rab11-FIP4 interacts with Rab11 in a GTP-dependent manner and its overexpression condenses the Rab11 positive compartment in HeLa cells. Biochem Biophys Res Commun 2002;299(5):770-9.

7. Prekeris R, Klumperman J, Scheller RH. A Rab11/Rip11 protein complex regulates apical membrane trafficking via recycling endosomes. Mol Cell 2000;6(6):1437-48.

8. Rodriguez OC, Cheney RE. Human myosin-Vc is a novel class V myosin expressed in epithelial cells. J Cell Sci 2002;115(Pt 5):991-1004.

9. Prekeris R, Davies JM, Scheller RH. Identification of a novel Rab11/25 binding domain present in Eferin and Rip proteins. J Biol Chem 2001;276(42):38966-70.

10. Hales CM, Vaerman JP, Goldenring JR. Rab11 family interacting protein 2 associates with Myosin Vb and regulates plasma membrane recycling. J Biol Chem 2002;277(52):50415-21.

11. Fan G-H, Lapierre LA, Goldenring JR, Sai J, Richmond A. Rab11-Family Interacting Protein 2 and Myosin Vb are required for CXCR2 recycling and receptor-mediated chemotaxis. Mol. Biol. Cell 2004;15(5):2456-2469.

12. Lindsay AJ, McCaffrey MW. The C2 domains of the class I Rab11 family of interacting proteins target recycling vesicles to the plasma membrane. J Cell Sci 2004;117(19):4365-4375.

13. Lindsay AJ, McCaffrey MW. Rab11-FIP2 functions in transferrin recycling and associates with endosomal membranes via its COOH-terminal domain. J Biol Chem 2002;277(30):27193-9.

14. Brock SC, Goldenring JR, Crowe JE, Jr. Apical recycling systems regulate directional budding of respiratory syncytial virus from polarized epithelial cells. Proc Natl Acad Sci U S A 2003;100(25):15143-8.

15. Pooley RD, Reddy S, Soukoulis V, Roland JT, Goldenring JR, Bader DM. CytLEK1 Is a Regulator of Plasma Membrane Recycling through Its Interaction with SNAP-25
10.1091/mbc.E05-12-1127. Mol. Biol. Cell 2006;17(7):3176-3186.

16. Volpicelli LA, Lah JJ, Fang G, Goldenring JR, Levey AI. Rab11a and myosin Vb regulate recycling of the M4 muscarinic acetylcholine receptor. J Neurosci 2002;22(22):9776-84.

17. Wakabayashi Y, Dutt P, Lippincott-Schwartz J, Arias IM. Rab11a and myosin Vb are required for bile canalicular formation in WIF-B9 cells. Proc Natl Acad Sci U S A 2005;102(42):15087-92.

18. Ducharme NA, Hales CM, Lapierre LA, Ham AJ, Oztan A, Apodaca G, et al. MARK2 Phosphorylation of Rab11-FIP2 Is Necessary for the Timely Establishment of Polarity in MDCK Cells. Mol Biol Cell 2006.

19. Barth AIM, Pollack AL, Altschuler Y, Mostov KE, Nelson WJ. NH2-terminal deletion of beta -catenin results in stable colocalization of mutant beta -catenin with adenomatous polyposis coli protein and altered MDCK cell adhesion. J. Cell Biol. 1997;136(3):693-706.

20. Breitfeld PP, Casanova JE, Harris JM, Simister NE, Mostov KE. Expression and analysis of the polymeric immunoglobulin receptor in Madin-Darby canine kidney cells using retroviral vectors. Methods Cell Biol 1989;32:329-37.

21. Apodaca G, Katz LA, Mostov KE. Receptor-mediated transcytosis of IgA in MDCK cells is via apical recycling endosomes. J Cell Biol 1994;125(1):67-86.

22. Maples CJ, Ruiz WG, Apodaca G. Both microtubules and actin filaments are required for efficient postendocytotic traffic of the polymeric immunoglobulin receptor in polarized Madin-Darby canine kidney cells. J Biol Chem 1997;272(10):6741-51.

23. Wang X, Kumar R, Navarre J, Casanova JE, Goldenring JR. Regulation of vesicle trafficking in madin-darby canine kidney cells by Rab11a and Rab25. J Biol Chem 2000;275(37):29138-46.

24. Ullrich O, Reinsch S, Urbe S, Zerial M, Parton RG. Rab11 regulates recycling through the pericentriolar recycling endosome. J Cell Biol 1996;135(4):913-24.

25. Ojakian G, Schwimmer R. The polarized distribution of an apical cell surface glycoprotein is maintained by interactions with the cytoskeleton of Madin-Darby canine kidney cells. J. Cell Biol. 1988;107(6):2377-2387.

26. Galperin E, Benjamin S, Rapaport D, Rotem-Yehudar R, Tolchinsky S, Horowitz M. EHD3: A Protein That Resides in Recycling Tubular and Vesicular Membrane Structures and Interacts with EHD1. Traffic 2002;3(8):575-589.

27. Naslavsky N, Rahajeng J, Sharma M, Jovic M, Caplan S. Interactions between EHD Proteins and Rab11-FIP2: A role for EHD3 in early endosomal transport. Mol. Biol. Cell 2006;17(1):163-177.

28. Lillie SH, Brown SS, Naslavsky N, Weigert R, Donaldson JG. Suppression of a myosin defect by a kinesin-related gene. Nature 1992;356(6367):358-61

29. Hume AN, Collinson LM, Hopkins CR, Strom M, Barral DC, Bossi G, et al. The leaden gene product is required with Rab27a to recruit myosin Va to melanosomes in melanocytes. Traffic 2002;3(3):193-202.

30. Nedvetsky PI, Stefan E, Frische S, Santamaria K, Wiesner B, Nielsen S, et al. Myosin Vb regulates recycling of aquaporin-2 in renal principal cells. Traffic 2006;In Press.

31. Cullis DN, Philip B, Baleja JD, Feig LA. Rab11-FIP2, an adaptor protein connecting cellular components involved in internalization and recycling of epidermal growth factor receptors. J Biol Chem 2002;277(51):49158-66.

CHAPTER IV

IDENTIFICATION OF PROTEINS COMPLEXED WITH RAB11-FIP2 REVEALS PROTEINS REGULATING PLASMA MEMBRANE RECYCLING

Nicole A Ducharme, Amy-Joan L. Ham[2], Lynne A Lapierre, and James R Goldenring[3]

From the Departments of Surgery and Cell & Developmental Biology, Vanderbilt University School of Medicine, [2]Department of Biochemistry and Mass Spectrometry Research Center, Vanderbilt University School of Medicine, Vanderbilt-Ingram Cancer Center and the [3]Nashville VA Medical Center, Nashville, TN 37232.

Submitted for publication to Molecular and Cellular Proteomics

Abstract

The Rab11 Family Interacting Proteins (Rab11-FIPs) are hypothesized to mediate sequential interactions in the apical recycling and transcytotic pathways of polarized epithelial cells. Previous studies have suggested that Rab11-FIP proteins assemble into multi-protein complexes regulating plasma membrane recycling. We have utilized an approach combining immunoprecipitation of overexpressed EGFP-Rab11-FIP2 and EGFP-Rab11-FIP2 mutant proteins from stable MDCK cell lines followed by mass spectrometric analysis of isolated proteins to identify proteins complexed with Rab11-FIP2. We analyzed protein complexes from cells expressing Rab11-FIP2 wild type as well as three mutant Rab11-FIP2 constructs, one of which causes a delay in the establishment of polarity while the other two serve as distinguishable dominant negative mutants in the transcytotic pathway. We identified over 400 potential components of Rab11-FIP2 complexes and have validated a subset of them here. We focused on the validation of proteins with clear putative relevance to trafficking: Rab5b, Rab10, epsinR, dynein, IQGAP1, clathrin heavy chain, and AP-1. This proteomic approach to analysis of proteins complexed with Rab11-FIP2 has led to new insights into the regulation of membrane recycling by multiprotein effector complexes.

Introduction

Cells have evolved complex processes to maintain a functional dynamic equilibrium. One of the fundamental tasks of a cell is to interact with its environment. The cell must receive information such as nutrient status in order to ascertain whether to grow, divide, or maintain the status quo. Thus, they must accurately assess life-sustaining requirements such as insulin and oxygen availability exemplified by the activation of the GLUT4 receptor in response to insulin and the recycling of the transferrin receptor for oxygen transport. To respond accurately and relay these signals, the cell has evolved an intricate system for the regulation of receptor expression and activity at the plasma membrane. This pathway begins with the recognition of the stimulus, which initiates an appropriate downstream response. The movement of cellular proteins via vesicle structures between donor and target membranes along the cytoskeleton facilitates many of these interactions, thus allowing coordination and regulation in distinct domains of the cell.

Over the past 10 years, a number of studies have led to the recognition that Rab11 family members regulate the plasma membrane recycling system. Rab11a is apically oriented and localized in discrete epithelial cell populations (1). The polarized cell utilizes an elaborate endosomal structure involving progression through an early sorting endosome, recycling endosome, and apical recycling endosome (ARE) (2). Rab11a containing tubular membranes localize to the ARE near the centrosome beneath the apical membrane. The integrity and function of the ARE is dependent upon intact

microtubules; and destabilization of the microtubule cytoskeleton causes Rab11 positive vesicles to disperse, while stabilization causes aggregation of vesicles near tight junctions (3).

Rab11 family members interact with a group of interacting proteins (Rab11-FIPs) discovered in the past five years: FIP1, FIP2, FIP3 (4), FIP4 (5), FIP5/pp75/Rip11 (6) and FIP1C/RCP (7). They each interact with Rab11 at their carboxyl-termini through predicted coiled-coil regions containing an amphipathic alpha helical Rab11 Binding Domain (RBD) (4, 8). Rab11a also interacts with the tail region of myosin Vb, which is essential for exit from the plasma membrane apical recycling system (9). The members of the Myosin V Family are unconventional myosins, which function in subcellular localization of organelles and intracellular transport (10). Thus, myosin Vb plays an essential role in Rab11a vesicle trafficking. Rab11-FIP2 also interacts with myosin Vb (11), suggesting the formation of a ternary complex between Rab11a, FIP2, and myosin Vb is a critical regulatory complex in plasma membrane recycling. In addition, FIP2 suppresses EGFR uptake and binds alpha-adaptin which associates with clathrin coated pits (12), implying a critical role for FIP2 in early endosomal processing.

We have recently reported the characterization of two dominant negative FIP2 mutants, FIP2(ΔC2) and FIP2(SARG) (13). These two mutants allowed us to identify separable aspects of the roles of FIP2 in polarized MDCK cells. FIP2(ΔC2) caused a aggregation of the EEA1 positive early endosomal system, while FIP2(SARG) altered a later step in the recycling system pathway. In addition, we have recently identified a role for FIP2 in the establishment of polarity via phosphorylation by MARK2 on serine 227 (14). These three roles for FIP2 suggested that additional functions for FIP2 have yet to

be elucidated. Therefore, we undertook an approach utilizing mass spectrometry to clarify the role of FIP2 in polarized epithelial cells. The FIP2(ΔC2) mutant has revealed the necessity of the C2 domain for numerous functional interactions. The FIP2(SARG) mutant interacts with proteins involved in late stages of recycling endosomes, but notably does not interact with many coat proteins. Finally, the wild type FIP2 protein revealed novel interactions with a number protein regulators of membrane trafficking.

Methods

Materials: Rabbit anti-Rab11a (VU57) antibodies were developed against the amino terminus of human Rab11a and were specific for Rab11a versus Rab11b and Rab25 (15). The other commercial antibodies used were goat anti-dynein (Santa Cruz), anti-GFP mouse monoclonal (8362-1 BD), anti-GFP rabbit AB290 (AbCam), anti-clathrin heavy chain (BD Transduction Labs), and anti-AP-1 (Sigma). In addition, we received anti-EpsinR from Margaret Robinson (MRC Laboratory of Molecular Biology) and anti-IQGAP1 from David Sacks (Harvard University).

Vectors: Human Rab5b and Rab10 sequences were amplified from full length human ESTs with Pfu Polymerase (Stratagene) using sense primers with in-frame EcoRI sites and anti-sense primers with SalI sites. The resulting fragments were cloned into pEGFP-C2 (Clontech) and mRFP-C2 (Clontech).

Cell Culture: Doxycycline-inhibitable expression vectors and stable inducible cell lines were generated as previously described (14). Parental T23 MDCKs (16) as well as the stably transfected cell lines described previously (13, 14) were grown in D-MEM

supplemented with 10% fetal bovine serum (Gibco), penicillin-streptomycin, 2mM L-glutamine, and 0.1 mM MEM non-essential amino acids (Gibco/BRL). Media for cell lines also contained 0.5mg/ml G418 sulfate (Cellgro), and 0.25ng/ml hygromycin (Invitrogen). In the stable cell lines, expression of the EGFP chimeras was inhibited with doxycycline (20ng /ml) (Calbiochem). To examine EGFP protein expression, cells were grown on 0.4 μm Transwell filters (Costar) without doxycycline in tetracycline screened fetal bovine serum (HyClone) media for 2-4 days.

Immunoprecipitation for isolation of protein complexes: Anti-rabbit IgG Dynabeads (Dynal) were loaded with either 5 μl of anti-GFP antibody AB290 serum (AbCam) or control rabbit serum for two hours at 4°C. Beads were washed 3 times with TBS. The antibody was cross-linked to the beads using the manufacturer's protocol with slight modifications. Briefly, beads were washed two times with 200 mM Triethaolamine (Sigma) followed by a 30 minute room temperature incubation with 20mM DMP in 200 mM Triethaolamine. The beads were washed with 50mM Tris ph 7.5 followed by a five-minute wash with 20 mM ethanolamine. The beads were washed three times with PBS. Lysate was diluted in PBS with protease inhibitors and phosphatase inhibitors and incubated with the beads overnight at 4°C. The beads were washed one time with PBS, one time with PBS supplemented with 0.1% CHAPS and then twice with PBS. The beads were eluted in 1% SDS buffer and proteins were run until the sample was fully contained in the 10% Bis-Tris Gels (NuPAGE, Invitrogen, Carlsbad, CA). Protein was visualized with colloidal Coommasie blue (GelCode Blue, Pierce) and the protein band was excised and prepared. The samples were analyzed by trypsin triple digestion and LC-MS-MS mass spectrometry.

Mass Spectrometry: LC-MS-MS analysis of the resulting peptides was performed using a ThermoFinnigan LTQ ion trap mass spectrometer equipped with a Thermo MicroAS autosampler and Thermo Surveyor HPLC pump, Nanospray source, and Xcalibur 1.4 instrument control. The peptides were separated on a packed capillary tip, 100 μm x 11 cm, with C_{18} resin (Jupiter C_{18}, 5 micron, 300 angstrom, Phenomonex, Torrance, CA) using an inline solid phase extraction column that was 100μm x 6cm packed with the same C18 resin (using a frit generated with from liquid silicate Kasil 1 (17)) similar to that previously described (18), except the flow from the HPLC pump was split prior to the injection valve. The flow rate during the solid phase extraction phase of the gradient was 1 μL/min and during the separation phase was 700 nL/min. Mobile phase A was 0.1% formic acid, mobile phase B was acetonitrile with 0.1% formic acid. A 95 min gradient was performed with a 15 min washing period (100 % A for the first 10 min followed by a gradient to 98% A at 15 min) to allow for solid phase extraction and removal of any residual salts. After the initial washing period, a 60 minute gradient was performed where the first 35 min was a slow, linear gradient from 98% A to 75 % A, followed by a faster gradient to 10 % A at 65 min and an isocratic phase at 10 % A to 75 min. MS/MS scans were acquired using an isolation width of 2 m/z, an activation time of 30 ms, and activation Q of 0.250 and 30% normalized collision energy using 1 microscan and maximum injection of 100 for each scan. The mass spectrometer was tuned prior to analysis using the synthetic peptide TpepK (AVAGKAGAR). Typical tune parameters were as follows: spray voltage of between 1.8 KV, a capillary temperature of 150ºC, a capillary voltage of 50V and tube lens 100V. The MS/MS spectra of the peptides were acquired using data-dependent scanning in which one full MS spectra, using a full mass

range of 400-2000 amu, was followed by 3 MS/MS spectra. Proteins were identified using a cluster version of the SEQUEST algorithm(Thermo Electron, San Jose, CA; (19) on a high speed, multiprocessor Linux cluster in the Advanced Computing Center for Research at Vanderbilt University, using the canine database from ENSEMBL. The SEQUEST results were then run through Peptide and Protein Prophet of the Trans Proteomic Pipeline (20, 21); http://tools.proteomecenter.org/TPP.php) for the statistical analysis of the peptide and protein matches.

Immunofluorescence: Staining for endogenous protein localization was done as previously described for Rab11a (14). Staining for dynein, IQGAP1, AP-1, and clathrin heavy chain was done as described (22). Briefly, cells were fixed in 70% ethanol for 20 minutes, permeabilized with 0.25% Triton X-100 for 10 minutes, and blocked in 2% BSA in PBS for at least one hour. Primary antibody was added in 1% BSA in a humid chamber overnight. Cells were washed with PBS and then incubated with secondary antibody in 1% BSA for 1 hour. Cells were washed and mounted.

Results

Utilization of immunoprecipated complexes from cell lines to identify proteins interacting with Rab11-FIP2.

We recently published results showing that FIP2 is phosphorylated by MARK2 and that this phosphorylation revealed a new role for FIP2 in the establishment of polarity (14). The involvement in polarity was an unexpected finding given that the FIPs were initially identified and characterized as participating in the Rab11 plasma membrane recycling system (4). Therefore, we sought to identify additional roles for FIP2 in

epithelial cells. We chose to utilize a technique combining immunoprecipitation and mass spectrometry. We utilized our previously characterized cells lines stably overexpressing FIP2 and FIP2 mutants (14). We gently lysed the cells in a buffer containing CHAPS to maintain any complexes associated with FIP2. The soluble lysate was incubated with Dynabeads crosslinked with anti-GFP antibodies to minimize contamination from the antibody in our analysis. The immunoprecipitated complexes were eluted in 1% SDS buffer with DTT and subsequently run approximately 1 cm into a 10% Bis-Tris NU-PAGE gel to stack proteins together. We cut the GelCode Blue stained band of proteins from the gel and digested it with trypsin for mass spectrometric identifications of peptides. This method allowed a clean separation from the sample buffer and a concentration of the sample. We also found that an in-gel digest recovered substantially more peptides than a digest in-solution. A similar protocol was used for parental T23 cells not expressing an EGFP construct to serve as a negative control for proteins that interacted non-specifically with the Dynabeads.

The peptides were analyzed by shot-gun 1-dimensional reverse phase LC followed by tandem mass spectrometry on a linear ion trap LTQ instrument. Three replicate analysis of each cell line was performed. Peptide sequences were compared with the canine database available from Ensembl (http://www.ensembl.org/Canis_familiaris/index.html) to match the peptides to protein sequences. We then compared the proteins found in each of the conditions with each other and with the negative control to ascertain proteins found in a complex with FIP2. We considered hits to be a potential interacting partner if the protein was found in at least two out of three FIP2 runs with a Protein Prophet probability greater than 0.8, but not in

at least two out of three runs using T23 parental cells with the same probability. This approach has revealed a number of novel potential interactions not previously anticipated (Table 3).

We chose to use this approach with four EGFP-Rab11-FIP2 over-expressing cell lines: FIP2 wild type, which identified 1079 peptides that met our criteria; FIP2(S227A), which identified 1897 peptides that met our criteria; FIP2(SARG), which identified 610 peptides that met our criteria; and FIP2(ΔC2), which identified 446 peptides that met our criteria. We hoped that a comparison of wild type cells with the MARK2 phosphorylation mutant, FIP2(S227A), would lend further clarity to the role of this phosphorylation event. We utilized two dominant negative trafficking mutants of FIP2, FIP2(ΔC2) and FIP2(SARG) (13), to dissect further individual components in the FIP2 pathway. While each of the conditions pulled-down FIP2, one of the wild type runs pulled down one peptide unique to canine FIP2, indicating that overexpressed human FIP2 can dimerize with canine FIP2. Overall, we identified 473 potential proteins that may form complexes with FIP2.

Table 3: Proteins in Complex with EGFP-Rab11-FIP2 and its mutants

A subset of proteins found by proteomics to be associated with the overexpressed EGFP-FIP2 cell lines. WT indicates wild type FIP2. 27A refers to FIP2(S227A). SARG refers to FIP2(SARG). C2 refers to FIP2(ΔC2). Xs indicate the protein was found associated with FIP2 by proteomics in that cell line.

Name	WT	27A	SARG	C2
Adapter-related protein complex 1 beta 1 subunit (Beta-adaptin 1)	x	x		
adaptor-related protein complex AP3 beta 1 subunit		x		
adipose differentiation-related protein	x			
A-kinase anchor protein 13 isoform 2	x			
alpha-cop protein	x	x		
Ankyrin 3 (ANK-3) (Ankyrin G)		x		
Annexin A2		x	x	
annexin VII isoform 2			x	
arsenate resistance protein 2		x		
beta prime cop		x		
beta-COP (coatomer protein complex, subunit beta)		x		
Clathrin heavy chain 1 (CLH-17)	x	x	x	x
coatomer protein complex, subunit gamma 1	x	x		
Coatomer zeta-1 subunit (Zeta-1 coat protein) (Zeta-1 COP)			x	
Dynein heavy chain, cytosolic	x	x		x
Endoplasmin (94 kDa glucose-regulated protein) (GRP94)	x	x	x	
epsilon globin	x			
epsilon isoform of 14-3-3 protein			x	
Epsin 4	x	x		
General vesicular transport factor p115 (Transcytosis associated protein) (TAP) (Vesicle docking protein)	x			
glyceraldehyde-3-phosphate dehydrogenase		x		
Host cell factor (HCF) (HCF-1)		x		
interleukin enhancer binding factor 2		x		
Interleukin enhancer-binding factor 3		x		
Keratin, type I cytoskeletal 12				x
KIAA0586		x	x	
Myosin-9	x	x		
Na+/K+ ATPase 1	x	x		
NDRG1 protein (N-myc downstream regulated gene 1 protein) (Differentiation-related gene 1 protein) (DRG1)	x			
proliferation associated gene (pag)		x	x	
Rab-10		x	x	
RAB11 family interacting protein 2	x	x	x	x
Rab-5B		x	x	
Rab-7		x	x	
Ras GTPase-activating-like protein IQGAP1 (p195)	x	x		
Ras-GTPase-activating protein binding protein 2		x		
SAR1a gene homolog 2			x	

Name	WT	27A	SARG	C2
Sec23a protein		x		
SFLQ611	x	x	x	
Spectrin beta chain, brain 1 (Spectrin, non-erythroid beta chain 1) (Beta-II spectrin) (Fodrin beta chain)				x
steroid dehydrogenase homolog		x		
SYNCRIP		x	x	
taste receptor, type 1, member 2			x	
Thioredoxin domain containing protein 1		x		
Thyroid receptor interacting protein 11	x			
TIP120 protein	x	x		
Tubulin	x	x		
Tubulin alpha-4 chain	x	x		
tubulin, alpha 1	x	x		
tubulin, beta 2	x	x		
Ubiquitin		x	x	x
UBIQUITIN ASSOCIATED 2	x	x	x	
ubiquitin associated protein 2 isoform 2	x	x		
Valosin			x	x
vesicle amine transport protein 1	x	x		
Vimentin	x	x	x	x
Xpo1	x	x		
YTH domain family protein 3	x		x	
ZO-1		x		

Novel interactions of FIP2 with proteins involved in general trafficking pathways

Trafficking components were the most obvious pathway associated with a FIP2 complex, since Rab11-FIP proteins initially were identified as a component of the Rab11a trafficking pathway. Therefore, we expected to identify additional proteins related to trafficking in our approach. Interestingly, while we did identify Rab11a in three runs, it did not reach criteria for inclusion in our proteomic list. In confirmation of our hypothesis, we found that FIP2 was able to complex with a number of proteins involved in trafficking pathways including dynein, Rab10, Rab5b, EpsinR/Epsin4 and Ras GTPase-activating-like protein IQGAP1 (Table 3). Unfortunately, antibodies to these proteins are not easily available or have limited applications towards western blotting,

especially in canine cells. Consequently, we have chosen to utilize a strategy of identifying evidence for association of these proteins with the recycling system by using two FIP2 mutants that inhibit recycling system function. The first mutant, FIP2(SARG) has two point mutations at serine 229 and arginine 413. It causes a generalized inhibition of the Rab11a positive recycling pathway. The other mutant lacks the carboxy-terminal C2 domain, FIP2(ΔC2), and causes a block at an early stage of the pathway resulting in an accumulation of the early endosomal protein EEA1 near FIP2(ΔC2) containing membranes.

The presence of dynein in a recycling system complex was not surprising because of the general importance of microtubules to the function of endocytic pathways. Dynein heavy chain is an extraordinarily large protein of more than 500 kDa and is not amenable to detection by western blot. Therefore, to confirm the association of dynein with the recycling system, we studied the localization of dynein in MDCK cells expressing the dominant negative FIP2(SARG) and FIP2(ΔC2) FIP2 trafficking mutants (Figure 30). Figure 30 demonstrates that both trafficking mutants cause accumulation of dynein in the collapsed tubular cisternae. In addition, the association was independent of Rab11a since a FIP2 chimera lacking the Rab11 Binding Domain (FIP2(Rab-)) also colocalized with dynein. The large size of the dynein heavy chain makes examination of direct association difficult in more conventional immunoprecipitation/immunoblot methodologies, thus demonstrating the utility of this approach in confirming protein association with the recycling system.

We also identified an unexpected Rab protein, Rab10, as a potential component of the FIP2 complex. Rab10 was implicated recently in the basolateral early endosome to

common endosome sorting and transcytotic pathways (23). In the proteomic studies, Rab10 was immunoprecipitated from FIP2(S227A) and FIP2(SARG) over-expressing cell lines. To validate this association, we examined the distribution of over-expressed mRFP-Rab10 in the FIP2(ΔC2) and FIP2(SARG) expressing cell lines. The mRFP-Rab10 accumulated with the FIP2(ΔC2) ring and FIP2(SARG) tubular cisternae (data not shown). In addition, when the FIP2(Rab-) mutant was overexpressed, Rab10 colocalized with the mutant at the plasma membrane of the cells (**Error! Not a valid link.**31), indicating that Rab10 associates in a complex with FIP2 that does not involve the Rab11 binding domain (data not shown). In support of this finding, we have utilized yeast two hybrid assays which did not show a direct interaction between Rab10 and FIP2, confirming that the Rab11 binding domain is not a general Rab protein binding domain (data not shown).

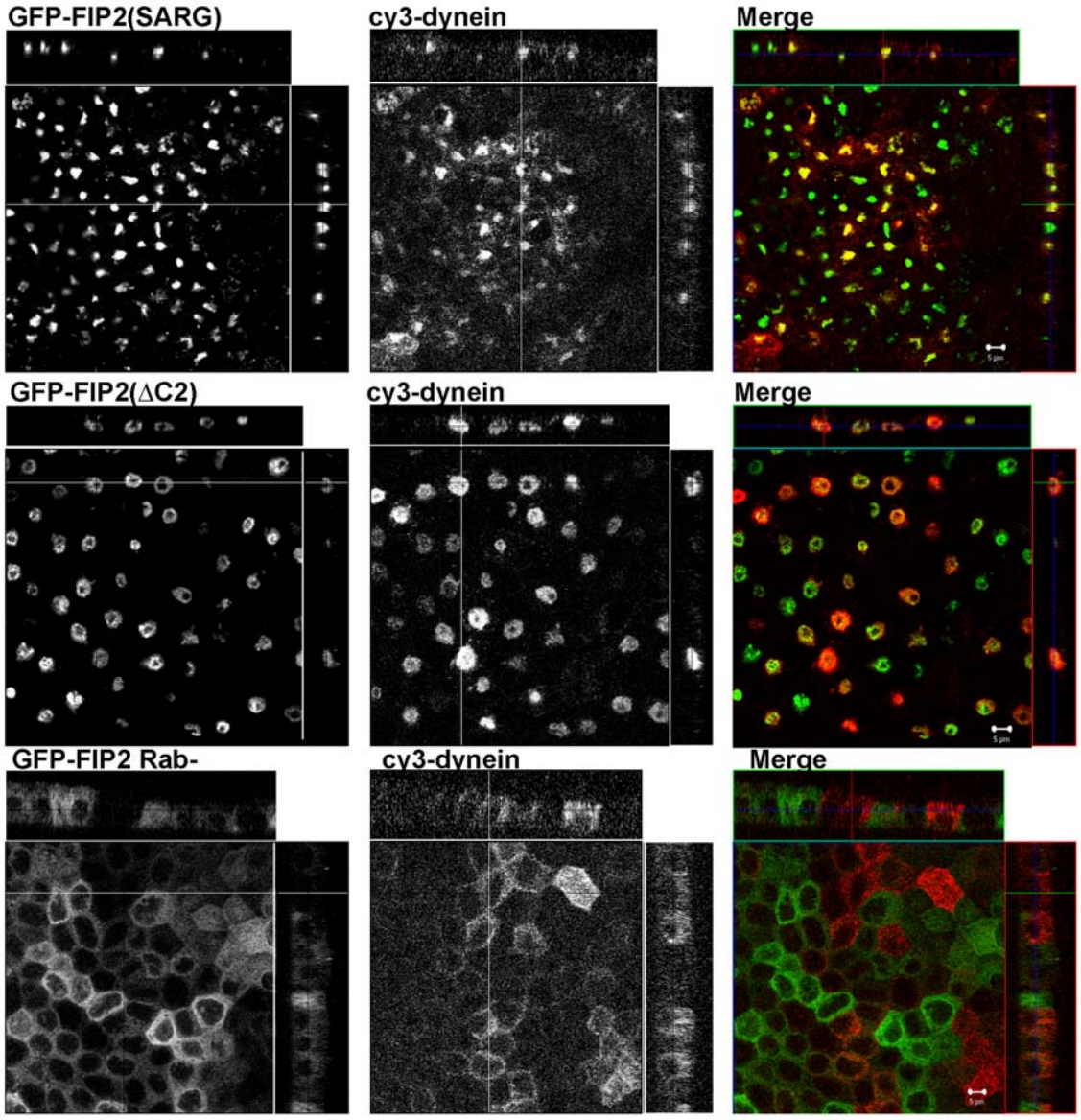

Figure 30: FIP2 mutants alter the localization of the microtubule motor protein dynein heavy chain

MDCK-T23 cells stably expressing each of the mutants (FIP2(SARG), (ΔC2) and Rab-) were imaged by confocal microscopy. All three mutants localized with endogenous dynein. Images were taken with a 100x lens. Scale bars represent 5 μm.

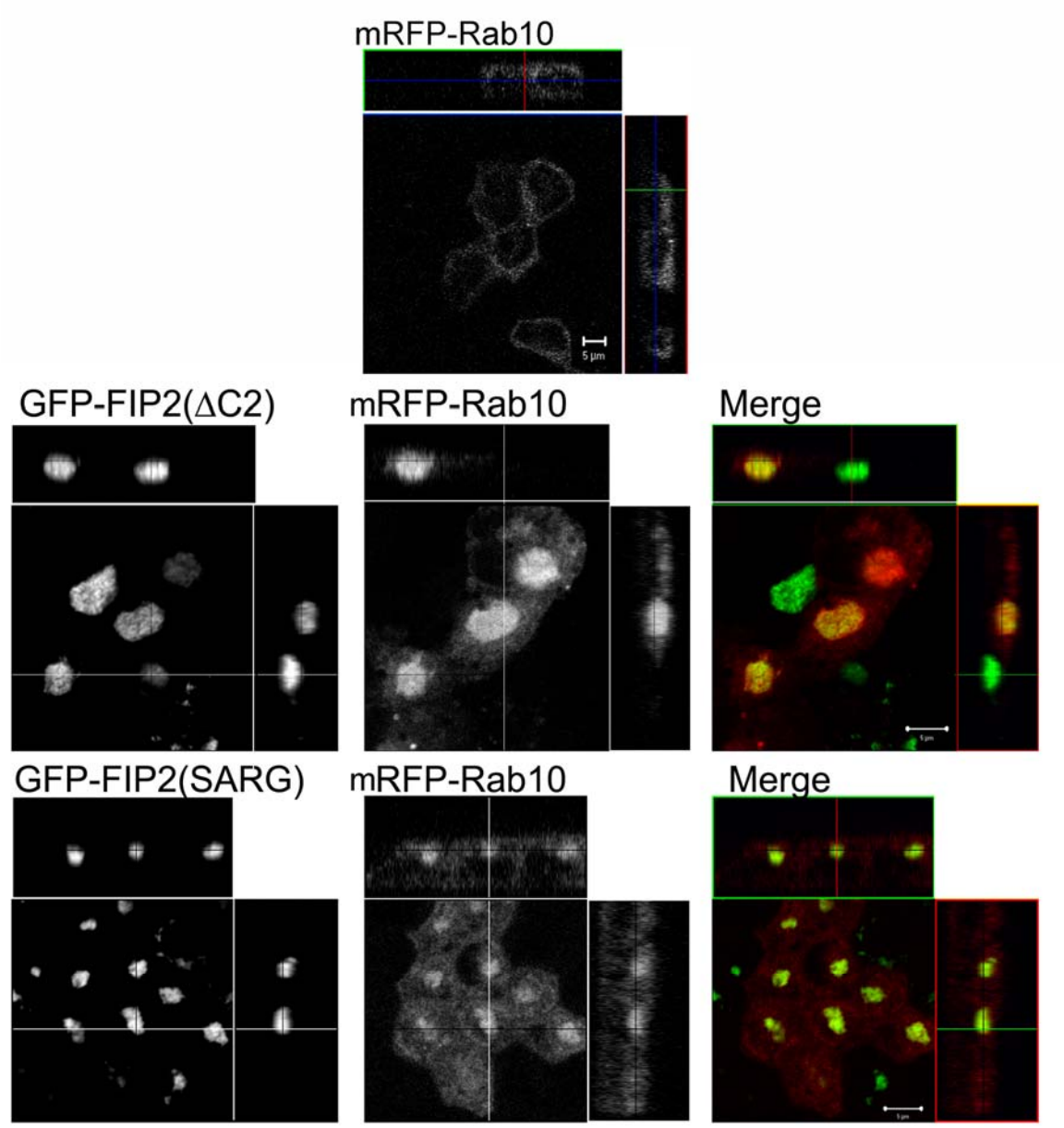

Figure 31: FIP2 interacts in a complex with Rab10

T23 cells stably expressing FIP2 wild type, FIP2(SARG) and FIP2(ΔC2) were transiently transfected with mRFP-Rab10 and imaged by confocal microscopy in the X-Y plane. The mRFP-Rab10 showed a collapse towards the FIP2 containing cisternae in cells over-expressing FIP2(ΔC2) and FIP2(SARG) compared to endogenous localization which is similar to that seen with FIP2 wild type. Images were taken with a 100x lens with a 3X zoom. Scale bars represent 5 μm.

FIP2(ΔC2) alters localization of additional early endosome proteins

The mass spectrometric analysis revealed that FIP2 was complexed with two early endosomal proteins, EpsinR/Epsin 4 (EpsinR) and Rab5b. These results support our assertion that FIP2 mutants allow dissection of different parts of the FIP2 pathway (13). EpsinR is an adaptor protein used in retrograde trafficking (24). To evaluate these findings, we examined the distribution of EpsinR with FIP2. While FIP2(SARG) did not pull EpsinR into collapsed cisternae (Figure 32), an altered localization of endogenous EpsinR was apparent in the FIP2(ΔC2) stable cell line (Figure 32). EpsinR containing vesicles were clustered around the FIP2(ΔC2)-containing membranes.

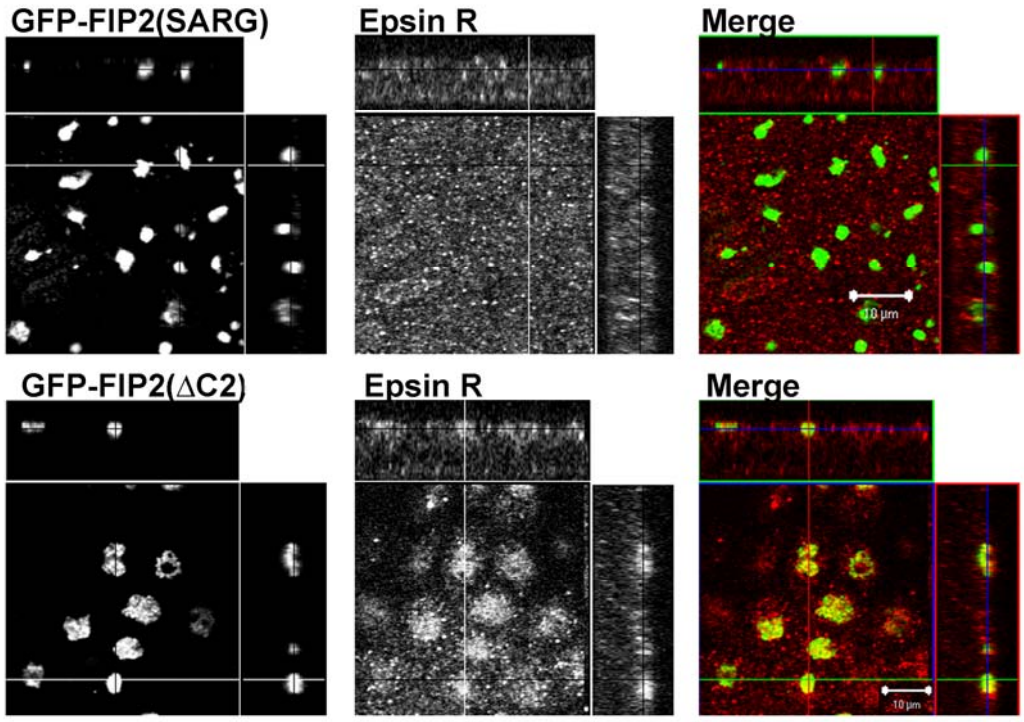

Figure 32: Differentiable interactions of FIP2 mutants in a complex with EpsinR

T23 cells stably expressing FIP2 (SARG) and FIP2(ΔC2) were imaged by confocal microscopy in the X-Y plane. Cells were stained for EpsinR (in cy5, but pseudo colored red for ease in visualization). While the FIP2(SARG) mutant had no impact on EpsinR localization, FIP2(ΔC2) caused a partial collapse of the structure. All images are cropped from 100X. Scale bars are 10 µm.

We also examined the association of FIP2 with Rab5b. Co-transfection of mRFP-Rab5b into parental T23 cells or FIP2 overexpressing cell lines revealed a diffuse distribution of Rab5b consistent with localization on early endosomal structures. In cells expressing FIP2(ΔC2), Rab5b containing vesicles were more concentrated towards the nucleus but did not directly colocalize with FIP2. FIP2(SARG) expression did not alter the distribution of Rab5b containing membranes (Figure 33). Because the interaction with FIP2(ΔC2) was positive, we analyzed the localization of a more traditional early endosome protein, mRFP-Rab5a, in parental T23 cells and the FIP2(ΔC2) cell line. In marked contract to Rab5b (Figure 33), EpsinR (Figure 32) and EEA1 (13), Rab5a distribution is not altered by FIP2(ΔC2) expression (Figure 34).

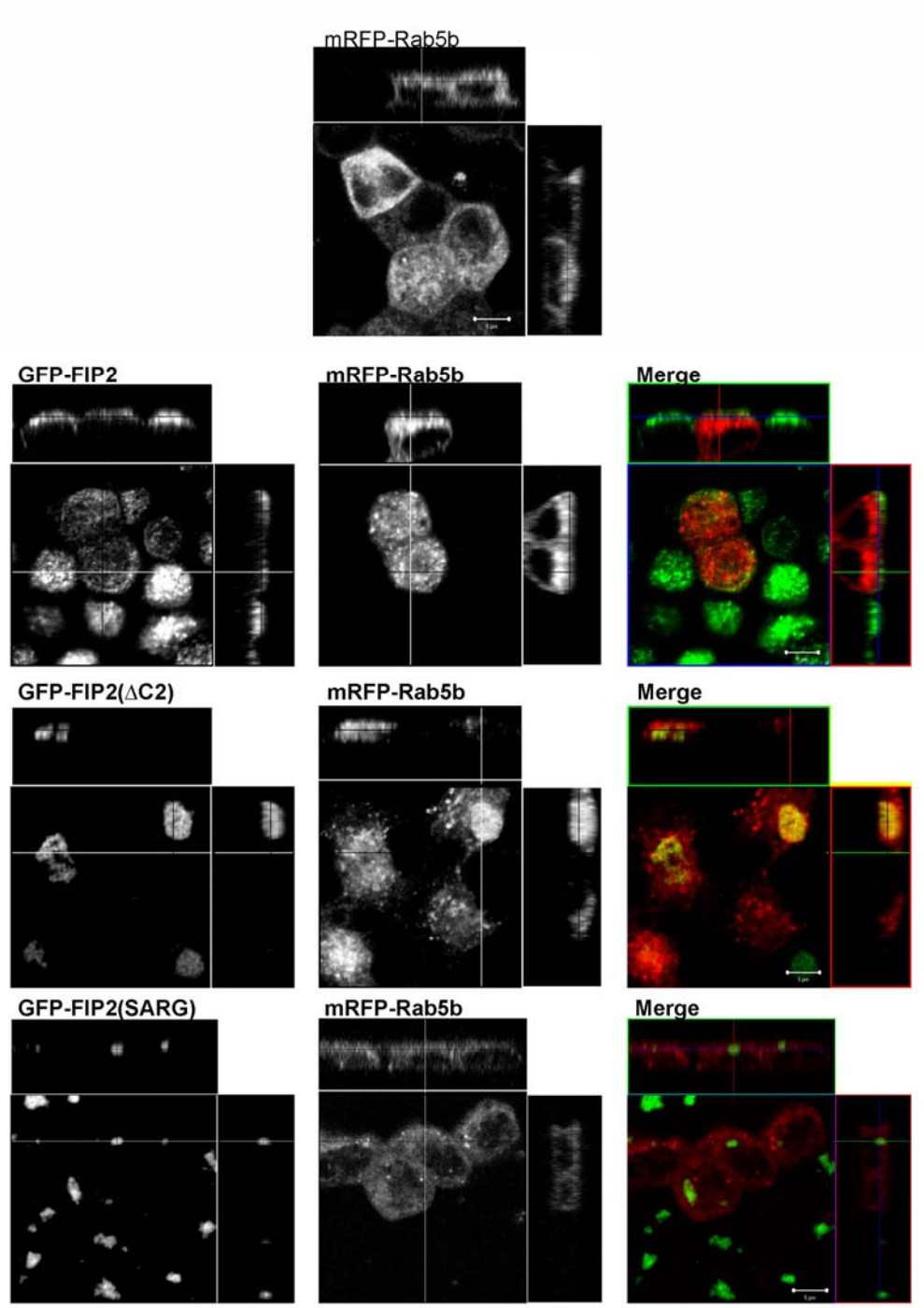

Figure 33: Differentiable interactions of FIP2 mutants in a complex with mRFP-Rab5b

T23 cells stably expressing FIP2 wild type and each of the mutants (FIP2(SARG) and (ΔC2)) were transiently transfected with mRFP-Rab5b and imaged by confocal microscopy in the X-Y plane. The mRFP-Rab5b showed a collapse towards the FIP2 containing cisternae in cells over-expressing FIP2(ΔC2) but not in cells overexpressing FIP2(SARG) or FIP2 wild type. Images were taken with a 100x lens with a 3X zoom. Scale bars represent 5 μm.

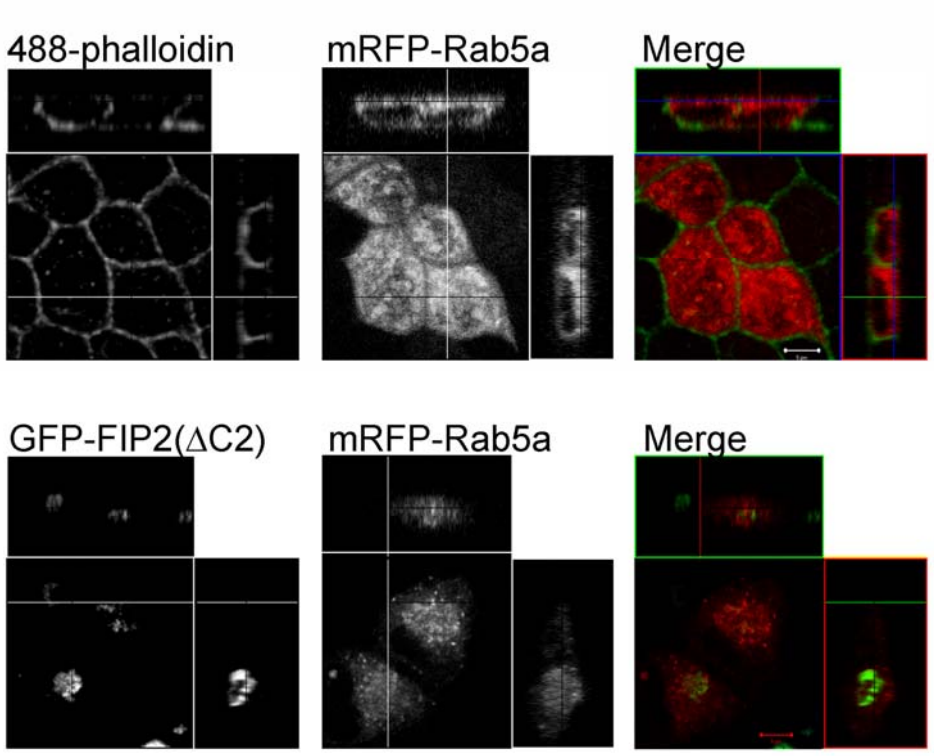

Figure 34: FIP2 does not alter the localization of Rab5a.

Parent T23 and T23 cells stably expressing FIP2(ΔC2) were transiently transfected with mRFP-Rab5a and imaged by confocal microscopy in the X-Y plane. Parent T23 cells were co-stained with 488-phalloidin and showed normal localization of mRFP-Rab5a. The mRFP-Rab5a did not show a collapse towards the FIP2 containing cisternae in cells over-expressing FIP2(ΔC2). Images were taken with a 100x lens with a 3X zoom. Scale bars represent 5 μm.

We also found that Ras GTPase-activating-like protein IQGAP1 (IQGAP1) was in complex with FIP2. In MDCK cells expressing the dominant negative FIP2(ΔC2) mutant, but not in cells expressing the wild type protein, IQGAP1 containing membrane vesicles were accumulated in the perinuclear region (Figure 35). IQGAP1 localization was altered in the FIP2(ΔC2) cells in a similar manner to other early endosome-associated proteins.

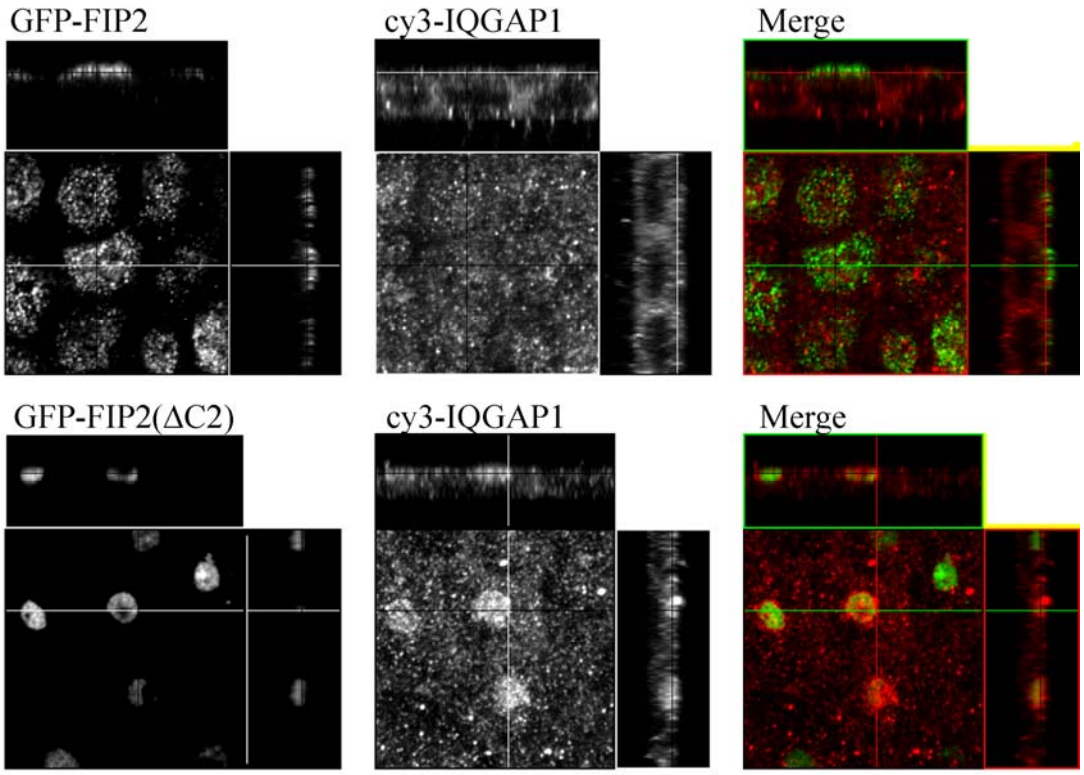

Figure 35: FIP2 and its mutants are in complex with IQGAP1

T23 cells stably expressing FIP2 wild type and FIP2(ΔC2) were stained for endogenous IQGAP1 (pseudo-colored red) and imaged by confocal microscopy in the X-Y plane. IQGAP1 showed a partial collapse towards the FIP2 containing cisternae in cells over-expressing FIP2(ΔC2) compared to endogenous localization akin to that seen with FIP2 wild type. Images were taken with a 100x lens with a 3X zoom. Scale bars represent 5 μm.

Interactions of FIP2 with coat proteins

Coat proteins were the third general type of protein revealed by this analysis. We have looked at two of these proteins: clathrin heavy chain and adaptor-related protein complex 1 (AP-1). Clathrin heavy chain was found by proteomics in each of the four overexpressing cell lines. Because clathrin heavy chain is expressed throughout the cell, we utilized our dominant negative mutants to enhance the visualization of a potential interaction. Both the FIP2(SARG) and FIP2(ΔC2) mutants elicited a partial accumulation of clathrin heavy chain into their collapsed structures (Figure 36).

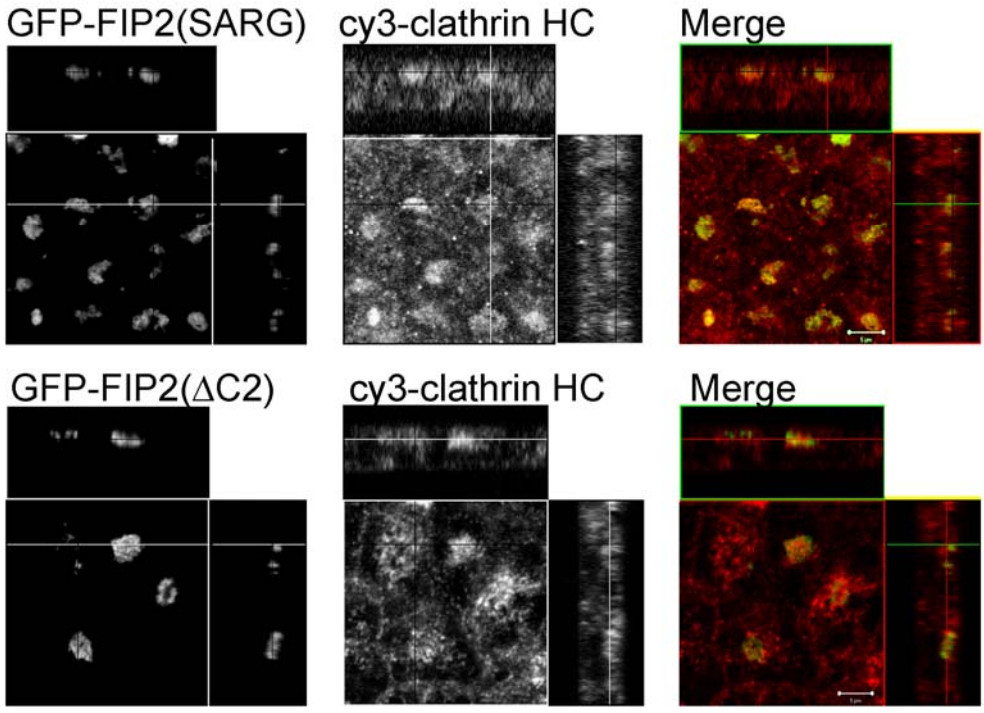

Figure 36: FIP2 mutants cause accumulation of clathrin heavy chain into the collapsed structures

T23 cells stably expressing FIP2(SARG) and FIP2(ΔC2) were stained for endogenous clathrin heavy chain (pseudo-colored red) and imaged by confocal microscopy in the X-Y plane. Clathrin heavy chain showed a partial collapse towards the FIP2 containing cisternae in cells over-expressing both mutants. Images were taken with a 100x lens with a 3X zoom. Scale bars represent 5 μm.

Finally, we found that AP-1 associated with EGFP-FIP2 wild type and FIP2(S227A) overexpressed chimeras in our proteomics results. We evaluated this potential complex by immunofluorescence and found that AP-1 accumulated with FIP2(SARG), but not with FIP2(ΔC2) (Figure 37). Therefore, AP-1 appears to be in complex with FIP2 during a specific subset of FIP2's functions or else requires the amino terminal C2 domain for interaction.

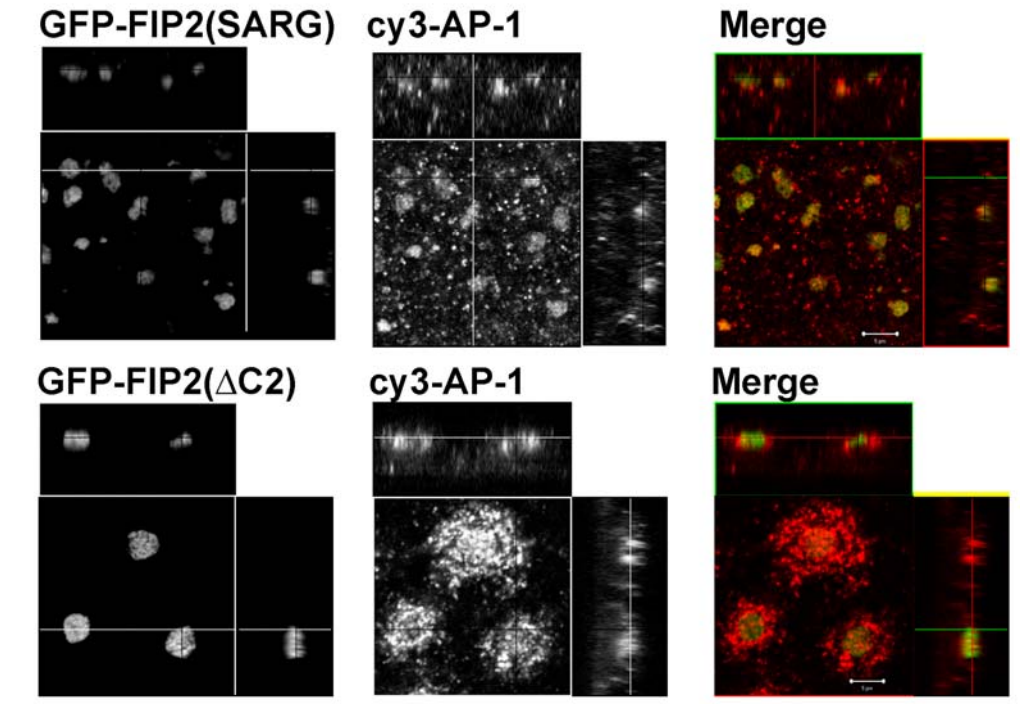

Figure 37: FIP2(SARG) causes a collapse of AP-1

T23 cells stably expressing FIP2(SARG) and FIP2(ΔC2) were stained for endogenous AP-1 (pseudo-colored red) and imaged by confocal microscopy in the X-Y plane. AP-1 showed a partial collapse towards the FIP2(SARG) containing cisternae but not the FIP2(ΔC2) structure in cells over-expressing the mutants. Images were taken with a 100x lens with a 3X zoom. Scale bars represent 5 μm.

Discussion

Rab11-FIP2 is a multifunctional regulator of multiple trafficking pathways. Recent investigations have implicated FIP2 in the regulation of early endocytosis, plasma membrane recycling and the establishment of polarity in epithelial cells. This range of functions suggests that FIP2 participates in multiple regulatory protein complexes. Therefore, we sought to ascertain unrecognized interactions of FIP2 with other proteins involved in trafficking within polarized epithelial cells. We utilized the available LC-MS/MS technology combined with immunoprecipitation to elucidate novel interacting

proteins with FIP2 regulated pathways. We analyzed proteins associating with EGFP-chimeras of wild type FIP2 as well as three mutant versions of FIP2 to maximize the identification of novel interactions by enhancing visualization of the recycling system. These studies have led to the identification of a number of previously unrecognized interactions of Rab11-FIP2 with components of the endocytic trafficking pathways.

Since our overall goal was to identify novel regulators of endocytic trafficking, we have validated eight of the potential interacting proteins using a combination of immunofluorescence staining for colocalization and fluorescent-chimeric protein overexpression studies. This approached focused on validation of the functional association of these proteins with the endocytic pathway. Because we utilized polarized MDCK cells in our studies, we often found that available reagents did not work well in canine cells. The use of trafficking mutants as a provocative test therefore avoids the need for specific immunoreagents against putative proteins. We have previously characterized two dominant negative mutants of FIP2, FIP2(ΔC2) and FIP2(SARG), which both inhibit transcytotic trafficking. Importantly, while both cause tubulation and collapse of the Rab11a-containing recycling system, only FIP2(ΔC2) also causes a aggregation of EEA-1-containg early endosome vesicles in proximity to the collapsed recycling system tubular cisternae (13). These two patterns allowed functional dissection of the possible roles of putative FIP interaction proteins along particular aspects of the endocytic recycling pathway. Two patterns emerged from our analysis. One pattern included proteins directly associated with the recycling endosome as exemplified by dynein and Rab10. Both FIP2 mutants affected the distribution of these proteins. The other pattern highlighted a presumed association of FIP2 with early endosome

compartments as demonstrated by Rab5b and EpsinR. These proteins were found in vesicles aggregated around the EGFP-FIP2(ΔC) containing cisternae.

Our approach sampled the entire gamut of protein complexes containing FIP2 in the overexpressing cell lines. Consequently, we have most likely missed potential interactions because of the size of the proteome. The use of multiple mutants, which can elucidate different aspects of FIP2 pathways, helped to ameliorate this concern. Therefore, even though some interactions were not seen in the mass spectrometry data sets, protein distribution was often altered by additional mutants. One of the caveats associated with proteomic approaches is the presence of false positives. Thus, we have used our results as a starting point to explore new roles for FIP2 and its associated proteins in endocytic trafficking.

We treated each potential interacting protein as if it were a general FIP2 binding partner, and used the mutant FIP2 constructs to validate these complexes. Some mutants appear to have generated false positives. For example, FIP2(SARG) pulled down Rab5b, but did not appear either to alter the localization of or colocalize with Rab5b. However, we did find that Rab5b was altered in one of the other mutant lines, FIP2(ΔC2), thus validating our approach of treating each proteomically identified protein as a entry point into studying potential interactions, as opposed to absolute indicators of *in situ* complexes. Our strategy initially implicated 473 proteins in complex with the EGFP-FIP2 chimeras. A logical assumption when examining complexes containing overexpressed proteins is that many proteins associated with biosynthetic pathways, endoplasmic reticulum function or chaperones would be identified. Indeed the assembled list does contain a number of endoplasmic reticulum components and chaperones and we chosen

to segregate these as non-specific interactors based on a general lack of data to support any role of FIP2 in endoplasmic reticulum function. Instead, we have chosen to focus our efforts on vesicle trafficking proteins that may be particularly relevant to the function of FIP2 in trafficking.

Proteins complexed with FIP2 throughout the FIP2 pathway

One set of proteins revealed in our approach associated with recycling endosome membranes containing Rab11a and the EGFP-FIP2 mutants. Two proteins analyzed here fit this pattern: dynein and Rab10. Both proteins associated with the two previously characterized dominant negative FIP2 mutants, indicating that they interact throughout the FIP2 positive recycling endosome pathway. FIP2 may escort protein complexes from the plasma membrane to endosomes through retrograde movement by recruiting dynein heavy chain for movement along microtubules. We have previously shown that FIP2 and Rab11a interact with the motor protein myosin Vb (9). Overexpression of the tail region of myosin Vb lacking the motor domain blocks Rab11 mediated trafficking events. However, we have noted that treatment of MDCK cells with the microtubule-stabilizing drug taxol caused relocation of Rab11a-contatining recycling vesicles to the apical corners of polarized cells. Polarized MDCK cells treated with the microtubule depolymerizing drug nocodazole showed dispersal of the apical recycling endosome as marked by Rab11a (3). These two pieces of data strongly implicate the importance of the microtubule cytoskeleton and microtubule motors in addition to the actin motor myosin Vb in regulation of endocytosis and plasma membrane recycling. Thus, the accumulation of dynein within the recycling system inhibited by FIP2 mutants suggests a critical role

for dynein in the movement of membrane vesicles within the plasma membrane recycling system.

Rab10 was recently identified as a component of the basolateral early and common endosomes in MDCK cells (23, 25). We have also recently described the presence of Rab10 on immunoisolated recycling vesicles from gastric parietal cells (15). Through the utilization of our dominant negative FIP2 mutants, we have seen that FIP2 has a more pronounced effect on transcytosis than on apical recycling (13). Thus, we have uncovered a potential interaction to account for this influence on transcytosis: a handoff between a Rab10 positive common/sorting endosome and a Rab11a positive apical recycling endosome may require fully functional Rab11-FIP2.

Early endosomal proteins complexed with FIP2(ΔC2)

The interaction of Rab11-FIP2 with dynein and Rab10 seems to indicate a general recycling system function for FIP2, because these proteins interacted with both dominant negative FIP2 mutants. In contrast, the localization of the early endosome proteins Rab5b, Epsin R and IQGAP1 was only altered by the FIP2(ΔC2) mutant. This specificity in association suggests that these proteins are acting with early components of the FIP2 pathway, likely before entry into a Rab11a-containing recycling system.

These studies have identified an association of FIP2 with a number of regulators of early endocytosis or the transition from early endosomes to recycling endosomes. Rab5b is a Rab5 family member that interacts with EEA1 and localizes presumedly to early endosome, but has a different GTPase activating protein than Rab5a (26). Each of the Rab5 family members are phosphorylated by different kinases suggesting that they may be regulated differentially and thus important for different aspects of early

endosome-mediated trafficking (27). A subset of these validated proteins allowed further confirmation of the results from our previous study, which showed that a dominant negative FIP2 mutant altered the localization of the early endosome marker, EEA1 (13). Because these interactions were positive, we analyzed the localization of a more traditional early endosome protein, Rab5a in these cell lines. In marked contrast to Rab5b and EEA1, Rab5a does not collapse near the FIP2(ΔC2)-containing structure. To our knowledge, this is the first study to find a functional difference between Rab5b and Rab5a. The association of FIP2 in a complex with Rab5b suggests the existence of an endosomal subdomain distinct from classically characterized Rab5a-containing early endosomes.

IQGAP1 localizes to adherens junctions in MDCK cells and is a putative downstream target of the Rho family small G proteins, Cdc42 and Rac (28). It is believed to be a Ras GAP by protein homology; however, direct evidence demonstrating IQGAP1 as a GAP effector for Cdc42 or Rac has not been reported. In fact, the presence of IQGAP1 seems to inhibit intrinsic GTPase activity in Cdc42 and Rac (reviewed in (29)). IQGAP1 interacts with a variety of proteins in signaling cascades and was recently found in association with an apical microvilli border in syncytiotrophoblast cells (30). This report suggested that it exists in complex with Rab7. Interestingly, trafficking and replication of the Moloney murine leukemia virus matrix protein utilizes IQGAP1 (31). We now demonstrate that IQGAP1 is in complex with FIP2. This new interaction may help to link the Rab11 pathway with the Cdc42/Rac pathway.

The alteration of Rab5b, EpsinR, and IQGAP1 localization with the FIP2(ΔC2) mutant but not the FIP2(SARG) mutant highlights the possibility that our proteomic

approach may have uncovered a novel dynamic compartment between the early and recycling endosomes that is not the traditional Rab4 positive sorting endosome. This compartment may be involved in the handoff between these two compartments mediated by FIP2. Alternatively, we may also have uncovered a separate early endosome pathway that utilized in different circumstances (i.e. distinct receptors or cargoes or a specific mode of internalization) than the Rab5a positive compartment.

Coat proteins in complex with FIP2

Our analysis also revealed coat proteins in association with FIP2. While a previous study has noted the interaction of FIP2 with alpha-adaptin (12), no study to date has shown an association with clathrin heavy chain. Clathrin heavy chain has previously been found on early endosomes and was implicated in early to late endosome trafficking (32). The presence of clathrin in a FIP2 complex lends credence to the growing hypothesis that FIP2 is involved in more aspects of cellular function than Rab11 positive apical recycling. Our approach found that AP-1 localized in a complex with FIP2(SARG). However, this association is not apparent in the FIP2(ΔC2) overexpressing cells. One of the controversies in studies of FIP2 is the function of the C2 domain. The McCaffrey lab has reported that this domain interacts with phosphatidylinositol-(3,4,5)-trisphosphate (33). However, we (data not shown) and others have not been able to duplicate this result using liposome association methods. The absence of AP-1 association with complexes containing FIP2(ΔC2) may suggest a more specific role for the C2 domain. Nevertheless, the exact role of FIP2 interaction with complexes containing coat proteins remains to be determined.

In summary, we have utilized the mass spectrometry technology to identify new, interesting and often unanticipated components of complexes with FIP2. This approach has proven useful in identifying new interactions relating to endocytic trafficking as well as additional interactions that remain uncharacterized. These results will lead to a broader understanding of Rab11-FIP2 as a multi-functional regulator of polarized epithelial cell function.

ACKNOWLEDGEMENTS

We thank Dr. S. Robinson for the gift of antibody reagent against EpsinR and Dr. David Sacks for the gift of antibody reagent against IQGAP1. Confocal images were generated through the use of the VUMC Cell Imaging Shared Resource (supported by NIH grants CA68485, DK20593, DK58404, HD15052, DK59637 and EY08126). This work was supported by NIH National Institute of Diabetes and Digestive and Kidney Diseases (NIDDK) Grants DK-070856, DK-48370 and DK-43405 (to J.R.G.). The authors also thank Vanderbilt University for institutional support of the Proteomics Laboratory in the Mass Spectrometry Research Center through the Academic Venture Capital Fund.

Nicole A Ducharme drafted the manuscript and performed the experiments relating to figures 29-35. Amy-Joan L. Ham supervised the mass spectrometry experiments. Lynne A. Lapierre assisted in experimental interpretation and manuscript editing. James R. Goldenring was involved in guiding the experimental design with Nicole Ducharme.

References

1. Goldenring JR, Smith J, Vaughan HD, Cameron P, Hawkins W, Navarre J. Rab11 is an apically located small GTP-binding protein in epithelial tissues. Am J Physiol 1996;270(3 Pt 1):G515-25.

2. Brown PS, Wang E, Aroeti B, Chapin SJ, Mostov KE, Dunn KW. Definition of distinct compartments in polarized Madin-Darby canine kidney (MDCK) cells for membrane-volume sorting, polarized sorting and apical recycling. Traffic 2000;1(2):124-40.

3. Casanova JE, Wang X, Kumar R, Bhartur SG, Navarre J, Woodrum JE, et al. Association of Rab25 and Rab11a with the apical recycling system of polarized Madin-Darby canine kidney cells. Mol Biol Cell 1999;10(1):47-61.

4. Hales CM, Griner R, Hobdy-Henderson KC, Dorn MC, Hardy D, Kumar R, et al. Identification and characterization of a family of Rab11-interacting proteins. J Biol Chem 2001;276(42):39067-75.

5. Wallace DM, Lindsay AJ, Hendrick AG, McCaffrey MW. Rab11-FIP4 interacts with Rab11 in a GTP-dependent manner and its overexpression condenses the Rab11 positive compartment in HeLa cells. Biochem Biophys Res Commun 2002;299(5):770-9.

6. Prekeris R, Klumperman J, Scheller RH. A Rab11/Rip11 protein complex regulates apical membrane trafficking via recycling endosomes. Mol Cell 2000;6(6):1437-48.

7. Lindsay AJ, Hendrick AG, Cantalupo G, Senic-Matuglia F, Goud B, Bucci C, et al. Rab coupling protein (RCP), a novel Rab4 and Rab11 effector protein. J Biol Chem 2002;277(14):12190-9.

8. Prekeris R, Davies JM, Scheller RH. Identification of a novel Rab11/25 binding domain present in Eferin and Rip proteins. J Biol Chem 2001;276(42):38966-70.

9. Lapierre LA, Kumar R, Hales CM, Navarre J, Bhartur SG, Burnette JO, et al. Myosin vb is associated with plasma membrane recycling systems. Mol Biol Cell 2001;12(6):1843-57.

10. Tsakraklides V, Krogh K, Wang L, Bizario JC, Larson RE, Espreafico EM, et al. Subcellular localization of GFP-myosin-V in live mouse melanocytes. J Cell Sci 1999;112(Pt 17):2853-65.

11. Hales CM, Vaerman JP, Goldenring JR. Rab11 family interacting protein 2 associates with Myosin Vb and regulates plasma membrane recycling. J Biol Chem 2002;277(52):50415-21.

12. Cullis DN, Philip B, Baleja JD, Feig LA. Rab11-FIP2, an adaptor protein connecting cellular components involved in internalization and recycling of epidermal growth factor receptors. J Biol Chem 2002;277(51):49158-66.

13. Ducharme NA, Williams J, Lapierre LA, Goldenring JR. Dominant Negative RAB11-FIP2 Mutants Uncover Differentiable Steps in Transcytosis. Traffic 2007;Submitted.

14. Ducharme NA, Hales CM, Lapierre LA, Ham AJ, Oztan A, Apodaca G, et al. MARK2 Phosphorylation of Rab11-FIP2 Is Necessary for the Timely Establishment of Polarity in MDCK Cells. Mol Biol Cell 2006.

15. Lapierre LA, Avant KM, Caldwell CM, Ham A-JL, Hill S, Williams JA, et al. Characterization of immunoisolated human gastric parietal cells tubulovesicles: identification of regulators of apical recycling. 10.1152/ajpgi.00505.2006. Am J Physiol Gastrointest Liver Physiol 2007:00505.2006.

16. Barth AIM, Pollack AL, Altschuler Y, Mostov KE, Nelson WJ. NH2-terminal deletion of beta -catenin results in stable colocalization of mutant beta -catenin with adenomatous polyposis coli protein and altered MDCK cell adhesion. 10.1083/jcb.136.3.693. J. Cell Biol. 1997;136(3):693-706.

17. Cortes HJ, Pfeiffer CD, Richter BE, Stevens T. Porous ceramic bed supports for fused silica packed capillary columns used in liquid chromatography. Journal of High Resolution Chromatography and Chromatography Communications 1987;10:446-448.

18. Licklider LJ, Thoreen CC, Peng J, Gygi SP. Automation of nanoscale microcapillary liquid chromatography-tandem mass spectrometry with a vented column. Anal Chem 2002;74(13):3076-83.

19. Yates JR, 3rd, Eng JK, McCormack AL, Schieltz D. Method to correlate tandem mass spectra of modified peptides to amino acid sequences in the protein database. Anal Chem 1995;67(8):1426-36.

20. Soukoulis V, Reddy S, Pooley RD, Feng Y, Walsh CA, Bader DM. Cytoplasmic LEK1 is a regulator of microtubule function through its interaction with the LIS1 pathway. Proc Natl Acad Sci U S A 2005;102(24):8549-54.

21. Babbey CM, Ahktar N, Wang E, Chen CC, Grant BD, Dunn KW. Rab10 regulates membrane transport through early endosomes of polarized Madin-Darby canine kidney cells. Mol Biol Cell 2006;17(7):3156-75.

22. Saint-Pol A, Yelamos B, Amessou M, Mills IG, Dugast M, Tenza D, et al. Clathrin Adaptor epsinR Is Required for Retrograde Sorting on Early Endosomal Membranes. Developmental Cell 2004;6(4):525-538.

23. Schuck S, Gerl MJ, Ang A, Manninen A, Keller P, Mellman I, et al. Rab10 is Involved in Basolateral Transport in Polarized Madin-Darby Canine Kidney Cells. Traffic 2006.

24. Callaghan J, Nixon S, Bucci C, Toh BH, Stenmark H. Direct interaction of EEA1 with Rab5b. Eur J Biochem 1999;265(1):361-6.

25. Chiariello M, Bruni CB, Bucci C. The small GTPases Rab5a, Rab5b and Rab5c are differentially phosphorylated in vitro. FEBS Lett 1999;453(1-2):20-4.

26. Katata T, Irie K, Fukuhara A, Kawakatsu T, Yamada A, Shimizu K, et al. Involvement of nectin in the localization of IQGAP1 at the cell-cell adhesion sites through the actin cytoskeleton in Madin-Darby canine kidney cells. Oncogene 2003;22(14):2097-109.

27. Brown MD, Sacks DB. IQGAP1 in cellular signaling: bridging the GAP. Trends in Cell Biology 2006;16(5):242-249.

28. Paradela A, Bravo SB, Henriquez M, Riquelme G, Gavilanes F, Gonzalez-Ros JM, et al. Proteomic Analysis of Apical Microvillous Membranes of Syncytiotrophoblast Cells Reveals A High Degree of Similarity with Lipid Rafts. J. Proteome Res. 2005;4(6):2435-2441.

29. Leung J, Yueh A, Appah FS, Jr., Yuan B, de los Santos K, Goff SP. Interaction of Moloney murine leukemia virus matrix protein with IQGAP. Embo J 2006;25(10):2155-66.

30. Raiborg C, Bache KG, Mehlum A, Stang E, Stenmark H. Hrs recruits clathrin to early endosomes. Embo J 2001;20(17):5008-21.

31. Lindsay AJ, McCaffrey MW. The C2 domains of the class I Rab11 family of interacting proteins target recycling vesicles to the plasma membrane. 10.1242/jcs.01280. J Cell Sci 2004;117(19):4365-4375.

CHAPTER V

CONCLUSION AND FUTURE DIRECTIONS

Rab11-FIP2 originally was identified as a member of the family of interacting proteins associated with Rab11a involved in transcytosis (Hales *et al.*, 2001). Rab11-FIP2 is unique in its ability to bind both GTP- and GDP-bound Rab11a; every other family member only binds GTP-bound Rab11a (Hales *et al.*, 2001). Therefore, it was hypothesized that FIP2 plays a separable role from that of the other FIP proteins. In addition, further work determined that only Rab11-FIP2 binds to myosin Vb (Hales *et al.*, 2002), a motor protein involved in the Rab11a pathway (Lapierre *et al.*, 2001). Thus, Rab11-FIP2 emerged as a critical multi-functional component of the Rab11a-positive apical recycling system. Our lab developed two dominant negative mutants to study this system in more detail, a Rab11-FIP2 construct lacking the amino-terminal C2 domain, Rab11-FIP2(ΔC2), and a truncated form of the motor protein lacking the motor domain, myosin Vb-tail. We and others have used these mutants to characterize receptor recycling of such diverse receptors as CXCR2 (Fan *et al.*, 2004), protease-activated receptor 2 (Roosterman *et al.*, 2003), and the M4 muscarinic acetylcholine receptor (Volpicelli *et al.*, 2002). The availability of these reagents has greatly enhanced the plasma membrane recycling field by allowing assays of cargo accumulation in the inhibited recycling system.

The body of work presented here represents a significant advance in our understanding of the role of Rab11-FIP2 in polarized epithelial cells. It also allows for

the postulation of a number of additional questions for future work. First, we demonstrated that Rab11-FIP2 is phosphorylated by MARK2 on a novel consensus site. This phosphorylation event is necessary for the timely re-establishment of polarity, specifically for the proper localization of adherens junction proteins. The polarized epithelial cell is the only cell culture system that could have revealed this new role for Rab11-FIP2 in the involvement of Rab11-FIP2 in polarity. The specificity of this role in polarized cells suggests that trafficking complexes may be involved in regulating junctional establishment, instead of simply serving as a general conduit for all junctional proteins regardless of the external cell conditions (Figure 38).

However, Rab11-FIP2 initially was described as a protein involved in the Rab11 trafficking pathway. In our efforts to follow up on this initial role, we have characterized a new dominant negative mutant that has allowed us to dissect differentiable roles of Rab11-FIP2 in the transcytotic pathway. More specifically, a previously characterized Rab11-FIP2 mutant lacking the amino terminal C2 domain, Rab11-FIP2(ΔC2), alters the distribution of the EEA1-containing early endosome membranes while the point mutant Rab11-FIP2(SARG) does not. However, both mutants cause a significant decrease in transcytosis, the delivery of cargo from the basolateral membrane to the apical plasma membrane. The availability of these two Rab11-FIP2 mutants will allow future work to understand the role of Rab11-FIP2 more fully. Finally, we have identified a number of candidate proteins that may be in complex with Rab11-FIP2 through a proteomic approach. The characterization of these interactions and the role of Rab11-FIP2 in both established and novel pathways may provide insights into the interconnection of recycling pathways with other trafficking systems. Altogether, these three facets of work

regarding Rab11-FIP2 demonstrate the diversity and complexity of the role of Rab11-FIP2 in polarized epithelial cells.

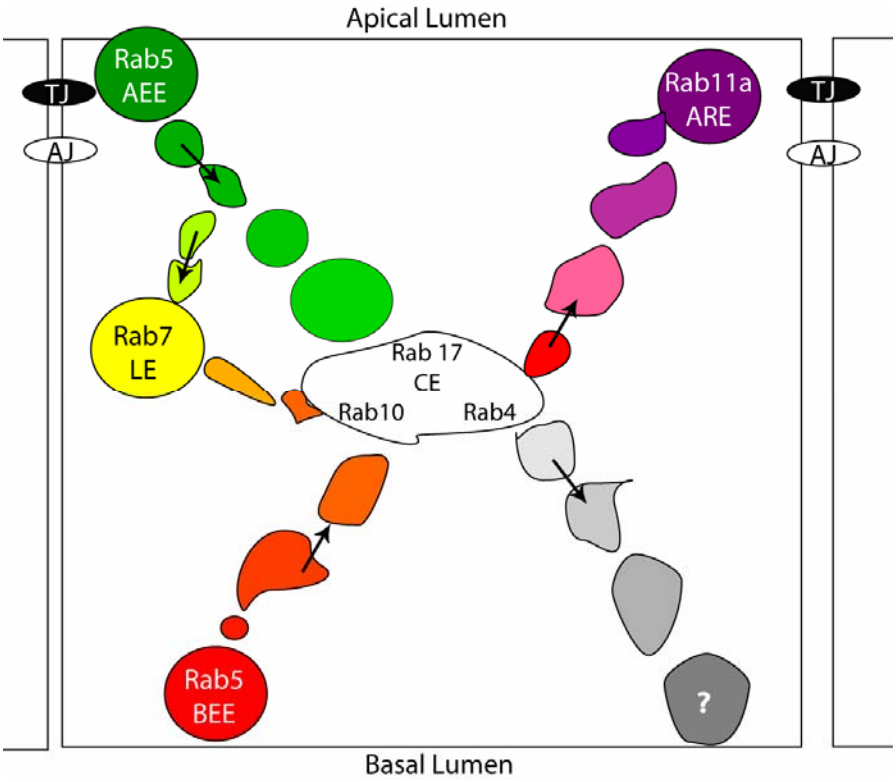

Figure 38: Generalized Model of Trafficking Pathways in Polarized Cells

Apical cargo is internalized via a Rab5a positive early endosome (EE). Basolateral cargo is internalized via a Rab10 positive basolateral early endosome (BEE). Both cargos are directed towards a common endosome (CE) or diverted to a Rab7 positive late endosome (LE). If the cargo is destined to the apical plasma membrane, it will be trafficked through a Rab11a positive apical recycling endosome (ARE).

Future Directions for Rab11-FIP2's Involvement in Polarity

Our work has demonstrated that Rab11-FIP2 is phosphorylated by MARK2 and that this event is necessary for the timely reestablishment of polarity. In addition, our proteomics work revealed both ankyrin G and ZO-1 as potential members of Rab11-FIP2 interacting complexes. The combination of these two results strongly suggests that the

involvement of Rab11-FIP2 in the establishment of polarity could be a critical regulatory component in the process. In addition, we have preliminary studies suggesting that the solubility of ZO-1 changes in cells expressing the Rab11-FIP2 phosphorylation mutant. Additional studies could confirm this alteration and attempt to understand more fully the impact of Rab11-FIP2 on tight junction proteins. We have preliminary evidence that Rab11-FIP2 is involved in apical membrane maintenance or establishment since expression of FIP2(ΔC2) causes a collapse of crumbs 3 (Figure 39) into the FIP2(ΔC2) containing compartment as well as the collapse of GP135 into the FIP2(SARG) compartment as shown in chapter 3. The involvement of Rab11-FIP2 with apically and junctionally targeted proteins may involve unique complexes that only have just been revealed through our proteomic analysis of interacting complexes.

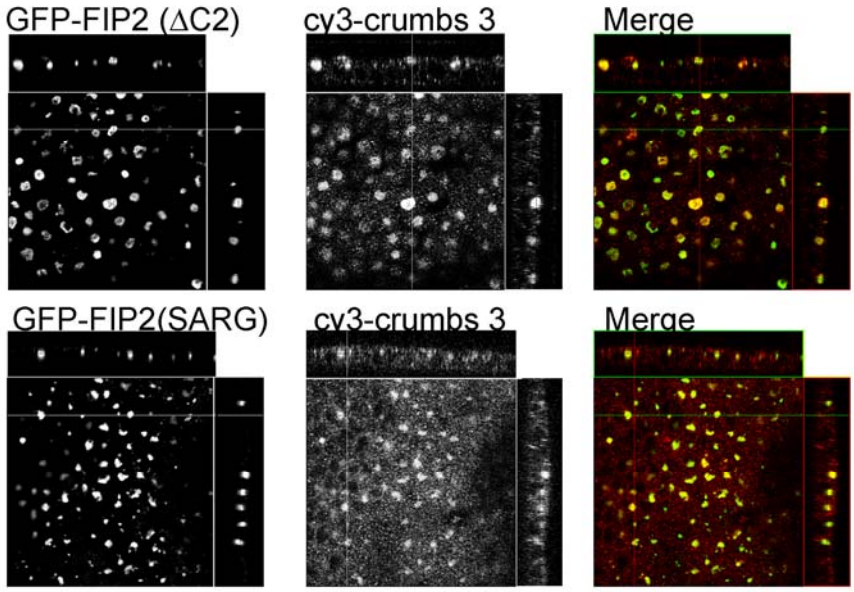

Figure 39: Rab11-FIP2 mutants cause a collapse of the apical protein crumbs 3

T23 cells stably expressing FIP2 (SARG) and FIP2(ΔC2) were imaged by confocal microscopy in the X-Y plane. Cells were stained for crumbs 3 (pseudo-colored red). Both FIP2(SARG) and FIP2(ΔC2) mutants caused a partial collapse of the structure. All images are 100X.

One of the major issues confronted during the generation of this data was the lack of a FIP2 antibody. We tried to generate an antibody on three separate occasions and were not successful in isolating antibodies that specifically recognize Rab11-FIP2. We generated inducible stable siRNA cell lines that knock down Rab11-FIP2, but these studies were difficult to pursue because of our inability to stain for endogenous Rab11-FIP2 to show that the expression level was decreased. We were able to show the knock-down by measuring mRNA levels by RT-PCR, but the differences between PCR and immunofluorescence studies made it difficult to correlate these results. However, according to FlyBase, loss of the *Drosophila melanogaster* Rab11-FIP2 homolog is reported to be lethal, even in the recessive form (Grumbling and Strelets, 2006). Our preliminary data suggest that knocking down Rab11-FIP2 in MDCK cells also is lethal. However, the use of the tetracycline inducible system should allow siRNA expression levels to be modulated, allowing for the study of events prior to cell death. While knock-down studies of Rab11-FIP2 have proven difficult thus far due to the lack of an antibody as well as the lethality of the knock-down, the lab is in the process of developing a new murine monoclonal Rab11-FIP2 antibody. If the generation of this antibody is successful, additional studies could be performed to examine the impact of the loss of Rab11-FIP2 on the establishment of polarity. A lack of Rab11-FIP2 could either hamper the formation of junctional complexes all together, or accelerate their formation.

Future Work Regarding Rab11-FIP2 in Novel Protein Complexes

We have found that Rab11-FIP2 complexes with two relatively unstudied Rab proteins, Rab5b and Rab10. The involvement of Rab11-FIP2 with additional Rabs allows the generation of a hypothesis suggesting that Rab11-FIP2 is involved in the hand-off of

cargo proteins between endosomal domains. Live cell imaging of cells actively trafficking fluorescently labeled ligand while expressing fluorescently tagged Rab11-FIP2 with fluorescent chimeras of Rab5b, Rab10 or Rab11a would allow a more thorough analysis of this hand-off process. The movement and interaction of Rab11-FIP2 between and with the distinct Rab-labeled endosomes would greatly further our knowledge of the mechanisms underlying trafficking events. The specific inhibition of transcytosis with our dominant negative mutants and not apical recycling (chapter 3) suggests that the specific routes of cargo may be determined by destination, origination, or some other as-yet-unknown factor. Rab10 colocalizes with both Rab5 near the basolateral membrane and Rab11 in the medial area of MDCK cells (Chen *et al.*, 2006). The involvement of Rab11-FIP2 in a basolaterally located Rab10 complex supports the finding that transcytosis is influenced more heavily by alterations of Rab11-FIP2 than apical recycling. Perhaps Rab11-FIP2 is involved in coordinating a Rab10/Rab11a handoff that is necessary for either delivery of previously internalized junctional complex proteins (chapter 2) or generalized transcytotic trafficking (chapter 3) (Figure 40).

The formation of a complex between Rab10 and Rab11-FIP2 does not involve direct interaction between these two proteins as demonstrated by yeast-two hybrid assays nor does it require the Rab11 Binding Domain as shown by immunoprecipitation studies (chapter 4). These interesting findings raise the possibility that an adaptor protein is involved in bringing these two proteins together. It has already been shown that Rab11-FIP2 can interact with both EHD1 and EHD3 (Naslavsky *et al.*, 2006; Ducharme *et al.*, 2007). One of the EHD proteins may be the linker between Rab11-FIP2 and Rab10.

Alternatively, the association of Rab10 with Rab11-FIP2 may require a third component in order to form a ternary complex as we have seen with Rab11/Rab11-FIP2/myosin Vb.

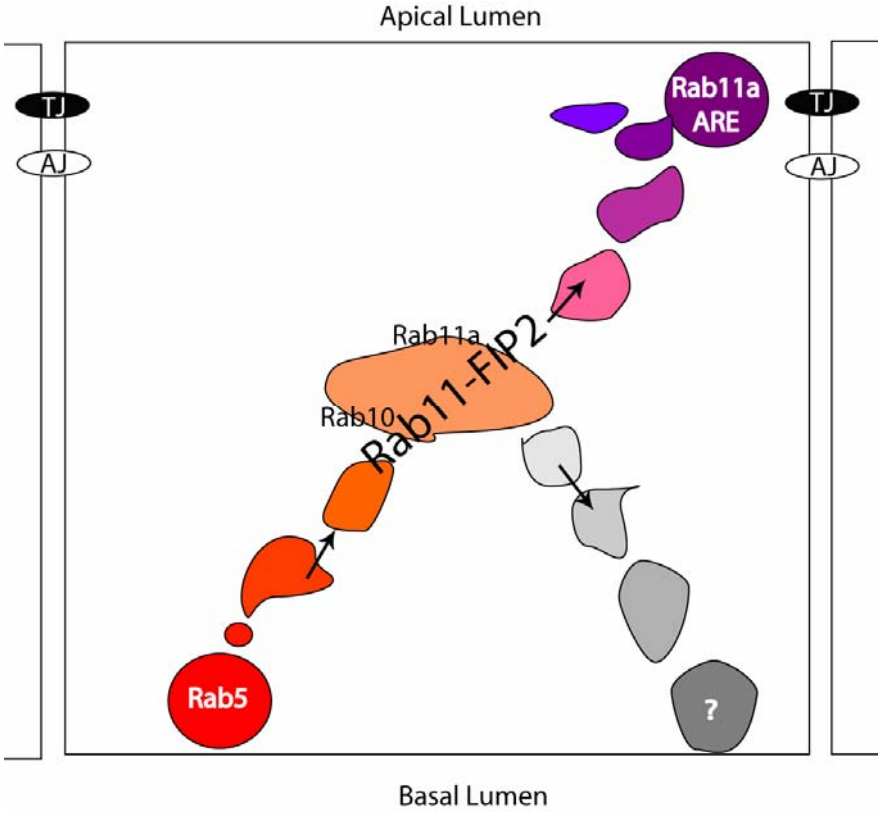

Figure 40: Model depicting Rab11-FIP2 escorting cargo throughout the entire transcytotic process from Rab10 internalization to the Rab11a recycling endosome.

Following basolateral endocytosis to a Rab5 positive early endosome (EE), Rab10 may escort cargo to and/or through the common endosome (CE). If the cargo is undergoing transcytosis, it will move to a Rab11 positive apical recycling endosome (ARE). The finding that Rab11-FIP2 is in a complex with Rab5b and Rab10 suggests that it may accompany cargo throughout the entire transcytotic pathway culminating in the previously known interaction with Rab11.

We have multiple lines of evidence to implicate Rab11-FIP2 in the hand-off between apical early endosomes and the Rab11a positive apical recycling endosome. We have found that the localization of the early endosomal proteins Rab5b, EpsinR (Chapter

4) and EEA1 (Chapter 3) is altered in cells stably expressing dominant negative Rab11-FIP2(ΔC2). Interestingly, we have data demonstrating that the Rab11-FIP2(ΔC2) mutant does not affect Rab5a, the traditionally defined early endosomal Rab. Our work allows us to postulate that multiple "early endosome" systems may exist that are coordinated separately (Figure 41), which is supported by their phosphorylation by different kinases (Chiariello *et al.*, 1999) and separable GAP activities (Callaghan *et al.*, 1999).

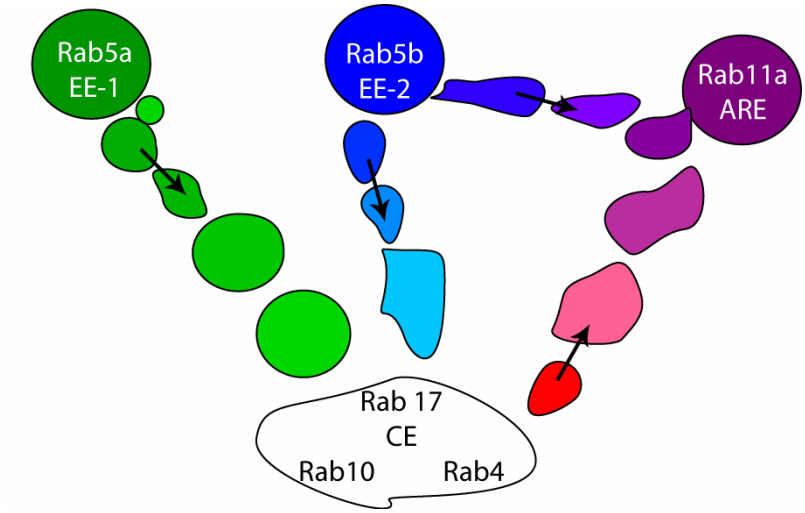

Figure 41: Model Depicting a New Early Endosomal Compartment

In a model with separable early endosomes, cargo would be internalized in either a Rab5a positive early endosome (EE-1) or a Rab5b positive early endosome (EE-2). Rab11-FIP2 would then escort cargo from the EE-2 to the Rab11a positive apical recycling endosome (ARE).

Alternatively, Rab5b could define an intermediary compartment between the Rab5a positive early endosome and the Rab11a apical recycling endosome (Figure 42). Rab11-FIP2 may help to define a subset of trafficking complexes, which can be used to track, and gain insight into, the distinctions between the early endosomal systems. Live cell imaging of cells stably expressing EGFP-Rab11-FIP2 utilizing several cargoes with

different destinations would be a logical starting place to begin understanding the dynamics of this system.

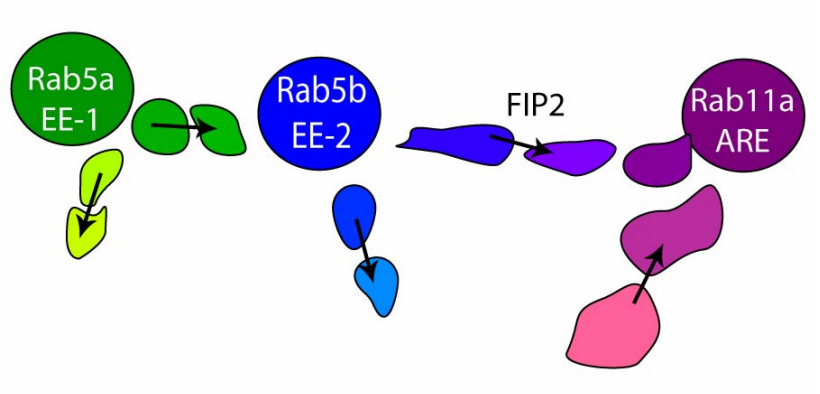

Figure 42: Model Depicting Sequential Early Endosomes

In a model with sequential early endosomes, cargo would be internalized in a Rab5a positive early endosome (EE-1). It would be trafficked to a second early endosome (EE-2) marked by Rab5b. Rab11-FIP2 would then escort cargo from the EE-2 to the Rab11a positive apical recycling endosome (ARE).

Finally, it is possible that Rab5b marks the basolateral early endosome (BEE) and Rab5a marks the apical early endosome (AEE) (Figure 43). Our data showing that Rab11-FIP2 inhibits transcytosis but not apical recycling supports this hypothesis (chapter 3). The difference between the Rab5 family members is still unknown. Most work to date has focused on examining Rab5a (Bucci *et al.*, 1994). Rab5a and Rab5b both interact with EEA1 (Callaghan *et al.*, 1999) at the Rab5 positive BEEs and AEE (Wilson *et al.*, 2000). Interestingly, these interactions are biochemically distinct. EEA1 at the BEE was disrupted by phosphoinositide 3 (PI-3) kinase depletion while the AEE population remained intact (Tuma *et al.*, 2001). By postulating that Rab5b is at the BEE, our finding that the Rab11-FIP2(ΔC2) mutant alters EEA1 localization generates a hypothesis that the BEE EEA1 population is effected by this mutant. The report that the

C2 domain of Rab11-FIP2 may bind to phospholipids such as phosphatidylinositol-(3,4,5)-trisphosphate (Lindsay and McCaffrey, 2004) may provide an additional functional connection with the EEA1-containing membranes. Thus, we can begin to ascertain the differences between the Rab5 family members as well as the AEE and BEE by following up on these observations. It would be beneficial to look at the colocalization of basolaterally-loaded cargo with Rab5b. If transcytotic studies show colocalization with Rab5b but apical recycling studies do not, this would greatly advance the field by defining these compartments. We have suggested that the block induced by Rab11-FIP2(ΔC2) occurs prior to that by Rab11-FIP2(SARG). If the hypothesis that Rab5b is at the BEE is supported, that allows us to place Rab11-FIP2 in the pathway as early as the BEE. The finding that Rab11-FIP2 interacts with Rab10 would suggest that Rab11-FIP2 is involved in coordinating events throughout the entire transcytotic pathway. Additionally, we could deplete PI-3K and look at the effect on Rab11-FIP2. If Rab11-FIP2 is mis-localized, that would strongly implicate a connection between the PI-3K pathway known to be involved in BEE EEA1 localization with Rab11-FIP2 localization. If Rab11-FIP2 is shown to be involved specifically in the basolateral transcytotic pathway, we could then ascertain if this is a general function or one specific to Rab11-FIP2. Most likely, the proposed involvement of Rab11-FIP2 throughout transcytosis would be specific to Rab11-FIP2.

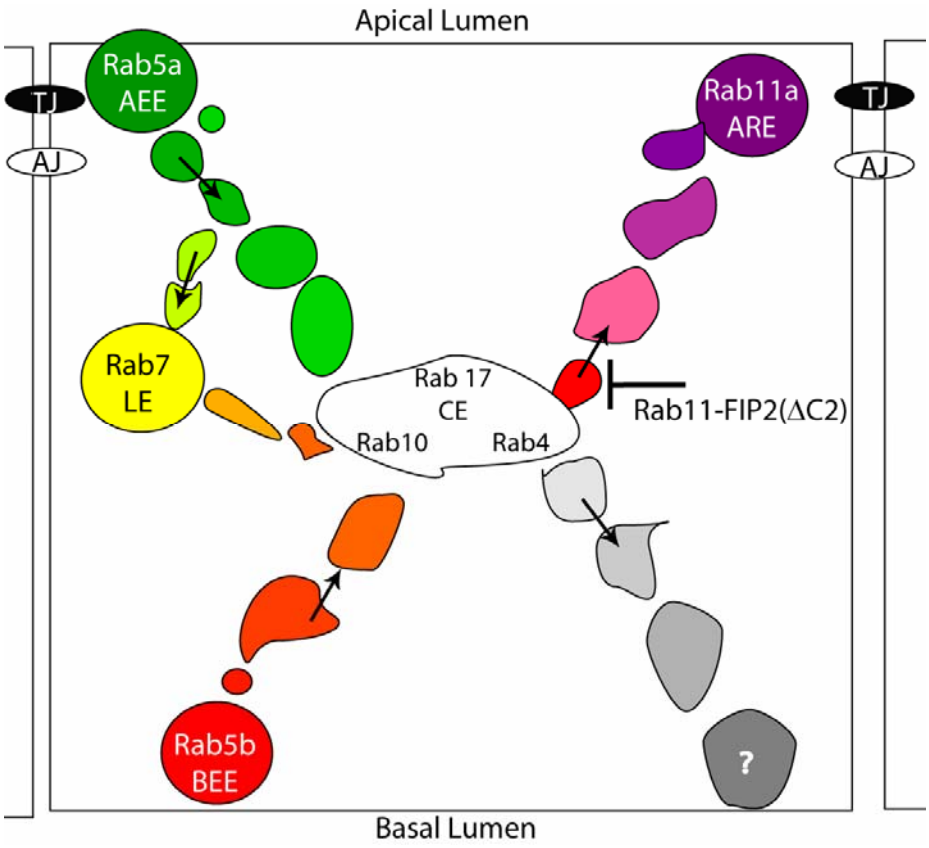

Figure 43: Model depicting Rab5b at the basolateral early endosome

This model shows Rab5b at the basolateral early endosome (BEE) and Rab5a at the AEE. In this model, Rab11-FIP2 would escort cargo from the Rab5b BEE through the CE and up to the ARE.

One of the main difficulties in the polarized trafficking field is that all trafficking assays in MDCK cells are done with exogenous cargo. This difficulty is exemplified by our first studies looking at wild type Rab11-FIP2 in MDCK cells (chapter 2). We struggled with the presence of two morphologically distinct populations of EGFP-Rab11-FIP2 in each of the stable lines we made. We eventually discovered that the difference in populations was correlated with the presence or absence of the polymeric IgA receptor, which was stably expressed in the parent line, but had variable expression levels. Our proteomic results may have revealed endogenous cargos for the Rab11-FIP2 pathway (chapter 4, e.g. vesicle amine transport protein 1, probable G-protein coupled receptor 82

and thyroid receptor interacting protein 11). It will be critical to explore the localization of these receptors with and without ligand stimulation. If we can engineer fluorescently tagged cargo as well as antibodies specific to these receptors, it would advance the trafficking field tremendously. The lack of endogenous cargo is one of the biggest caveats in the use of MDCK cells in the trafficking field. With these reagents in hand, we also would be able to explore the hypothesis that Rab11-FIP2 is a continually present escort through the entire endocytotic/recycling process.

One of the most exciting findings of this work is the interaction of Rab11-FIP2 with dynein. Little work has been done exploring the role of dynein-mediated trafficking in polarized MDCK cells. The presence of dynein in complex with Rab11-FIP2 allows the exploration of a myriad of previously un-testable hypotheses. The first of these involves the retrieval of Rab11a from its destination membrane back to the apical recycling endosome (ARE). Dynein may be involved in returning the complex back to the ARE (Figure 44A). Alternatively, dynein may be involved in the Rab10-positive basolateral endosome pathway (Figure 44B). Both of these hypotheses can be tested now that dynein has been identified as a component of the Rab11-FIP2 complex, which has known cargo. Ideally, a dynein truncation mutant akin to myosin Vb-tail would be generated and explored in this system. This truncation mutant could be used to assess trafficking of either pIgAR or one of the endogenous cargoes discussed above. However, a dynein mutant may have global effects that would preclude exploring its role specifically in Rab11-FIP2 mediated pathways. Additionally, protocols could be modified to allow immunoprecipitation of dynein from polarized cells allowing for a greater understanding of the complex. If the truncated dynein mutant can be cloned, it

would also be very beneficial to examine direct interactions between dynein and Rab11-FIP2, Rab10, Rab11a, and the other FIP members via yeast-two hybrid assays. Currently, we do not have a handle on the hierarchy of complex formation. Parsing out this hierarchy would aid us in understanding the sequence of events involved in the Rab11-FIP2 pathway.

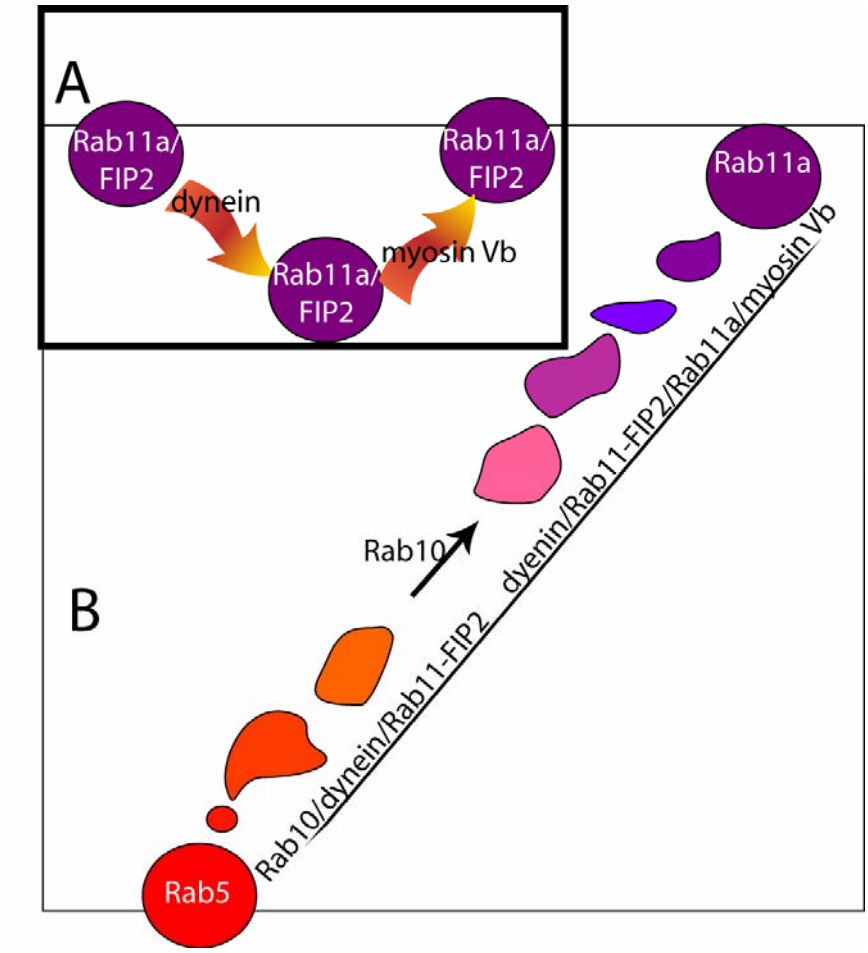

Figure 44: Model for Potential Roles of dynein in Rab11a trafficking

A) Rab11a may complex with myosin Vb and FIP2 as it moves to the plasma membrane. It would then be retrieved using a dynein dependent mechanism. B) Rab10 may complex with dynein and FIP2 during basolateral early endocytosis. As cargo transcytoses through the cell, Rab10 would be exchanged for Rab11a.

The combination of the identification of new proteins in complex with Rab11-FIP2 and the functional implications of our mutant work allows us to postulate a definitive role for Rab11-FIP2 (Figure 45). Rab11-FIP2 may accompany basolaterally-internalized cargo throughout the entire transcytotic process from the Rab5b positive BEE through the Rab10 positive CE culminating in the Rab11 positive ARE. Phosphorylation of Rab11-FIP2 by MARK2 may allow cargo to exit the apical recycling pathway and instead be delivered directly to a forming junction. Thus, cells expressing the non-phosphorylatable Rab11-FIP2 had a delay in junctional establishment because junctional proteins were forced to continue through the apical recycling route before delivery to the lateral membrane. The phosphorylation event may instigate an early release of cargo from the pathway mediated by extracellular signals such as calcium concentrations. In essence, it provides an alternate emergency route when cells are in danger (Figure 45).

The work presented here was initiated in order to investigate the hypothesis that Rab11-FIP2 is a critical regulator of plasma membrane recycling. We have provided ample data to support this hypothesis including information implicating Rab11-FIP2 in vesicle trafficking through the early endosomal system and the basolaterally originating transcytotic pathway. In the process of addressing this question, we have not only established an important role for Rab11-FIP2 in Rab11a mediated plasma membrane recycling, we have also uncovered additional roles for Rab11-FIP2 in other pathways.

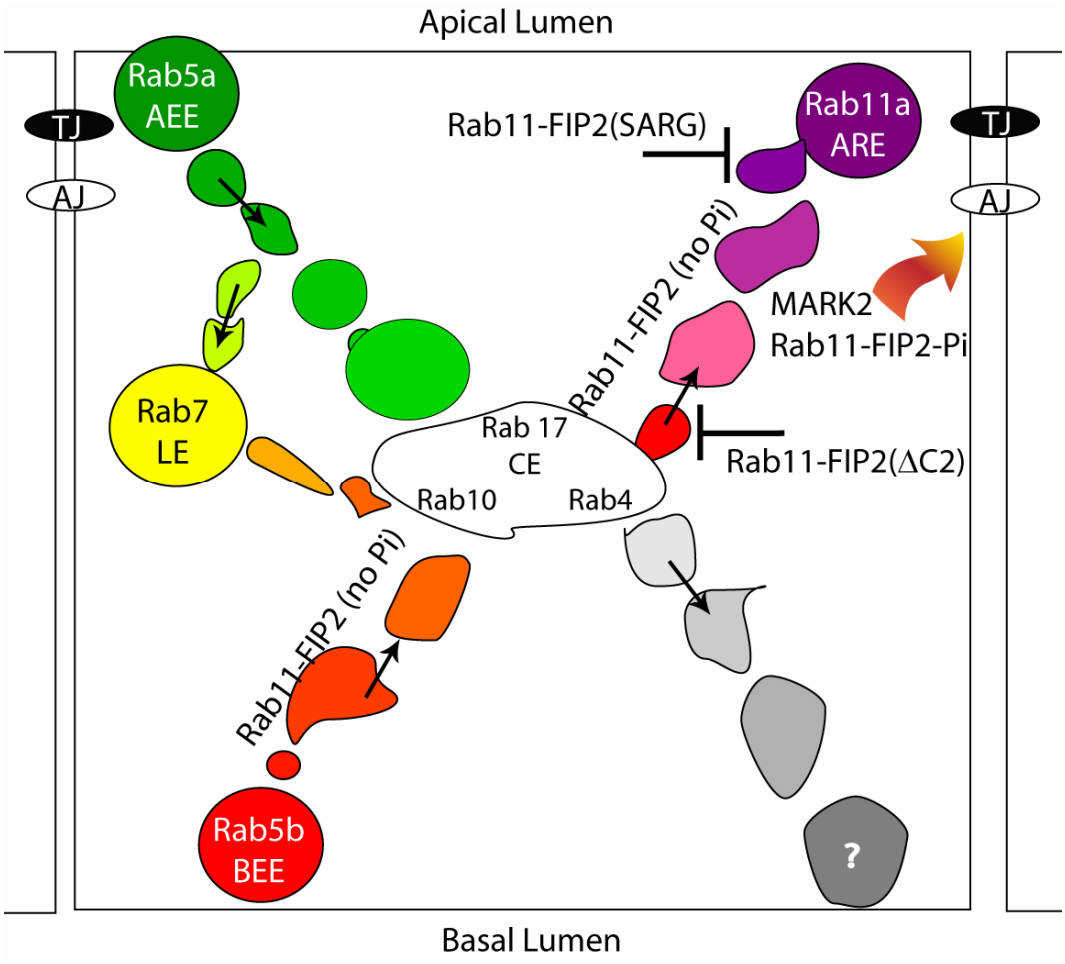

Figure 45: Model denoting the role of Rab11-FIP2 in polarized epithelial cells.

A postulated role of Rab11-FIP2 in polarized cells is presented. Rab11-FIP2 interacts with the Rab5b positive BEE. It then escorts the vesicle to the Rab10 positive CE. In normal conditions, Rab11-FIP2 and its associated vesicle continue to the Rab11 ARE. When the polarity of cells is altered, MARK2 phosphorylates Rab11-FIP2 allowing for an early release from the pathway.

References

Bucci, C., Wandinger-Ness, A., Lutcke, A., Chiariello, M., Bruni, C.B., and Zerial, M. (1994). Rab5a is a common component of the apical and basolateral endocytic machinery in polarized epithelial cells. Proc Natl Acad Sci U S A *91*, 5061-5065.

Callaghan, J., Nixon, S., Bucci, C., Toh, B.H., and Stenmark, H. (1999). Direct interaction of EEA1 with Rab5b. Eur J Biochem *265*, 361-366.

Chen, C.C.-H., Schweinsberg, P.J., Vashist, S., Mareiniss, D.P., Lambie, E.J., and Grant, B.D. (2006). RAB-10 Is Required for Endocytic Recycling in the Caenorhabditis elegans Intestine. Mol. Biol. Cell *17*, 1286-1297.

Chiariello, M., Bruni, C.B., and Bucci, C. (1999). The small GTPases Rab5a, Rab5b and Rab5c are differentially phosphorylated in vitro. FEBS Lett *453*, 20-24.

Ducharme, N.A., Williams, J., Lapierre, L.A., and Goldenring, J.R. (2007). Dominant Negative RAB11-FIP2 Mutants Uncover Differentiable Steps in Transcytosis. Traffic *Submitted*.

Fan, G.-H., Lapierre, L.A., Goldenring, J.R., Sai, J., and Richmond, A. (2004). Rab11-Family Interacting Protein 2 and Myosin Vb are required for CXCR2 recycling and receptor-mediated chemotaxis. Mol. Biol. Cell *15*, 2456-2469.

Grumbling, G., and Strelets, V. (2006). FlyBase: anatomical data, images and queries. Nucleic Acids Res *34*, D484-488.

Hales, C.M., Griner, R., Hobdy-Henderson, K.C., Dorn, M.C., Hardy, D., Kumar, R., Navarre, J., Chan, E.K., Lapierre, L.A., and Goldenring, J.R. (2001). Identification and characterization of a family of Rab11-interacting proteins. J Biol Chem *276*, 39067-39075.

Hales, C.M., Vaerman, J.P., and Goldenring, J.R. (2002). Rab11 family interacting protein 2 associates with Myosin Vb and regulates plasma membrane recycling. J Biol Chem *277*, 50415-50421.

Lapierre, L.A., Kumar, R., Hales, C.M., Navarre, J., Bhartur, S.G., Burnette, J.O., Provance, D.W., Jr., Mercer, J.A., Bahler, M., and Goldenring, J.R. (2001). Myosin vb is associated with plasma membrane recycling systems. Mol Biol Cell *12*, 1843-1857.

Lindsay, A.J., and McCaffrey, M.W. (2004). The C2 domains of the class I Rab11 family of interacting proteins target recycling vesicles to the plasma membrane. J Cell Sci *117*, 4365-4375.

Naslavsky, N., Rahajeng, J., Sharma, M., Jovic, M., and Caplan, S. (2006). Interactions between EHD Proteins and Rab11-FIP2: A role for EHD3 in early endosomal transport. Mol. Biol. Cell *17*, 163-177.

Roosterman, D., Schmidlin, F., and Bunnett, N.W. (2003). Rab5a and rab11a mediate agonist-induced trafficking of protease-activated receptor 2. Am J Physiol Cell Physiol *284*, C1319-1329.

Tuma, P.L., Nyasae, L.K., Backer, J.M., and Hubbard, A.L. (2001). Vps34p differentially regulates endocytosis from the apical and basolateral domains in polarized hepatic cells. J Cell Biol *154*, 1197-1208.

Volpicelli, L.A., Lah, J.J., Fang, G., Goldenring, J.R., and Levey, A.I. (2002). Rab11a and myosin Vb regulate recycling of the M4 muscarinic acetylcholine receptor. J Neurosci *22*, 9776-9784.

Wilson, J.M., de Hoop, M., Zorzi, N., Toh, B.H., Dotti, C.G., and Parton, R.G. (2000). EEA1, a tethering protein of the early sorting endosome, shows a polarized distribution in hippocampal neurons, epithelial cells, and fibroblasts. Mol Biol Cell *11*, 2657-2671.